Synthesis and Characterization of Polymeric Materials as Sequestrants for Biological Applications

Ophelia J. Wadsworth

Dissertation submitted to the faculty of the Virginia Polytechnic Institute and State University in partial fulfillment of the requirements for the degree of

Doctor of Philosophy
in
Chemistry

Michael D. Schulz, Chair
Alan R. Esker
Kevin J. Edgar
Andrew N. Lowell

May 13, 2025

Blacksburg, VA

Keywords: Hepatocellular carcinoma, Chemofilter, TACE, Doxorubicin, Glycomaterials, Post-polymerization Modification

Synthesis and Characterization of Polymeric Materials as Sequestrants for Biological Applications

Ophelia J. Wadsworth

ABSTRACT (academic)

To address the systemic toxicity attributable to doxorubicin (Dox) following targeted chemotherapy treatments for hepatocellular carcinoma, we explored drug-capture strategies using both DNA-functionalized substrates and synthetic polymeric materials. DNA-modified cotton substrates were prepared with and without using silane linkers and surprisingly, DNA-only modified substrates demonstrated comparable Dox capture efficacy to those functionalized with DNA and the control silane linker. DNA quantification revealed apparent increases in DNA concentration due to thermally induced denaturation during adsorption, suggesting the need for milder reaction conditions for future experiments.

We also synthesized poly(methacrylic acid) (PMA) resins to electrostatically bind Dox at physiological pH. Comparative capture studies with uncharged PMA at low-pH conditions confirmed an 18-fold increase in Dox capture efficacy due to ionic interactions. Crosslink density and polymer flexibility also played pivotal roles, with more rigid materials demonstrating greater capture efficacy and more flexible materials exhibiting the opposite trend due to increased hydrophobicity. These results underscore the importance of tuning network rigidity and hydrophobicity in subsequent drug-capture material design.

Finally, to explore alternatives to traditional antibiotics, we synthesized varied molecular weights of mannose-functionalized polynorbornenes and modified the polymer backbone with thiolated-mannose and thiolated-amine moieties. Our objective was to increase the antibacterial

properties observed with unmodified glycopolymers by increasing glycan density to inhibit bacterial growth and separately, introducing cationic charges to disrupt bacterial membranes. Our approach used the oxo-norbornene derivative, a key procedural change as these materials are not widely explored for post-polymerization modification, particularly with biologically relevant molecules such as glycans and cationic compounds. While we observed partial functionalization of the polymer backbone at longer reaction times, we demonstrated that the backbone alkenes of these glycopolymers are amenable to thiol-ene chemistry. We also generated a set of materials with precise architecture that differed only in their pendant functionalities. Comprehensive biological assays will follow to assess the antimicrobial and hemolytic performances and determine the structure-activity relationships.

Synthesis and Characterization of Polymeric Materials as Sequestrants for Biological Applications

Ophelia J. Wadsworth

GENERAL AUDIENCE ABSTRACT

For liver cancer patients receiving targeted chemotherapy treatments, a drug called doxorubicin (Dox) is delivered directly to the tumor. However, about half of the drug can escape into the bloodstream and cause serious damage to the heart. To help prevent this, we generated materials that could capture the excess drug before it circulates throughout the body. We found that DNA cotton fabric and crosslinked polymers worked well at capturing Dox and that the stiffness of the polymers affected how much drug they can bind to. We continue to explore different materials that potentially can be fabricated into a device for use to filter the excess Dox during chemotherapy treatments.

In a separate project, we tackled the growing problem of antibiotic-resistant bacteria by generating carbohydrate materials that mimic how bacteria attach to cells. These materials were designed to block bacteria from attaching to the cells in the body, preventing bacterial infections from progressing. By changing parts of the molecule's structure, we can fine-tune how effective it is at binding to different bacterial strains. Together, these studies show how we can design smart materials that either protect the body from harmful side effects or act as new tools in the fight against drug-resistant bacteria.

Acknowledgements

This has been an incredible and mind-bending journey towards becoming an esteemed professional researcher. I had no idea what I was signing up for; however, I am happy I signed up. I absolutely could not have completed this endeavor without the valuable assistance of people I admire and will always be indebted to. The following is my personal style paying homage to these individuals who will remain with me forever:

I commend myself for daring to embark on this journey, especially at a time in life when I feel the urge to wind down and look forward to meeting my grandchildren (they are still not yet born but I am waiting with bated breath). I felt “naked and afraid” when I decided to apply to graduate school but was primarily motivated by my unwillingness to add another “what if” to my list of regrets. I learned so much more about myself while persevering through this experience and I am more in awe of science.

I am forever grateful to myself that my son Brandon was born to me. You will never know how you have inspired and motivated me in ways no one else could. Through you I learned to remove my self-imposed limits on what to do and where to go professionally and personally. I remember a specific time when I failed my preliminary exam, and you failed the portion of your training necessary to advance to the next step. We were crushed emotionally, and we acknowledged that those were consequences of “aiming high”. We laughed about finishing for the sake of family pride and proceeded to make the most of our second chances. We did it and I am ridiculously proud of us both. In the same breath, the woman who willingly sacrificed so much for her children and asked nothing in return will always be my inspiration. You made certain we were able to access the opportunities that were unavailable to you. Mom, I thank you for your love and encouragement throughout my lifetime and dedicate my accomplishments to you.

I am a wise woman for choosing to work with Dr. Michael Schulz. I was inspired and impressed at your scientific intelligence, ambition and humility during our first conversation and when I learned that you are three years older than my son, I instantly knew it would be an even more humbling experience for me. For the past eight years (yes, my head is hard), you have been extremely patient, compassionate and encouraging. These attributes helped me to endure the many professional and personal challenges I encountered while enrolled at Virginia Tech. During one of our early meetings, you told me that one of your goals for me is to become the expert and teach you about my projects. You have helped me to improve my overall proficiency, and I am forever grateful. Angela Schulz, your heart is infinitely larger than your stature. Thank you for your necessary encouragement throughout these years with words and delicious meals.

I greatly appreciate me for integrating with my research group in a way that defies typical boundaries. I was able to persevere through those days when research output was disappointing because you all encouraged me, made me laugh and willingly contributed ideas to help me clean out the cobwebs. The camaraderie among the Schulz Research Group is astounding and I hope that it remains for future research generations. During my tenure, I witnessed the United Nations in action in our lab (St. Kitts, Jamaica, Saudi Arabia, Bangladesh, China, Indonesia and the United States). This offered a valuable education that we could not attain by reading books or watching documentaries. As the first-generation group members, Brady Hall, Ryan Archer and I established the group culture among ourselves. Now, I am very proud of Dr. Brady Hall and Dr. Ryan Archer for their accomplishments and am so happy to finally join you as an OG alum.

The second-generation members added so much real-estate value to the group with their drive for excellence. I am still in awe of Dr. Hanan Almuzaini. As a wife and mother, you were superbly organized and were able to accomplish so much, making the most of each day. As my

cubby mate for five years, we enjoyed many personal and professional conversations that helped me endure this journey. I look forward to meeting you in Riyadh someday soon. Dr. Rachel Bianculli, you are what I wish my younger self had been. Among so many amazing attributes, you willingly contribute to the betterment of everyone and everything around you. You even use surrogates to provide your necessary hugs since you dared to ambitiously leave Virginia Tech for greener pastures. I am honored to know you and will do so until one of us glamorously expire. Dr. Tiffany Thompson (TNT), if you know how brilliant you are, your head will not fit on your body. Even more astounding is that your heart is so much larger than your brain. When we met thirteen years ago, I could not know the depths and heights our friendship would grow to. Our honest conversations have enriched my life and no matter where our journeys lead us, I intend to keep you in my life forever.

The Schulz Research Group is currently led by some amazing human beings. Jon Mase and Connor Gallagher, thank you both for giving so much of yourselves personally and professionally. Gillian Su-Kropp, I am amazed at your growth and capabilities. You are now the teacher. Zhen Shi, my graveyard shift buddy, your encouragement and willingness to help with whatever circumstance developed, helped me survive the last six months in the lab. To the newer group members, you acclimated quickly to the teamwork atmosphere and have truly increased our value in the department. Amira Muhamed, Tyler Bridges, Cassell McMillan, Lane Kennedy, Matthew Williams, Chris Armstrong, Destiny Matthews, Nishat Adiba and Muhamed Ali, thank you all for choosing this group and helping to maintain the unity among us.

My past research advisors have played key roles in my aspiration to become a proficient scientist. To Dr. Omar Christian, thank you for my first chemistry research experience and patiently allowing me to mess up some stuff. I won't hold being Jamaican against you. Dr. Natalie Arnett, you were and sometimes still are more ambitious for me than I am. Thank you for leading by example. I will forever appreciate our personal conversations and the reminders about who I am made to be. I will not hold being Bahamian against you.

To my VT research committee – you are a very patient group of distinguished scholars, and I apologize for testing that patience. Dr. Alan Esker, Dr. Kevin Edgar and Dr. Andrew Lowell, thank you all for consistently making yourselves available to me and therefore helping me get out of here. Thank you for helping me rise to this challenge and finally overcome it. I will appreciate you always.

Attributions

This dissertation consists of chapters that were written with the help of several co-workers, colleagues, and collaborators. They are acknowledged below along with their affiliations:

Dr. Brady A. Hall, Research Scientist, Luna Innovations Inc.

Dr. W. Ryan Archer, Post Doctoral Researcher, Princeton University

Dr. Tiffany N. Thompson, Research Scientist, Dow Inc.

Dr. Michael D. Schulz, Associate Professor, Virginia Tech

Mr. Landon Dehart, Manager, DAX Copilot Adoption Company

Ms. Simran Kala, Consultant, Deloitte Business Consulting and Services

Ms. Gillian A. Su, Ph.D. Candidate, Virginia Tech

Ms. H. Suzanne Muller, Graduate Student, University of North Carolina-Chapel Hill

Dr. Steven W. Hetts, Chief of Neuroendovascular Surgery, University of California-San Francisco

Chapter 1. Literature Review

This chapter partially contains material previously published in *Polymer International* and *Journal of Materials Chemistry B*.

Archer, W.R.; Hall, B.A.; Thompson, T.N.; Wadsworth, O.J.; Schulz, M.D. *Polym. Int.* **2019**, *68*, 1220-1237.

W. Ryan Archer, Brady Hall, Tiffany Thompson, and Ophelia Wadsworth wrote and edited the manuscript. Michael Schulz is the advisor and helped with writing and editing the manuscript.

Su, G.A.; Wadsworth, O.J.; Muller, H.S.; Archer, W.R.; Hetts, S.W.; Schulz, M.D. *J. Mater. Chem. B*, **2023**, *11*, 8449-8455.

Gillian Su synthesized the materials, conducted FTIR characterization and BET analysis, and wrote the manuscript. Ophelia Wadsworth and Suzanne Muller conducted drug capture studies. William Archer conducted BET analysis. Steven Hetts helped with writing the manuscript. Michael Schulz is the advisor and helped with writing and editing the manuscript.

Chapter 2. Modification of Cellulose in Cotton Fabric for Chemotherapy Drug Capture

Ophelia Wadsworth synthesized the materials, conducted SEM characterization and drug capture studies, and wrote the manuscript. Landon Dehart and Simran Kala synthesized the materials and conducted drug capture analysis. Michael Schulz is the advisor and helped with writing and editing the manuscript.

Chapter 3. Methacrylic acid-based Resins for Chemotherapy Drug Capture Applications

Chapter to be submitted for publication

Ophelia Wadsworth synthesized the materials, conducted FTIR characterization and drug capture studies, and wrote the manuscript. Gillian Su and Suzanne Muller conducted drug capture studies. Steven Hetts helped with writing the manuscript. Michael Schulz is the advisor and helped with writing and editing the manuscript.

Chapter 4. Synthesis and Post-polymerization Modification of Mannose-Containing Glycopolymers to Improve Antimicrobial Properties while Reducing Hemolytic Activity

Chapter to be submitted for publication

Ophelia Wadsworth synthesized the materials, conducted NMR and SEC analysis, and wrote the manuscript. Brady Hall helped with writing the manuscript. Michael Schulz is the advisor and helped with writing and editing the manuscript.

Chapter 5. Summary and Future Outlook

Ophelia Wadsworth wrote the manuscript. Michael Schulz is the advisor and helped with writing and editing the manuscript.

Table of Contents

Chapter 1. Literature Review

1.1. Introduction

The versatility of polymers as sequestrants has received much attention because they show promise to mitigate the hazards of biological and environmental contaminations.[1] Polymer sequestrants are designed to bind to and remove specific molecules from complex solutions, often targeting organic micropollutants in the soil and wastewater,[2] radioactive materials,[3] heavy metals from wastewater sources,[4] and bacterial endotoxins in the gastrointestinal tract.[5] A more recent application is their use as drug capture materials to adsorb excess chemotherapy agents during cancer treatments.[6] Procedures to limit the delivery of chemotherapy drugs to the targeted tumor are highly advantageous to mitigate toxicity to healthy tissue. Several approaches have shown promise towards sequestering the excess drug during chemotherapy treatment,[7-9] and additional work is in the research pipeline.

While the exploration of polymer sequestrants to bind chemotherapy drugs is relatively new, they have been widely investigated as viable replacements for traditional antibiotics. Antibiotics have significantly mitigated the global impact of bacterial infections; however, many ba*cterial strains have adapted resistance mechanisms over time, leading to diminished antibiotic efficacy.[10] Consequently, there is now an overwhelming need for new antibacterial therapeutics with equal or enhanced efficacy that can evade the drug-resistance that plague current antibiotics.[11, 12] Polymers with pendant carbohydrate side chains (glycopolymers) are a promising alternative antibacterial therapeutic to treat infections attributable to antibiotic resistant bacterial strains because the sidechains can mitigate bacterial infections by competing for the binding sites on the bacterial surfaces.

The fundamental challenge to developing polymer sequestrants is to incorporate moieties with high affinity for the targeted compound. This literature review explores the synthetic strategies and limitations of polymer sequestrants designed to capture chemotherapy drugs during cancer treatments and those developed to bind to pathogenic bacteria to inhibit growth and mitigate bacterial infections.

1.2. Biological Toxicity due to Chemotherapy Drugs

Cancers develop when mutations occur within the cell cycle that disrupt the genes that regulate cell growth (proto-oncogenes) and tumor suppressor genes. Controls within the cell cycle are arrested and the rate of cell division increases while that of cell death is decreased or altogether halted.[13] Proto-oncogenes transform into oncogenes when they experience mutations that disrupt their functionality. As a result, cancer cells grow and divide at a considerably faster rate than normal cells, resulting in tumor growth.[14] The rates of cancer incidence and mortality have increased exponentially within the last decade, with 19.3 million new cases and 10 million deaths occurring in 2020.[15] While resection is often prescribed for early stage detection (tumors of a certain size), many patients are diagnosed in the late stages, when radiation therapy and/or chemotherapy are required to decrease the tumor size before surgical removal.[13, 16]

Chemotherapy is prescribed to destroy rapidly dividing tumor cells; however, healthy cells are also targeted. The destruction of healthy cells leads to side effects such as chemotherapy-induced nausea and vomiting, fatigue, mouth sores, nerve damage, and low white blood cell count that leads to infections (neutropenia), diarrhea, constipation and hair loss.[17] There are currently five classes of chemotherapy drugs categorized by their mechanisms of action for suppressing tumor growth (**Fig. 1.1**):[13] alkylating agents [18, 19] antimetabolites;[20, 21] antitumor antibiotics,[22-24] topoisomerase inhibitors, [25] and tubulin-binding drugs.[26, 27] Treatment options often involve combination therapy due to the complexity of the tumor and the type of cancer diagnosed; a single chemotherapy drug may not provide effective treatment.[16] While more than 130 anticancer drugs have been approved by the US Food and Drug Administration, doxorubicin (Dox) (**Fig. 1.2)** and paclitaxel are among the most prescribed due to their effective treatment capabilities for a wide variety of cancers; however, they are also known to cause severe cardiotoxicity and acute hypersensitivity, respectively.[16, 28] Cardiotoxicity impairs the heart muscle and poses the most serious adverse effect to cancer patients being treated with Dox. Irreversible cardiomyopathy and congestive heart failure were observed in patients whose cumulative dose of Dox exceeded 550 mg/m^2. Consequently, Dox is administered in limited doses and is often combined with other chemotherapeutic drugs such as etoposide (**Fig. 1.1**) to access different anticancer mechanisms, in accordance with the type of cancer treated.[28-30]

Hepatocellular carcinoma (HCC), a primary liver cancer, is the third leading cause of cancer mortality globally. It is often undetected until late stages, resulting in a mortality rate of 95% within five years of diagnosis.[31-33] While transplantation or resection are primary treatment options, many patients do not qualify and are instead prescribed chemotherapy.[34, 35] Transarterial chemoembolization (TACE), a procedure in which chemotherapy drugs are directly administered to the tumors via catheter (**Fig. 1.2**), is the standard therapeutic treatment for these patients.[36-39] Despite this site-specific delivery, approximately 50% of the administered drug exits the liver and circulates throughout the body, harming healthy tissues. The development of a filtration device to remove the excess chemotherapy drugs would enable higher doses to be administered resulting in faster tumor shrinkage while mitigating systemic toxicity.[32]

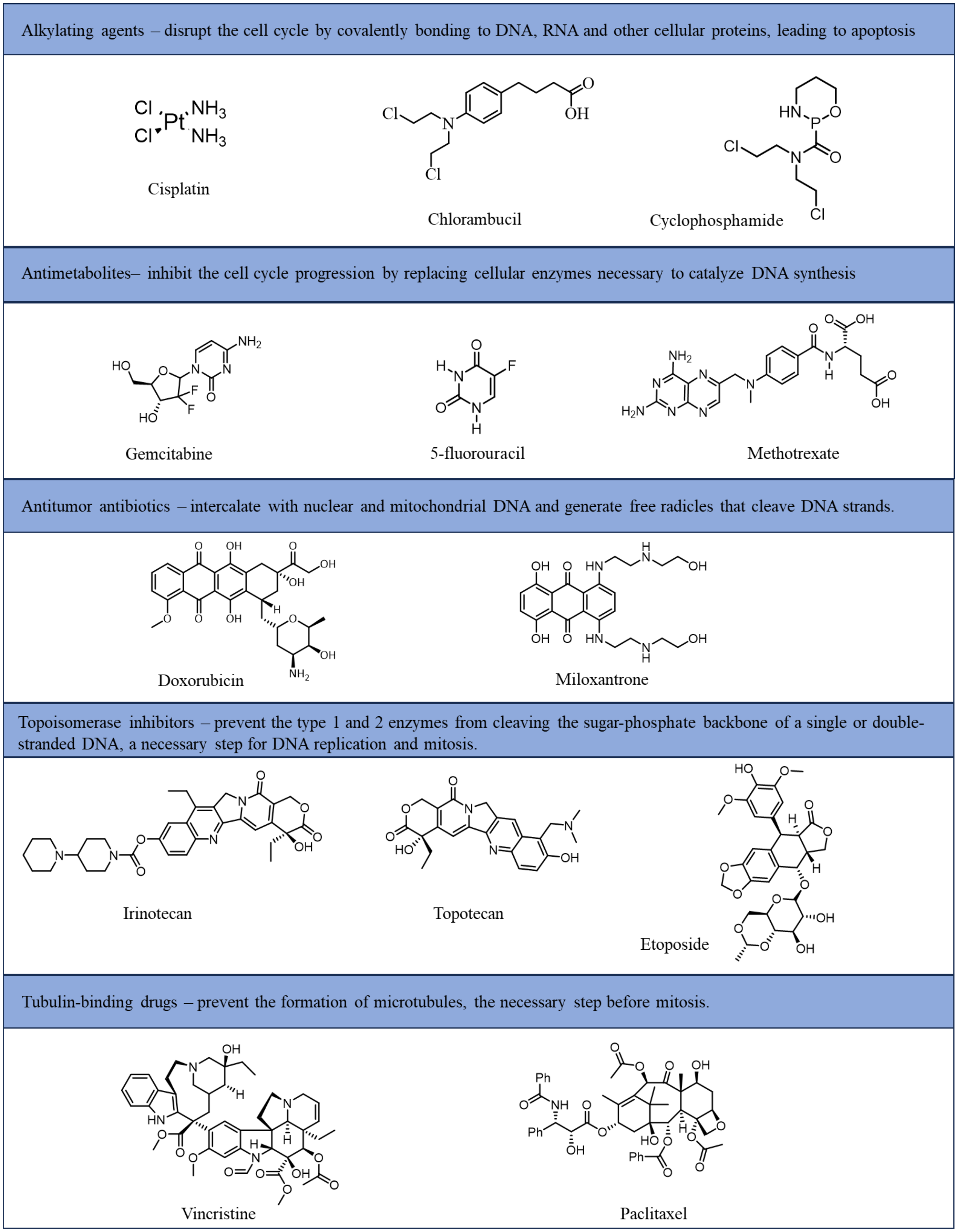

Figure 1.1. Representative molecular structures of tumor suppressing agents within the five classes of chemotherapy drugs

(a) (b)

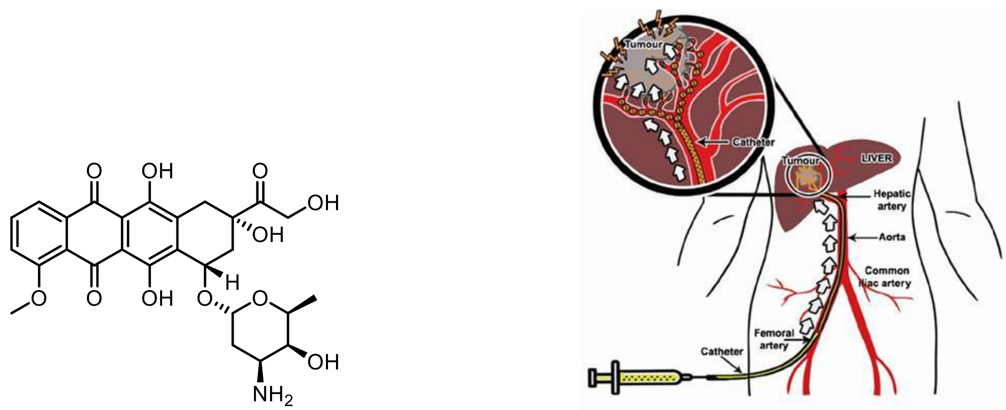

Figure 1.2. (a) Molecular structure of doxorubicin (b) schematic of TACE procedure used to administer chemotherapeutic to liver cancer patients[31]

1.3. Approaches to Mitigating Off-target Dox Toxicity

To mitigate or eliminate off-target toxicity during TACE procedures, Patel *et al.* proposed using a filtration device, temporarily deployed via catheter downstream from the liver, to capture excess Dox leaving the liver vasculature. This chemofilter approach (**Fig. 1.2b**) can be integrated with the TACE procedure, which has already proven to be a successful treatment method to localized chemotherapy drugs in the liver.[6, 32, 40, 41] This approach, however, requires materials that are capable of binding to Dox or other chemotherapy drugs in the blood, leading to research efforts to develop such materials.

1.3.1. Anionic Resins to Facilitate Electrostatic Attraction with Dox

To assess the viability of removing excess Dox from the bloodstream during chemotherapy treatments, Patel *et al.* designed a flow circuit experiment that mimicked TACE and tested Dox sequestration in phosphate buffered solution, blood serum and live porcine subjects (**Fig. 1.3**). An anionic polyethylene-polystyrene sulfonate triblock copolymer (PSS-PE-PSS) film was used to electrostatically bind to Dox, which is positively charged at physiological pH. The resin was immobilized in a mesh and the Dox solution was passed through a peristaltic pump. Within 10 minutes, the resin captured 76% of Dox from the PBS solution and 52% from the serum solution. *In vivo* results showed that the membrane manufactured from the same resin captured 85% of Dox after three minutes of introducing the drug into the hepatic vein.[32]

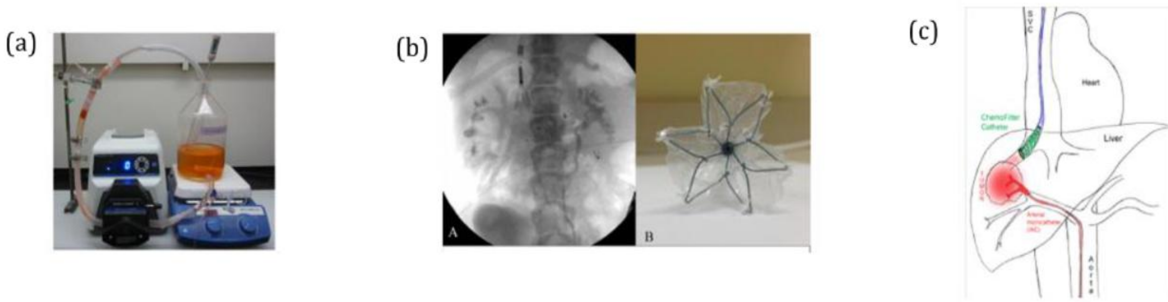

Figure 1.3. (a) TACE simulator – 76% Dox capture in 10 mins; (b) *in vivo* swine model – 85% Dox capture in 3 mins; (c) schematic of Dox and chemofilter treatment[32]

Oh *et al.* subsequently fabricated a porous absorber that was used to selectively bind to and sequester excess Dox leaving the liver within one hour without obstructing blood flow or causing thrombosis. The 2000 mm^2 substrate was 3D-printed from poly(ethylene glycol) diacrylate (PEGDA) with dimensions and features that allowed insertion and removal by a minimally invasive guide-wire approach (**Fig. 1.4**). It was then coated with a poly-(*tert*-butylstyrene)-*b*-poly(ethylene-*co*-propylene)-*b*-poly(styrene-*co*-styrenesulfonate)-*b*-poly(ethylene-*co*-propylene)-*b*-(*tert*-butylstyrene) (PtBS-PEP-PSS-PEP-PtBS) triblock copolymer; the PtBS and PEP blocks facilitated adhesion to the substrate while the PSS block captured the drug. The coated substrate was then inserted into live porcine subjects before a clinical Dox dose was infused into the iliac vein leading to the liver. Once Dox was administered, blood samples were withdrawn from the vein at the positions immediately before and after the adsorber placement. UV absorbance analysis of Dox removed from the blood samples withdrawn after the absorber showed an average capture efficiency of 64±6% (n=3). The capture efficiency of the uncoated absorber was negligible.

After removing Dox, the coated absorbers were flushed for one month to assess the binding strength between Dox and the absorber; less than 0.001 mg/mL of a starting concentration of 50 mg/mL was released, showing that Dox was irreversibly bound to the absorber.[9]

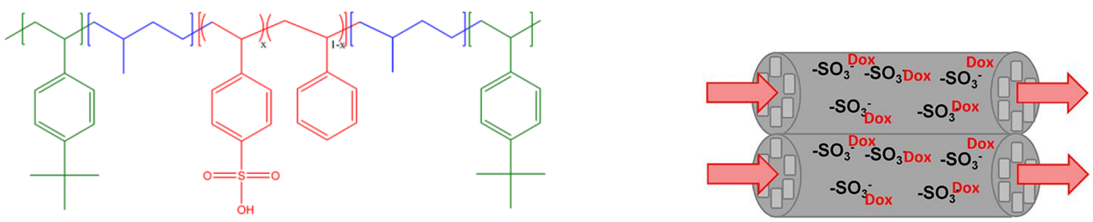

Figure 1.4. (a) Chemical structure of the PtBS-PEP-PSS-PEP-PtBS triblock copolymer used to coat the absorber (b) used to sequester Dox in porcine subjects[9]

1.3.2. Genomic DNA as an Adsorption Substrate

DNA was explored as a Dox-capture material because Dox's superior antitumor activity arises from its DNA-targeting mechanism of action. Dox destroys cells by binding preferentially to cytosine-guanine sites in DNA which prevents DNA replication and causes apoptosis. DNA-based capture materials form hydrogen bonds between Dox and the cytosine-guanine base pairs, resulting in a strong attachment and likely more sustained Dox capture.[42, 43]

A chemofilter device was also developed by Aboian *et al*. that utilized salmon DNA embedded in a polyester mesh (**Fig. 1.5**). A flow model was developed to simulate the circulatory system, and the mesh was positioned to filter solutions containing Dox. Within 1 minute, 95.1% of the initial Dox concentration was removed from PBS solution, 91% from porcine serum and 82% from porcine blood.[44] Despite the favorable Dox capture efficacy, the architecture does not facilitate *in vivo* applications. It is necessary to immobilize DNA on a solid support that can be deployed before Dox is administered during TACE and removed after the procedure.

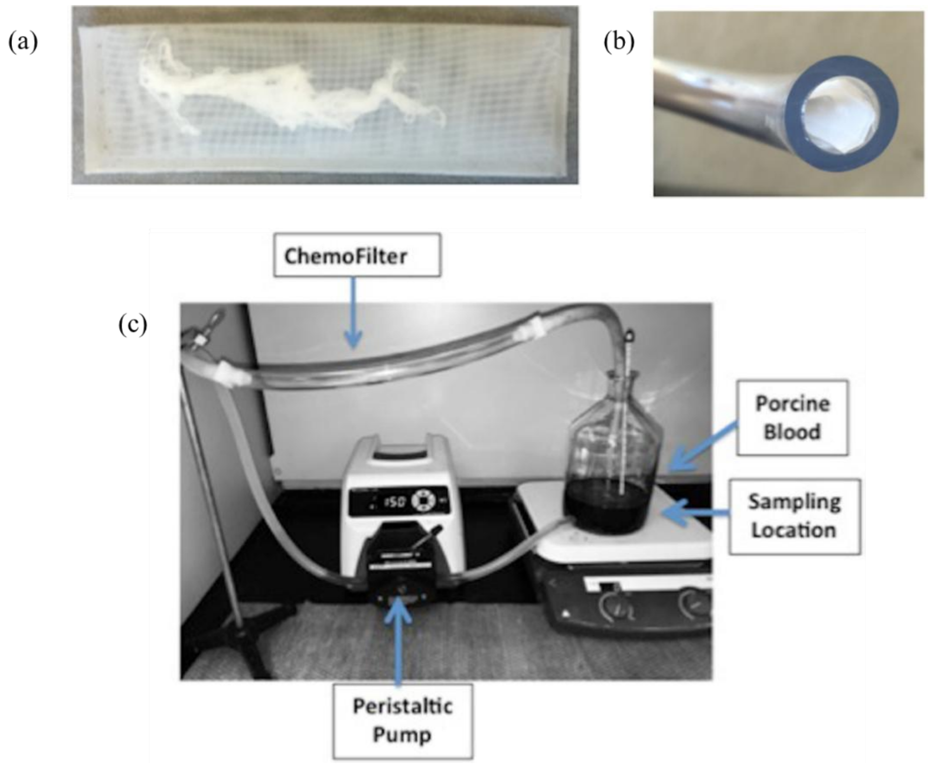

Figure 1.5. (a) Salmon DNA in polyester mesh; (b) cross-section of mesh in tube representing artery; (c) TACE simulator[44]

Blumenfeld *et al.* also explored enhancing Dox capture using DNA. Magnetite nanoparticles coated with an amine that was functionalized with nitrogen mustard were reacted with genomic DNA to form a covalent linkage. Sequestration of Dox, along with cisplatin and epirubicin, which target different moieties in DNA, were assessed in porcine serum, porcine blood and a live porcine model. While promising results were attained for cisplatin and epirubicin, the DNA-coated surface captured significantly more Dox from serum (65% in 1 minute; 93% in 25 minutes), blood (92% in 10 minutes) and in the bloodstream of the *in vivo* porcine model (82% in 3 minutes).[8]

Genomic DNA was also coated onto a 3D-printed polyacrylate substrate then crosslinked via UVC radiation. This approach could potentially lead to chemofilter devices that could be tailored to the vasculature dimensions of individual patients. Yee *et al.* prepared and utilized the following substrates and compared their Dox capture capabilities: 1) non-coated lattice; 2) lattice coated with DNA; 3) DNA-coated lattice exposed to UVC radiation to induce DNA crosslinking; 4) lattice coated with an amine linker; 5) amine-coated lattice with DNA; and 6) amine-DNA lattice exposed to UVC radiation (**Fig. 1.6**). The amine linker and crosslinking method were employed to mitigate DNA leaching from the lattice surface. Energy Dispersive Spectroscopy showed that the treated lattices that were subjected to crosslinking retained a higher quantity of DNA on the surface. UV-Vis spectroscopy verified that the Dox capture efficacy for the same materials increased 2-fold in PBS and human serum, compared to the control lattices, although some DNA leaching was detected.[40]

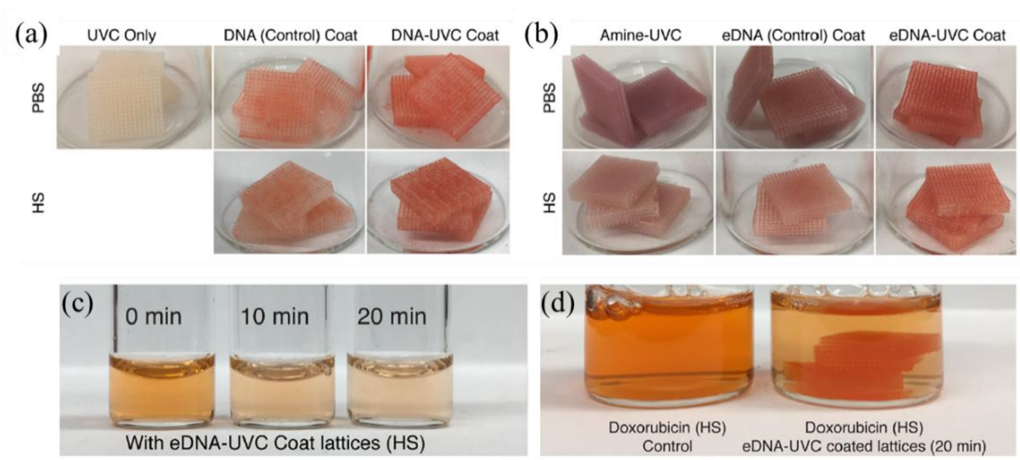

Figure 1.6. a) DNA-UVC lattice and its controls and (b) eDNA-UVC lattice and its controls after Dox capture experiments in PBS and HS. (c) Color of the doxorubicin HS solution at various time points during the doxorubicin binding experiments. (d) Comparison of color between the initial doxorubicin HS solution and the solution 20 min after the eDNA-UVC lattices have been introduced[40]

1.3.3. DNA Nucleobases Embedded in Crosslinked Polymer Resin

Inspired by the increased Dox-capture efficiency of DNA-based devices, Su *et al.* explored using DNA nucleobases to capture Dox in lieu of whole DNA, which may elicit an immune response in some patients. Adenine, cytosine, thymine and xanthine were individually incorporated into a cross-linked polymer resin synthesized by free-radical copolymerization of methacrylic acid with ethylene glycol dimethacrylate (**Fig. 1.7**). Polymer composites were subjected to elemental analysis to determine the amount of nucleobase loaded in the polymer network. To evaluate the Dox capture efficacy, 100 mg of polymer-nucleobase composite was stirred in a solution of 0.05 mg mL^{-1} Dox in phosphate buffered saline at 37 °C and UV-Vis spectroscopy was used to measure how much Dox was captured in 20 minutes.

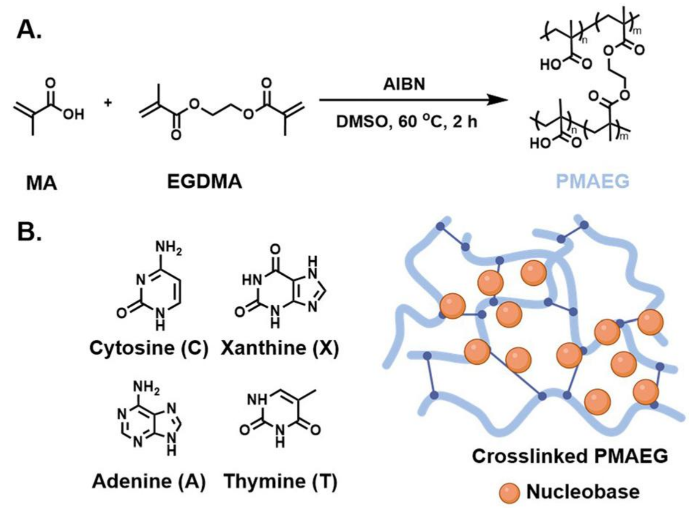

Figure 1.7. (A) Free-radical copolymerization of methacrylic acid (MA) and ethylene glycol dimethacrylate (EGDMA), initiated using AIBN, enabled the synthesis of the cross-linked resin PMAEG. (B) Nucleobases embedded into the PMAEG matrix during polymerization[7]

Compared to the control polymer resin and the cytosine, thymine and xanthine polymer composites, the adenine polymer composite demonstrated superior Dox capture with 22 mg of Dox capture and 8.78 mg of nucleobase loaded per gram of polymer resin. The pore size of each material was similar; therefore, it did not play a role in Dox capture efficacy. The nucleobases were then removed from the polymer network to determine if their presence alone contributed to capture efficacy or if a molecularly imprinted effect (template) contributed to the overall performance.

Subsequently the nucleobases were reincorporated to determine whether the materials could be regenerated. The polymer composites synthesized with adenine, thymine and xanthine showed significantly decreased Dox capture when the nucleobases were removed, and the same efficacy was observed when the materials were regenerated with the corresponding nucleobases. It was concluded that the capture mechanism of these materials depended primarily on Dox interactions with the nucleobases as well as secondary contributions from molecular imprints that were present when the nucleobases were removed (**Fig. 1.8**). Cytosine, however, demonstrated the inverse effect. When cytosine was removed, the polymer resin captured more Dox than the polymer-nucleobase composite, indicating that the primary capture mechanism was interactions with the molecular imprints. As with the other composites, Dox capture with the regenerated material was similar to that of the as-synthesized composites.

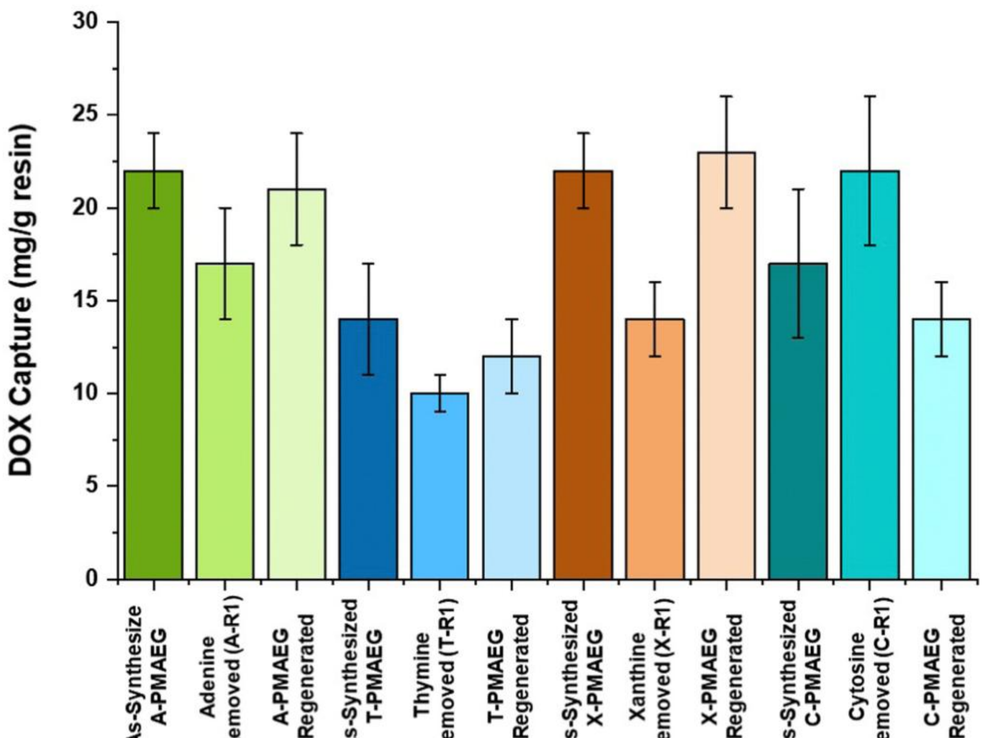

Figure 1.8. Dox capture after 20 minutes, assessing the effect of nucleobase content on capture efficacy. 100 mg of each resin was used for these measurements. Error bars are standard deviations of three samples measured[7]

1.3.4. In-situ Imine Formation to Covalently Bind Dox

Chemofilter materials that used DNA as the capture motif demonstrated higher Dox capture than ion-exchange resins; however, risks included DNA fragmentation *in situ* and possible adverse reactions to foreign DNA *in vivo*. In contrast, Krishnamoorthy and Grubbs investigated using immobilized aldehydes to covalently bond to Dox via Schiff base formation, preventing drug leaching in situ and consequently providing greater capture capability.[45] Proof of concept was established by first reacting pyridoxal-5'-phosphate (VB6) with Dox (**Fig. 1.9**) and ^{1}H NMR characterization was used to confirm successful imine formation. VB6 was then anchored to iron oxide nanoparticles via the phosphate group to generate IONP-VB6, which successfully captured Dox from DI water, PBS, and human serum; however, VB6 leaching occurred when the phosphate group hydrolyzed during Dox capture experiments. Further Dox capture experiments with various aldehydes anchored with catechol and siloxane functional groups also demonstrated excessive leaching. Subsequently, the phosphonate anchoring group proved to be the most stable (least amount of leaching detected) and the corresponding aldehyde-functionalized iron-oxide nanoparticle (IONP-3F4CPP) was used for further Dox studies (**Fig. 1.10a**).

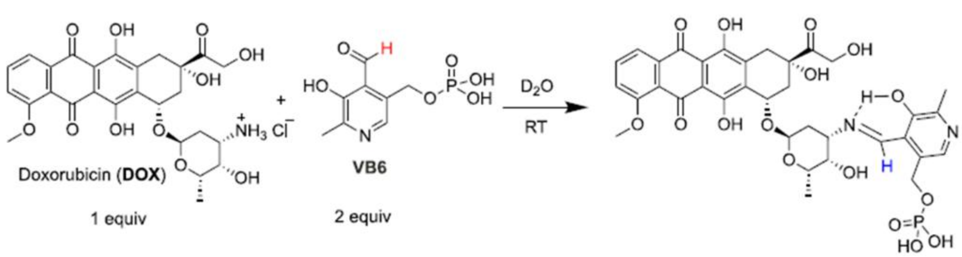

Figure 1.9. Scheme of Schiff base formation with Dox and VB6[45]

Dox capture efficacy was evaluated in PBS and human serum at varying Dox concentrations. The amount of Dox captured in both media was proportional to the concentration of Dox in solution, owing to the Schiff base reaction. Dox capture significantly decreased in human serum, where available proteins competed with Dox for Schiff base formation. IONP-3F4CPP was then modified with sulfonate and PEG groups (**Fig. 1.10b-c**) to mitigate the competing reactions by enhancing the overall hydrophilicity. Although the modifications with sulfonate and PEG groups did improve the capture efficacy in human serum, aldehyde- leaching persisted.

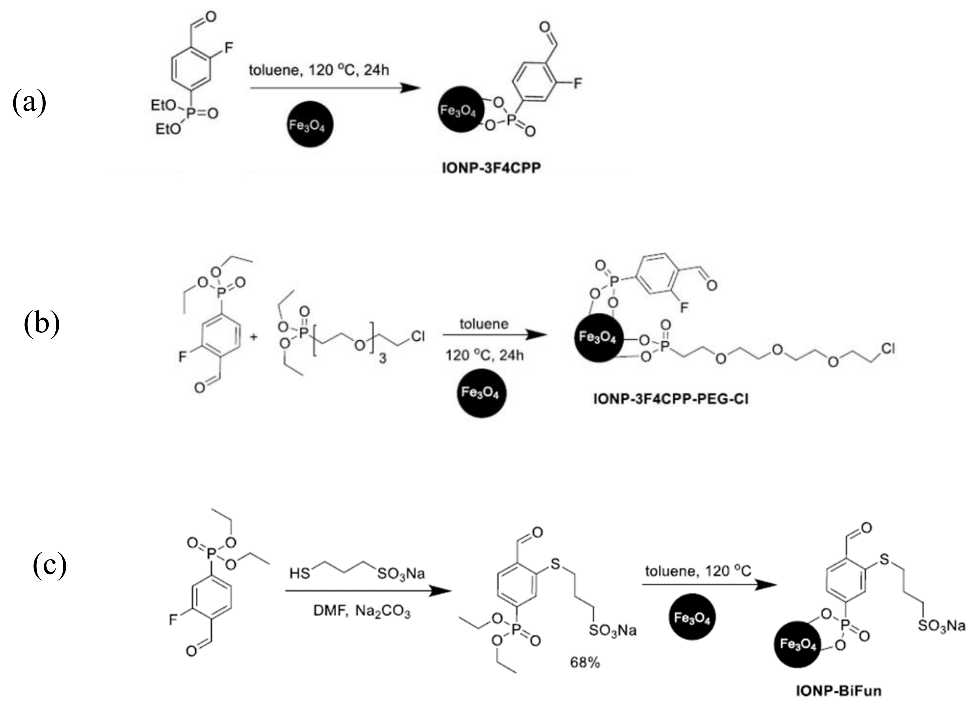

Figure 1.10. Modification of parent phosphonate-aldehyde (a) to promote increased hydrophilicity with PEG (b) and sulfonate (c) groups[45]

1.4. Global Impact of Bacterial Infections

Bacterial infection-related deaths have been categorized as an urgent priority globally and are projected to increase annually, with a projected mortality rate of 10 million per year by 2050.[46] Ikuta *et al* evaluated the deaths due to infections caused by 33 different bacteria among the population in 204 countries (**Fig. 1.11**). The 2019 study concluded the following: 1) There were 7.7 million deaths due to bacterial infections, which represented 13.6% of all deaths; 2) this was the second leading cause of deaths globally, and 3) the poorest regions of the world experienced the highest mortality rates. Additionally, among the 33 bacteria associated with these infection-related deaths, *S. aureus* and *E. coli* were the two leading pathogens that produced the highest mortalities.[47] Bacterial infections can also contribute to tumor growths in the bladder, colon and gallbladder.[48]

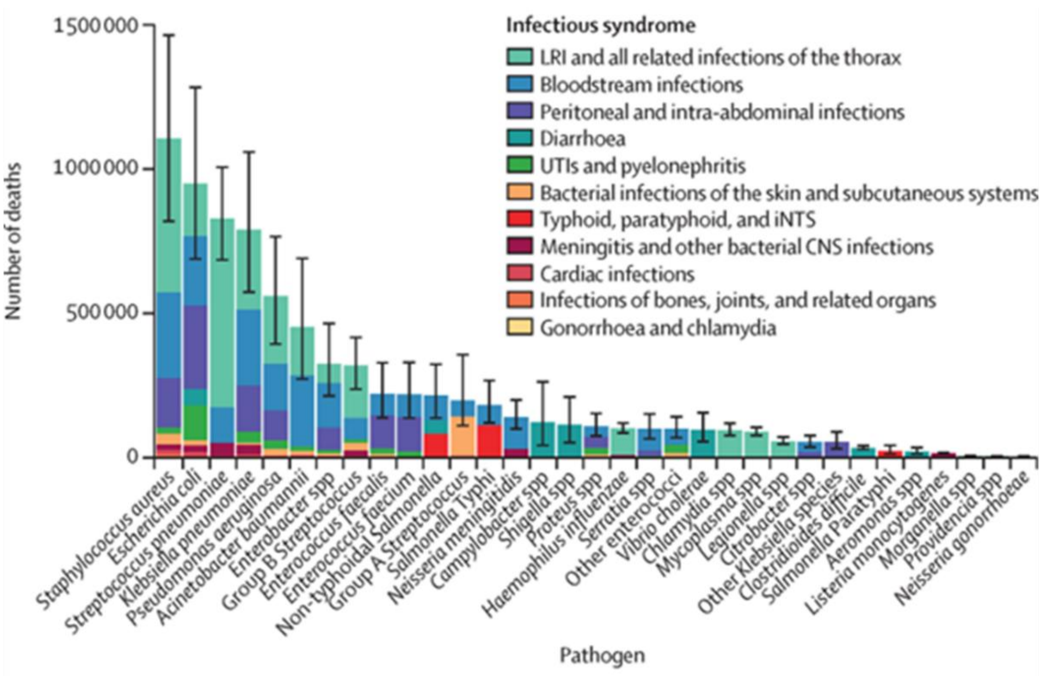

Figure 1.11. Global deaths due to bacterial infections attributed to 33 different bacteria[47]

Bacterial infection begins when binding ligands on the bacterium cell surface attach to glycoproteins or glycolipids receptors on the host cell's surface. As contact progresses, the host cell wraps its outer membrane around the bacterium and eventually encloses the bacterium completely (endocytosis) (**Fig. 1.12a**). [49-51] Alternatively, bacteria colonize the tissue surface and form a biofilm (**Fig. 1.12b**).[52] Invasion commences when these binding interactions spread throughout the tissue or the entire body leading to infection of major organs such as the lungs, stomach and heart.[53, 54]

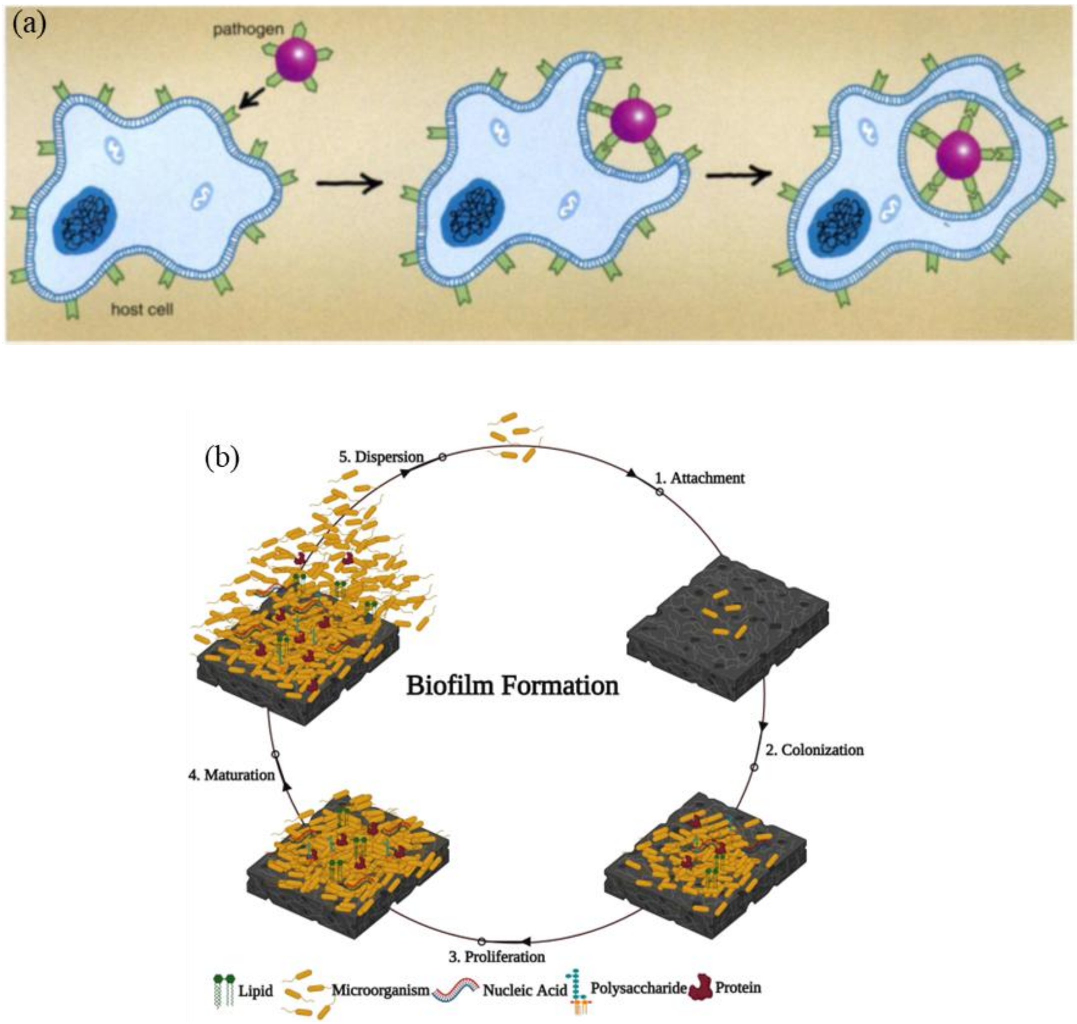

Figure 1.12. Internalization of a bacterium by a host cell (a)[51] and bacteria colonization leading to biofilm formation (b)[52]

1.5. The Emergence of Antibiotic-Resistant Bacterial Strains

Antibiotics have been used for over a century to mitigate the effects of bacterial infections and disease transmission and play a vital role in extending human life through medical intervention. The use of antibiotics has also contributed to the success of invasive medical procedures such as organ transplantations, open-heart surgeries, and cancer treatments, which are often plagued by the patients contracting bacterial infections while hospitalized.[46, 55, 56] They have been widely used for so long because they are highly effective in treating bacterial infections, are cost-effective, and many can be administered orally.[57] Prior to the development and use of antibiotics, greater than 50% of deaths were attributable to bacterial infections.[55] As of 2019, there were more than 30 classes of antibiotics (approximately 40 drugs) that had been used to treat bacterial infections with multi-targeted approaches based on their mechanisms of action (**Fig. 1.13**).[46] Among the most prescribed classes of antibiotics and their antibacterial mechanisms are: glycopeptides and carbapenems inhibit the synthesis of peptidoglycan, the polysaccharide envelope that constitutes the bacteria wall;[58, 59] macrolides and aminoglycosides inhibit the synthesis of proteins by binding to the A-site on ribosomal RNA, preventing bacterial cell growth;[60, 61] lipopeptides and polymyxins disrupt bacterial cell membranes; ansamycin and fluoroquinolones inhibit bacteria's synthesis of DNA and RNA.[46, 62]

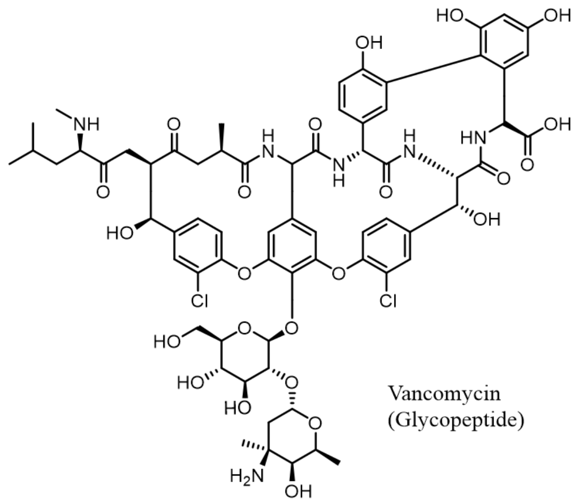

Vancomycin
(Glycopeptide)

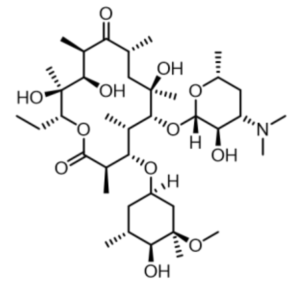

Erythromycin
(Macrolide)

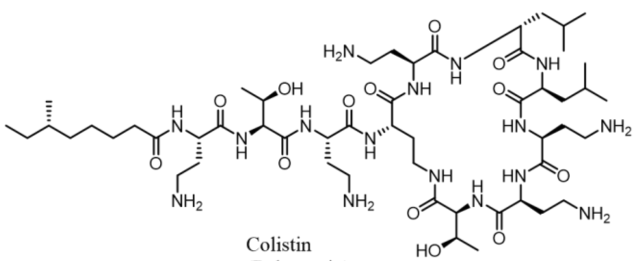

Colistin
(Polymyxin)

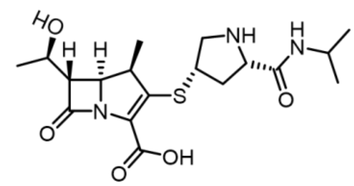

Meropenem
(Carbapenem)

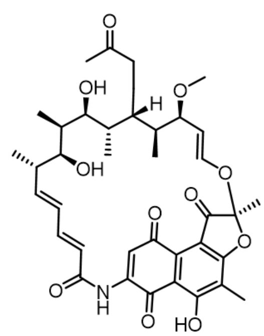

Rifamycin
(Ansamycin)

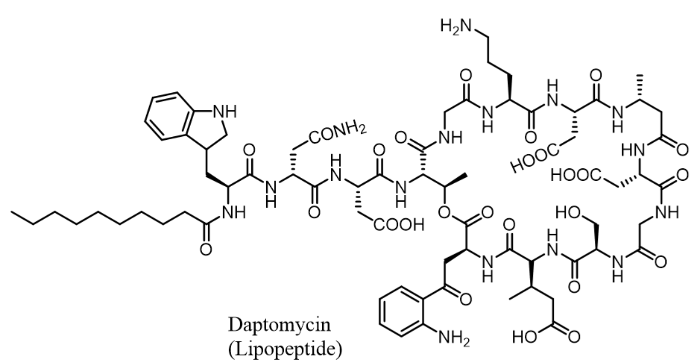

Daptomycin
(Lipopeptide)

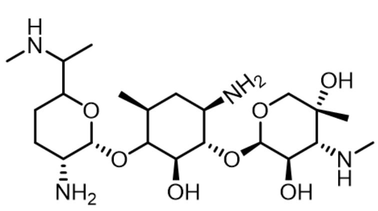

Gentamicin
(Aminoglycoside)

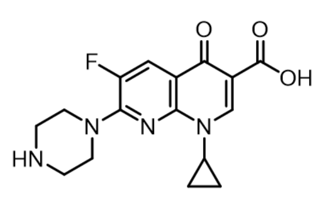

Ciprofloxacin
(Fluoroquinolone)

Figure 1.13. Structures of commercially available antibiotics

Antibiotics have significantly mitigated the global impact of bacterial infections; however, bacteria have adapted and become resistant over time, leading to a reduction in antibiotic efficacy. Additionally, overprescription of these drugs has enabled bacterial strains to develop resistance at a faster rate and some infections are now untreatable; therefore, antibiotic resistance has emerged as a global threat.[46, 63-65] Antibiotic-resistance to multiple drugs was first detected during the late 1950s[65] and later determined to occur via the following pathways (**Fig. 1.14**): 1) bacterial cell enzymes modify or degrade the antibiotic, rendering it ineffective, 2) the membrane effluxes the drug out of the cell, 3) the membrane also modifies the cell wall to change its permeability to the antibiotic drug, or 4) intracellular components alter the antibiotic target site.[10, 11] The increase in antibiotic-resistant bacterial strains has resulted in higher morbidity and mortality.[66, 67] A 2019 Centers for Disease Control report determined that 2.8 million antimicrobial-resistant infections and 35,000 related deaths occurred annually in the U.S. since 2013.[68] Therefore, there is now an overwhelming need for new antibacterial therapeutics with equal or enhanced efficacy that can evade the drug-resistance that plagues current antibiotics.[11, 69, 70] Polymeric materials, particularly those that mimic host-cell surface glycans, offer a promising approach due to their potential to target bacterial adhesion mechanisms rather than traditional pathways.[71, 72]

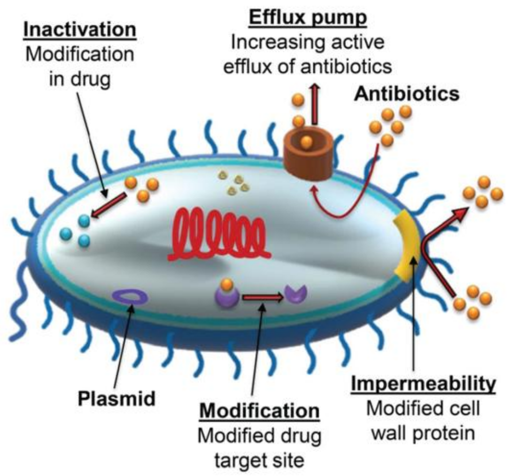

Figure 1.14. Multiple bacteria have developed several mechanisms to ensure survival in the presence of antibacterial drugs.[10]

1.6. Biological Applications for Glycopolymers

Glycopolymers are macromolecules that incorporate various pendant carbohydrates as sidechains[54, 73] and are synthesized either by functionalization of a carbohydrate monomer or post-polymerization modification to append the carbohydrate side chains.[74, 75] Similarly to other polymers, they can be synthesized as homopolymers or copolymers using various polymerization methods that facilitate control of the molecular weight, chemical functionality and stability, architecture, and degrees of flexibility of the polymer backbone and sidechains.[76] Well-defined architecture can be achieved by nitroxide-mediated polymerization (NMP),[77] atom-transfer radical polymerization (ATRP),[78] reversible addition fragmentation chain-transfer (RAFT),[79] and ring-opening metathesis polymerization (ROMP).[80, 81]

Glycopolymers have played a pivotal role in advancing biological research with their ability to mimic the carbohydrate moieties present on the membrane surface of host cells, which is the docking site for viruses, bacteria and other pathogens to begin infection and cell-cell signaling (**Fig. 1.15**).[82] Their presence *in vivo* provides decoy targets to minimize pathogen-cell interactions, thereby mitigating infection at the host site. Additionally, they forge stronger binding interactions to lectins due to the multivalency enabled by increased carbohydrate density, commonly known as the glyco-cluster effect.[83, 84] Glycopolymers have been widely explored and show great promise for pharmaceutical applications such as anticoagulants,[85] coatings for medical implants,[86] vaccine design,[87, 88] anticancer agents,[82, 89, 90] and as antiviral[91-93] and antibacterial[94, 95] alternatives.

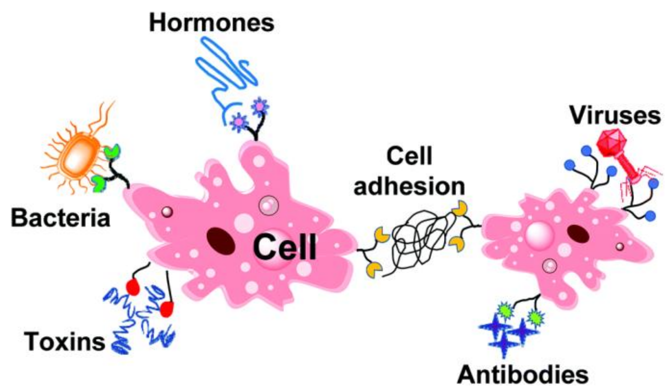

Figure 1.15. Various biological recognition processes that use lectin's high and specific affinity for carbohydrates[82]

1.6.1. Drug Delivery Vehicles

Targeted drug delivery enables therapeutic treatment to specific tissues in the body while reducing side effects and enhancing drug efficacy. Drug delivery vehicles must stabilize the drug *in vivo*, provide controlled release of the drug at the targeted site, and exhibit low toxicity, biodegradability, and chemical inertness.[96, 97] Natural polysaccharides have been heavily explored for this purpose as they are abundant in nature, have relatively low toxicity, and many are inherently bioactive.[98] Alginate, extracted from brown seaweed, is widely used as a stabilizer in a variety of drug formulations to extend drug release. The carboxylic acid functional groups remain protonated in acidic environments below pH 3.5, ensuring limited drug release in the stomach and its ability to crosslink with calcium or zinc in the bloodstream enhances its stability until the drug reaches the targeted site.[99] Chitin is extracted from the exoskeletons of shellfish and the cell walls of fungi. Chitosans, which are partially deacetylated derivatives of chitin, are utilized as hemostatic, antibacterial and mucoadhesive coatings in wound dressing applications.[100-102] Hyaluronic acid (HA) is a component of the extracellular matrix and its CD44 receptors are overexpressed on the surface of tumor cells. HA is attractive as a carrier for chemotherapeutics as it provides enhanced drug targeting to the tumor sites.[103, 104] Cellulose and its derivatives (ethers, esters) are used to synthesize hydrogels that survive specific biological environments and facilitate sustained release of drugs, while bacterial cellulose has been heavily explored including as a transdermal drug delivery-system.[105-107]

Although natural polysaccharides are sustainable, there are limitations to their continued use as drug-delivery materials. Some polysaccharides are difficult to dissolve and therefore more energy-inefficient methods are required to process the desired materials. Batch-to-batch variation is another common challenge even when the materials are derived from the same sources, which impacts large-scale production when there are variations in molecular weight and composition. Additionally, impurities such as proteins and metal ions are difficult to remove and additional treatment steps are necessary during the processing of the desired materials.[75]

Galactose-azobenzene copolymers were synthesized by Pearson *et al.* as light-responsive micelles to deliver chemotherapeutic agents to melanoma cells. Galactose was modified to append a methacrylate moiety and incorporated to facilitate cellular uptake via ligand-receptor binding to galectin-3 receptors on the surface of melanoma cells, as they are known to strongly bind to galactose.[108] The amphiphilic copolymers were synthesized via RAFT with precise block lengths and, loaded with drug mimic Nile red, demonstrated high cellular uptake in human melanoma A375 cells (**Fig. 1.16**). The success of cellular uptake and proven non-toxicity in the absence of the loaded drug validated these materials as effective drug delivery vehicles to improve targeted chemotherapy.[109]

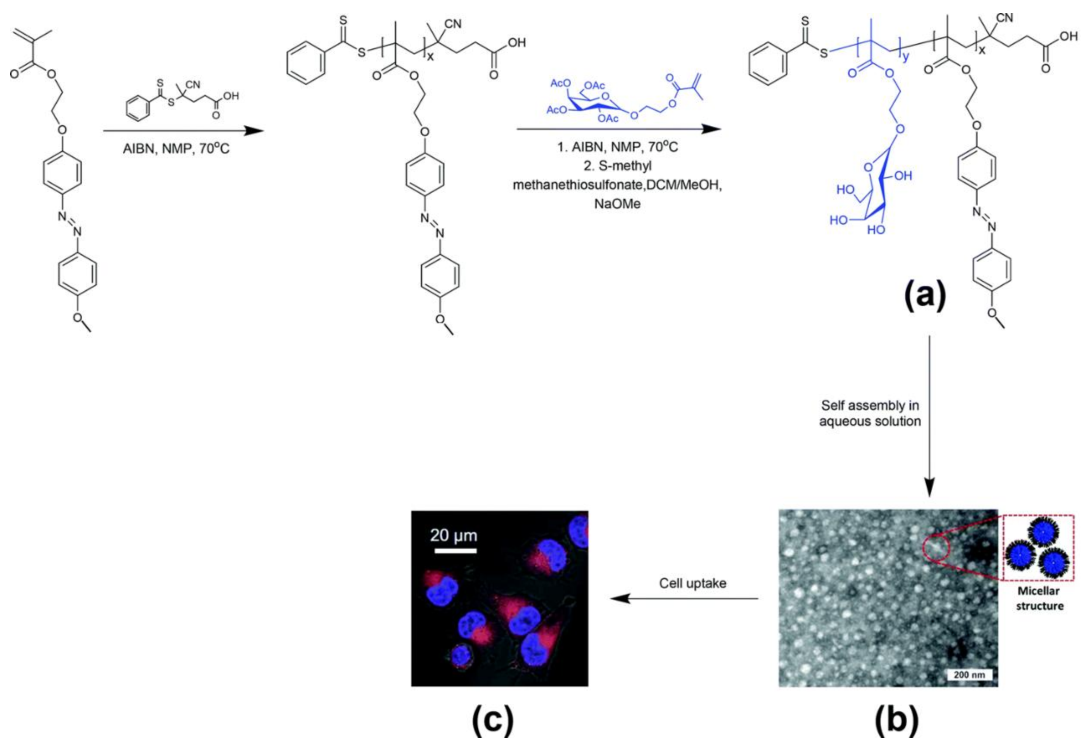

Figure 1.16. (a) Synthetic scheme of galactose-azobenzene copolymer; (b) TEM imaging of micelle formation; (c) Confocal microscopy imaging of A375 melanoma cells incubated with Nile red loaded polymer[82, 109]

Dag *et al.* synthesized mannose-containing diblock copolymers with varying mannose concentrations to facilitate self-assembly of nanoparticles with varied morphologies. The materials were used to assess the effect of morphology on cellular uptake by macrophages. Confocal fluorescence microscopy revealed that uptake increased with mannose concentration rather than morphology, demonstrating the validity of these glyco-nanoparticles as promising drug delivery materials to tissues with surface mannose.[110]

Similarly, amphiphilic block copolymers were synthesized in a two-step process in which a functionalized glucose monomer was polymerized via RAFT followed by post-polymerization modification of the terminal end with an amino initiator that facilitated polymerization of an amino acid block (glutamate or isoleucine) (**Fig. 1.17**). The length of the amino acid polymer block was varied to assess any impact on nanoparticle stability. The copolymer was used to encapsulate paclitaxel, a chemotherapeutic agent and its viability as a drug-delivery system was assessed. Cytotoxicity assays revealed that each variation of copolymer composition was non-toxic up to the concentration used for drug encapsulation. Although the IC_{50} values of the drug-loaded NPs were significantly greater when tested against human breast cancer cells, they were similar to those of the free drug when tested against human lung cancer cells.[111]

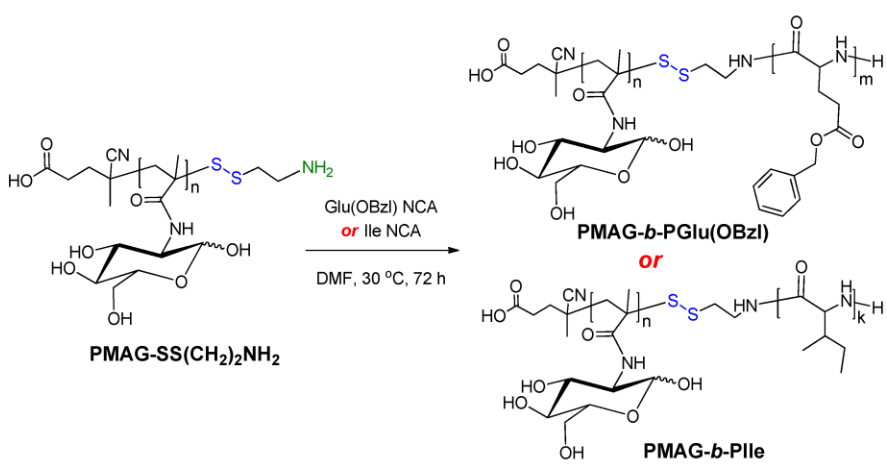

Figure 1.17. Synthesis of glucose-amino acid block copolymer to encapsulate paclitaxel[111]

1.6.2. Vaccine Design

Natural carbohydrate-based vaccines that have been approved for commercial use are isolated from microbes and conjugated to carrier proteins.[112] They are available in limited quantities due to arduous purification methods, heterogeneous products and often irreproducible chemistry methodologies for protein conjugation.[113] Synthetic carbohydrate-based vaccines are heavily investigated to surmount these limitations because well-defined antigen structures can be synthesized in large quantities and with greater purity to minimize undesirable immune responses.[114] Quimi-Hib, the first commercially available synthetic vaccine was developed in Cuba to treat *Haemophilus influenzae* type b bacterial infections, which caused over 600,000 infant deaths annually in developing countries as of 2004. In addition to bacterial infections, both versions are being explored for the treatment of viral infections and cancer.

Healthy mammalian cells are characterized by the presence of N-acetyl-glucosamine-D-glucosamine (GlcNAc) on the cell surface whereas cancerous mammalian cells show the presence of α-N-acetyl-D-galactosamine (αGalNAc).[115] This difference was leveraged to develop a treatment regimen for cancer immunotherapy with the goal of generating a viable vaccine (**Fig. 1.18**). RAFT was used to copolymerize the αGalNAc monomer in varying compositions with poly(ethylene glycol) methyl ether methacrylate (PEGMA). Gold nanoparticles were then prepared with each polymer, and the materials were tested for their ability to induce an immune response in rabbits, as evidenced by the presence of IgG antibodies in blood serum. The free polymer generated little to no immune response while the nanoparticles that incorporated 20-25 αGalNAc repeat units generated approximately 5-fold more antibodies than the material with 50 repeat units. The reduced efficacy was attributed to the induced crosslinking of B cell coreceptors caused by increased αGalNAc density. The researchers further investigated the ability of the antibodies to recognize naturally occurring αGalNAc. Bovine mucin contains sialylated αGalNAc and samples containing the sialylated and desialylated αGalNAc were reacted with serum samples collected from rabbit subjects at day 0 and 70 after immunization with nanoparticles that incorporated 20 and 25 αGalNAc repeat units. ELISA results showed a noticeable increase in antibody production specific to the sialylated and desialylated αGalNAc when those samples were reacted with the immunized serum sample. Furthermore, the number of antibodies specific to the desialylated αGalNAc were significantly higher than those specific to the sialylated version. This study highlights the successful design of fully synthetic glycopolymers that are promising candidates for anticancer vaccine development.[87] Additional synthetic and clinical research has demonstrated promising results towards a multivalent approach for multiple cancers[116] or all cancers.[117-119]

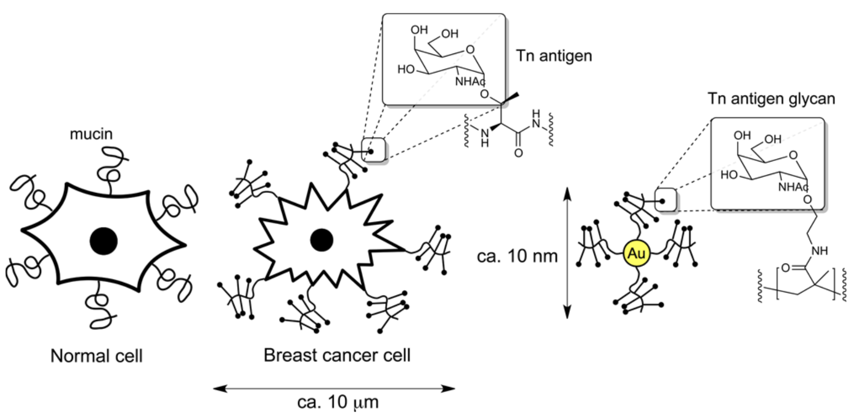

Figure 1.18. Design approach to synthesize PEGMA-αGlcNAc vaccine for the treatment of mammalian cancer[87]

Closteridium difficile (*C. difficile*) is the leading cause of health-care related bacterial infections in humans with symptoms such as colitis and diarrhea persisting throughout the active phase.[112, 120] In 2011, 453,000 new cases were detected and 29,000 deaths resulted within 30 days of diagnosis.[121] Although vancomycin and metronidazole are the primary antibiotics prescribed for severe and mild cases, respectively, alternative treatments are necessary due to the rise in antibiotic-resistant strains.[112, 120]

PSII is a glycan that is abundantly present on the surface of different *C. difficile* strains and has the been the target for vaccine design. Adamo *et al.* isolated PSII from a strain of *C. difficile* and conjugated it to a carrier proteins to test its efficacy to elicit an immune response. Three additional glycans representing PSII variations were synthesized and conjugated to carrier protein to determine which functionality is essential to successfully mitigate *C. difficile* infections (**Fig. 1.19**). Among the four glycans used to immunized mice subjects, the native PSII and the phosphorylated conjugate elicited immune responses with production of IgM and IgG antibodies (the immune system's response to the presence of antigens and to fight infections, respectively). These are now being explored as vaccine candidates to treat *C. difficile* infections, providing a necessary alternative to combate antibiotic-resistant bacteria strains.[122]

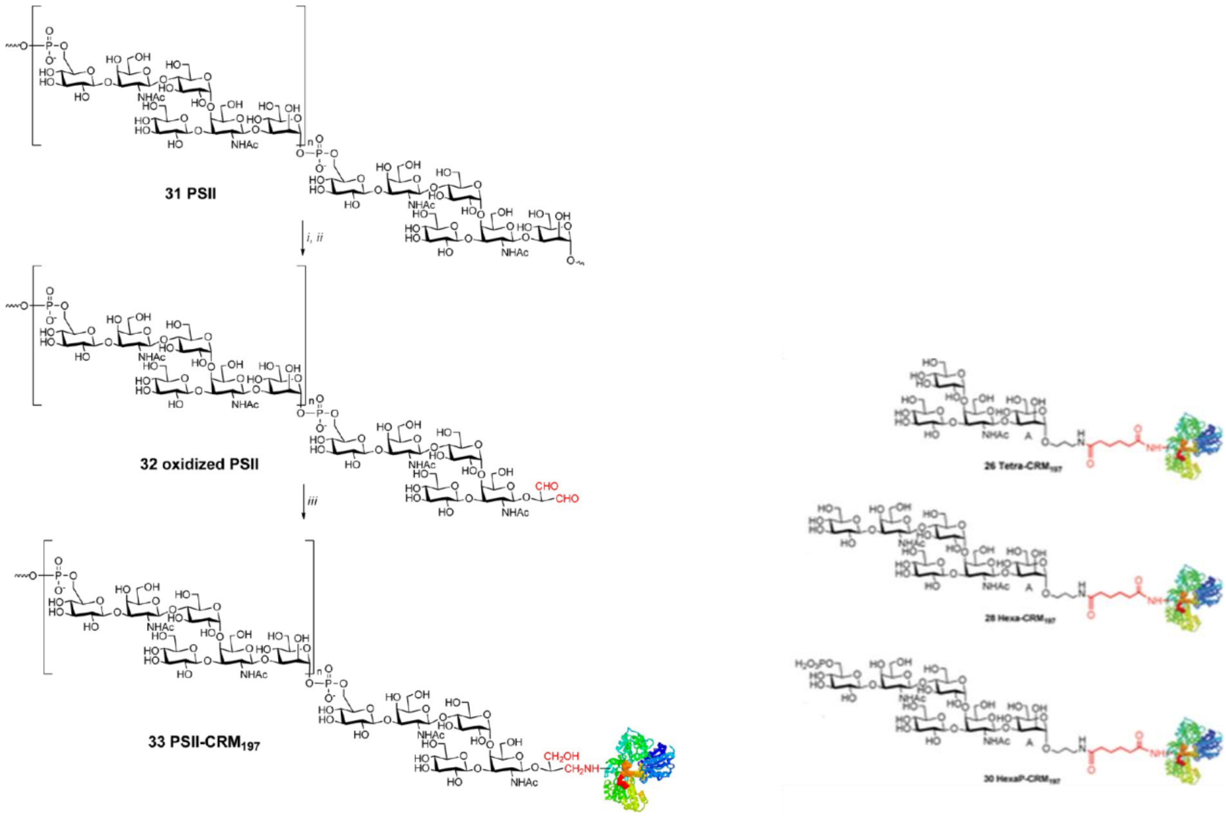

Figure 1.19. Scheme used to conjugate protein carrier to glycans tested as candidates to elicit an immune response (a) and structures of the glycan variations (b)[122]

1.6.3. Biosensors

Poly(NIPAM-co-GEMA) microgels with glucose sidechains were synthesized as potential glucose sensors by Wei *et al*. Glucose is known to bind strongly with Con A, therefore the pores contract when the protein interacts with the polymer in solution. The abundance of free glucose promoted competitive binding with Con A, which is released from the pores leading to the pores reswelling. The refractive index of the solution was lowered as the pores expand, and surface plasmon resonance was used to detect the decrease in the amount of light reflected, which was then used to quantify the amount of glucose in solution. (**Fig. 1.20**). The side chains can be modified to facilitate binding with various proteins that will competitively bind to different small molecules/toxins, allowing medical personnel to quantity the concentrations present.[123]

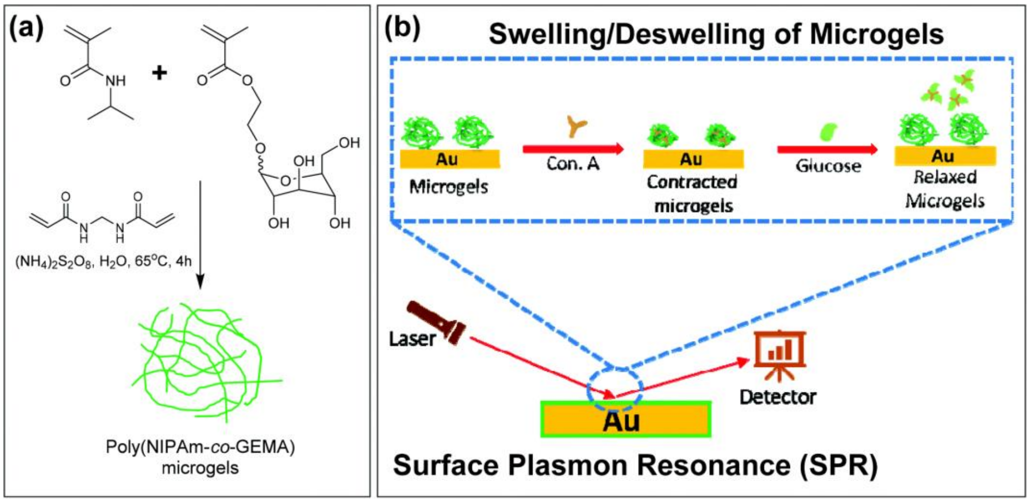

Figure 1.20. (a) Synthesis of Poly(NIPAM-co-GEMA) microgel; (b) sensing mechanism for glucose detection[82, 123]

1.6.4. Alternative Antibacterial Therapeutics

Bacterial infection begins when the pathogen adheres to the surface of the host cell. This critical step involves attachment via ligand-receptor interaction between the bacterial fimbriae and specific carbohydrates abundantly present on the surface of mammalian cells.[124] *E. coli*, a prevalent pathogenic bacterium the is known to cause serious illness in humans with as little as 10 cells,[125] uses D-mannose specific lectins (FimH) to bind to mannose receptors on the surface of host cells before invasion and infection begin.[126-130] Other bacteria that bind to mannose receptors are *L. plantarum*, *K. pneumoniae*, *S. typhi*murium and *S. cerevisiae*,[54] while *P. aeruginosa* uses LecA and LecB lectins to bind to galactose and fucose receptors, respectively.[131] Therefore, glycopolymers are vastly interesting and widely explored materials because the sidechains mimic the binding sites on host cell surfaces and can be leveraged to mitigate bacterial infections.[54, 56] The variety of synthetic methods including ATRP, RAFT and ROMP, enable polymerization of different monomeric structures to produce a variety of well-defined glycopolymers.[132, 133] Additionally, compared to glycomonomers (monosaccharides), glycopolymers provide multiple binding sites (multivalency) (**Fig. 1.21**) resulting in stronger ligand-receptor binding interactions and enhanced efficacy, known as the cluster glycoside effect.[133-136]

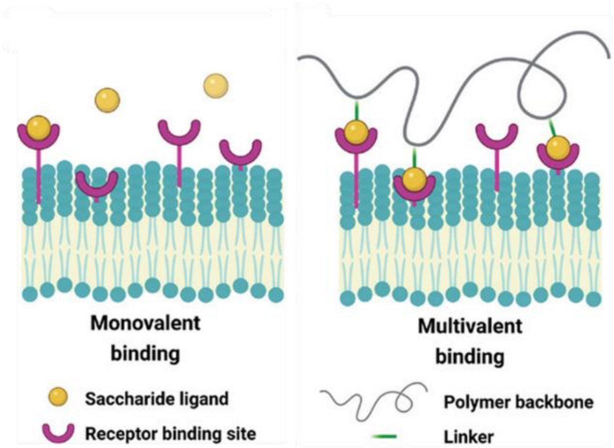

Figure 1.21. Multivalency advantage of glycopolymers vs. monosaccharides[134]

Hanheiser *et al.* synthesized linear polyglycerols with mono and di-mannoside side chains to determine the direct binding affinity to *E. coli* strain ORN178, the bacterium that causes urinary tract infections.[137] While previous binding experiments to elucidate the relevant binding interactions between bacteria and host cells have utilized pathogen extracts, this approach targeted the binding affinity with the intact bacteria. Aminopentyl functionalized α-D-mannoside and Manα-1,2-Man dimannoside were synthesized and conjugated to linear polyglycerol to produce the mono- and divalent side chains as shown in **Scheme 1.2**. The label-free microscale thermophoresis (MST) method was used to determine and compare the apparent binding constants ($K_{d,app}$) between the bacterial strain and functionalized glycopolymers, unfunctionalized linear PG as a negative control and the monosaccharide α-D-methylmannopyranoside (MeMan). The divalent-chain glycopolymer demonstrated a six-fold increase in $K_{d,app}$ for the E. coli strain that infects the urinary tract, compared to the monosaccharide, while the monovalent-chain glycopolymer exhibited a five-fold higher $K_{d,app}$, suggesting the divalent-chain glycopolymer was slightly more potent than the monovalent counterpart. The adhesion-inhibition assay results revealed that both functionalized glycopolymers successfully decreased bacterial adhesion to human colon cancer cells, with the monovalent-chain glycopolymer demonstrating a two-fold potency compared to the divalent chain glycopolymer. This synthetic approach can be adapted to incorporate alternative glycomonomers that will target other pathogens, especially larger ones.

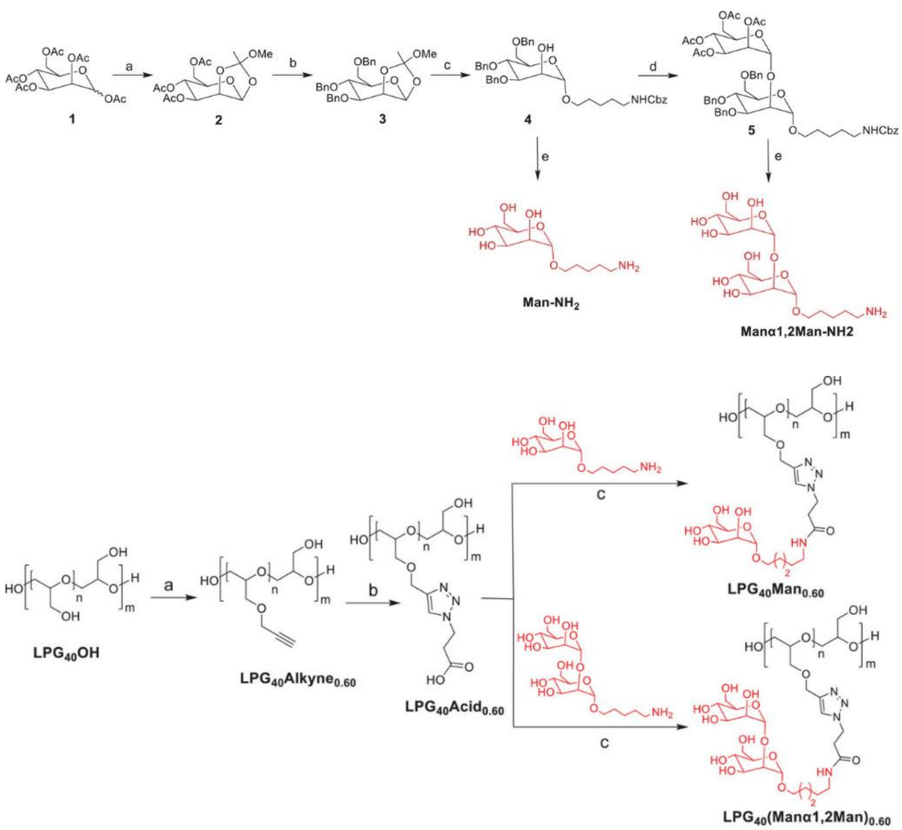

Scheme 1.2. Synthesis of mannose-functionalized glycopolymers with mono and di-valent side chains[137]

Yan *et al* synthesized n-heptyl α-D-mannose (HM)-based glycopolymers with linear and star architecture and varied side chain lengths to investigate the effect of polymer architecture on bacterial adhesion (**Fig.1.22**).[138] Adhesion assays were performed with intestinal epithelial cells and the *E. coli* strain that causes Crohn's disease. At similar degrees of polymerization and concentration, linear polymer PHMM (mannose heptyl methacrylamide) demonstrated 100X more potency than the HMM monosaccharide, while the linear polymer PEMM (mannose ethyl methacrylamide) did not inhibit bacterial adhesion. These results suggest that the number of binding sites alone did not contribute to enhanced activity, but rather the optimal spacings facilitated better ligand-receptor binding. Among the star-shaped glycopolymers, the 3-arm star PHMM demonstrated similar antiadhesion activity to the linear analogue, while potency decreased significantly with the 8-arm star PHMM. Fluorescence microscopy and differential light scattering analyses of the polymers before and after adhesion assays revealed that the increased potency of the glycopolymers compared to the monovalent ligands was attributed to induced crosslinking interactions with the live bacteria and the ability to generate aggregation among the bacterial cells, hindering some of the cells from binding to the intestinal cells. The antiadhesive capabilities of the PHMM materials demonstrate their potential as a treatment for *E. coli* related intestinal diseases.

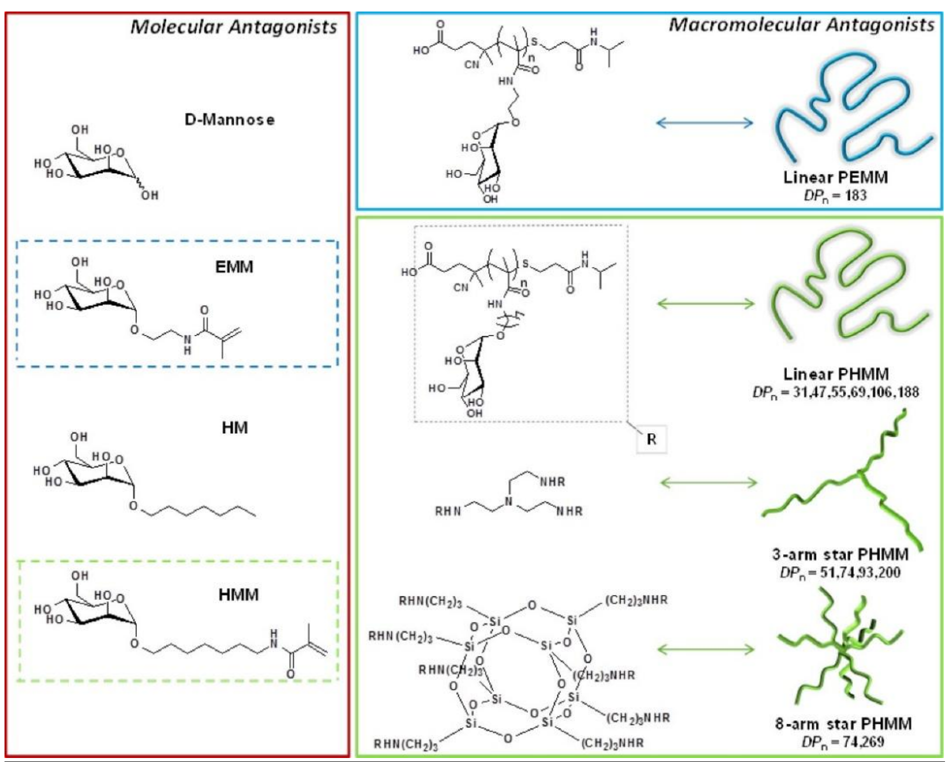

Figure 1.22. Synthetic route to linear and star glycopolymers to inhibit *E. coli* bacteria growth[138]

Polyethylene imine (PEI) has broad-spectrum antibacterial activity due to its cationic functionality[139-141] and its antibacterial activity and cytotoxicity are molecular weight and architecture dependent.[142] Liu *et al* investigated the effect of functionalizing PEI (MW=600, 1800, 10,000 Da) with mannose to enhance the antibacterial properties and mitigate its cytotoxic effects (**Fig. 1.23**). Copolymer particles (CPs) were synthesized via nucleophilic addition between the primary amine and aldehyde to generate Man-PEI CPs. The antibacterial performance of each molecular weight PEI was improved 10, 4 and 1.4-fold, respectively, when the corresponding Man-PEI CP, owing to the preferential binding between E. coli's Fim H receptor and mannose. At 600 Da, the inhibitory concentration for Man-PEI CP was 10 μg/mL while that of PEI was 200 μg/mL. Furthermore, cytotoxicity was reduced as cell viability remained at approximately 75% after 24 hours incubation time, even when the Man-PEI CP concentration was increased to 500 μg/mL.[64]

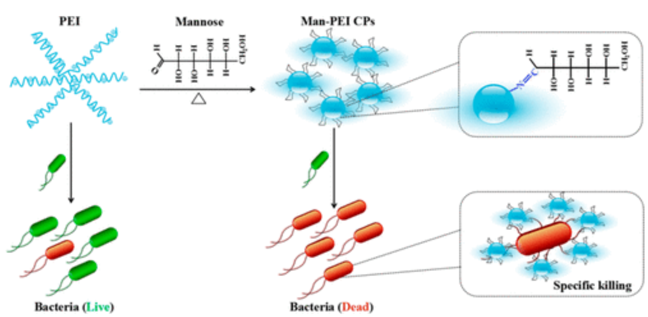

Figure 1.23. Illustration of PEI and Man-PEI CPs antibacterial strategy[64]

In our group, a series of glycopolymers was investigated for antibacterial activity in the absence of traditional antibacterial moieties (antibiotics, cationic groups) to determine their potential as antimicrobial agents. Hall, Wadsworth, and coworkers synthesized norbornene glycomonomers containing pendant β-D-galactose (Gal), β-D-glucose (Glc), β-D-*N*-acetylglucose (GlcNAc) or α-D-mannose (Man), then used ROMP to generate polymers with four degrees of polymerization (DP = 50, 100, 250 and 500) (**Scheme 1.3**). The antibacterial activity of each polymer series was compared to that of the corresponding monosaccharide.

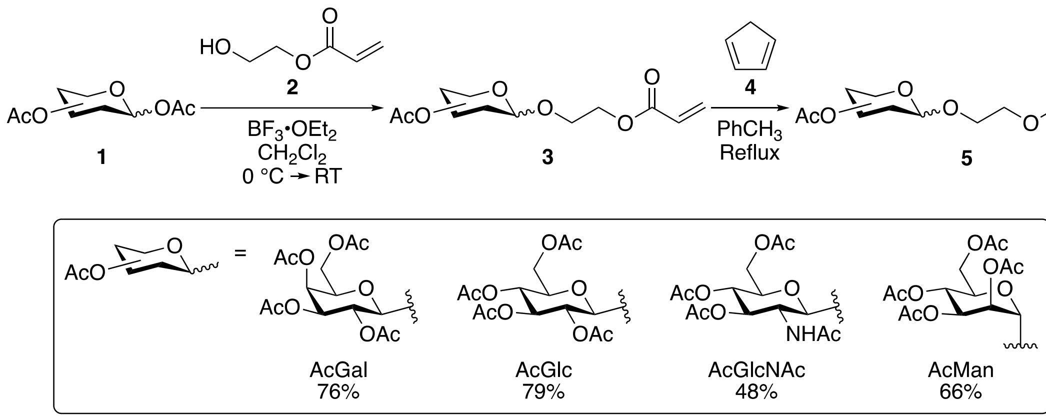

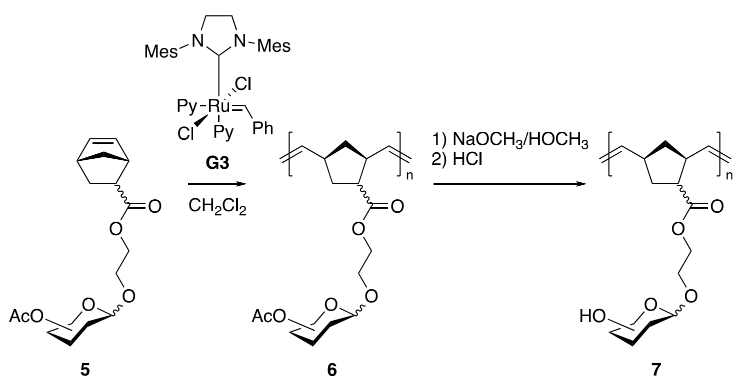

Scheme 1.3. Synthetic route to sugar-containing polynorbornenes; overall yields shown below each sugar-containing monomer[143]

Disk diffusion assays revealed glycopolymers containing pendant mannose only generated zones of inhibition against *E. coli*. Their selectivity towards the Gram-negative bacteria signified that the outer membrane may be the targeted feature to inhibit growth. The activity of the four series of glycopolymers was determined via broth dilution assays along with 600-kDa polyethyleneimine as the positive control. The mannose-pendant glycopolymers displayed the greatest potency, with the higher DP polymers (250 and 500) showing a four-fold greater activity than the lower DP polymers (50 and 100) and the mannose monosaccharide. These results showed a molecular weight dependence on the mechanism of action and that the activity was enhanced by the polymer structure. Their ability to inhibit bacterial growth in the absence of specific antimicrobial functionalities suggests that these glycopolymers have inherent antibacterial properties. Hemolysis assays, however, revealed that the higher DP polymers (the best *E. coli* growth inhibitors), caused greater lysis to red blood cells than the lower DP polymers, indicating that these glycopolymers were not selective for bacterial cells.

1.7. Conclusion

The use of polymeric sequestrants to adsorb chemotherapy drugs has emerged as a promising strategy to reduce systemic toxicity and enhance the efficacy of cancer treatments. A wide range of materials, from templated resins to coated absorbers, has been explored for their ability to selectively bind chemotherapy agents such as Dox. The key factor influencing sequestration is the binding affinity between the polymer and the targeted drug. The approaches covered in this review represented design concepts that targeted the known drug characteristics to maximize binding interactions and will influence the development of next-generation materials.

Polymer sequestrants also play a vital role in mitigating bacterial infections with the development of glycopolymers as promising replacements for traditional antibiotics. By mimicking the glycan structures recognized by bacterial lectins, these polymers can inhibit pathogen adhesion and colonization and possibly overcome the antibiotic-resistance mechanisms employed by many bacterial strains. As glycopolymer research continues to advance, future efforts will focus on designing materials with improved biocompatibility and broad-spectrum antibacterial activity, along with the development of glycopolymer-based materials for both antibacterial and anticancer vaccines. As with any other field, an interdisciplinary approach is required to ensure that the materials developed are viable solutions to improve overall patient care.

1.8. References

(1) Archer, W. R.; Hall, B. A.; Thompson, T. N.; Wadsworth, O. J.; Schulz, M. D. Polymer sequestrants for biological and environmental applications. *Polym. Int.* **2019**, *68* (7), 1220-1237.

(2) Marican, A.; Durán-Lara, E. F. A review on pesticide removal through different processes. *Environ. Sci. Pollut. Res.* **2018**, *25*, 2051-2064.

(3) Husnain, S. M.; Um, W.; Chang, Y.-S. Magnetite-based adsorbents for sequestration of radionuclides: a review. *RSC Adv.* **2018**, *8* (5), 2521-2540.

(4) Diallo, M. S.; Kotte, M. R.; Cho, M. Mining critical metals and elements from seawater: opportunities and challenges. *Environ. Sci. Technol.* **2015**, *49* (16), 9390-9399.

(5) Bär, A.; Til, H.; Timonen, M. Subchronic oral toxicity study with regular and enzymatically depolymerized sodium carboxymethylcellulose in rats. *Food Chem. Toxicol.* **1995**, *33* (11), 909-917.

(6) Chen, X. C.; Oh, H. J.; Yu, J. F.; Yang, J. K.; Petzetakis, N.; Patel, A. S.; Hetts, S. W.; Balsara, N. P. Block copolymer membranes for efficient capture of a chemotherapy drug. *ACS Macro Lett.* **2016**, *5* (8), 936-941.

(7) Su, G. A.; Wadsworth, O. J.; Muller, H. S.; Archer, W. R.; Hetts, S. W.; Schulz, M. D. Polymer–nucleobase composites for chemotherapy drug capture. *J. Mater. Chem. B* **2023**, *11* (35), 8449-8455.

(8) Blumenfeld, C. M.; Schulz, M. D.; Aboian, M. S.; Wilson, M. W.; Moore, T.; Hetts, S. W.; Grubbs, R. H. Drug capture materials based on genomic DNA-functionalized magnetic nanoparticles. *Nat. Commun.* **2018**, *9* (1), 1-7.

(9) Oh, H. J.; Aboian, M. S.; Yi, M. Y.; Maslyn, J. A.; Loo, W. S.; Jiang, X.; Parkinson, D. Y.; Wilson, M. W.; Moore, T.; Yee, C. R. 3D printed absorber for capturing chemotherapy drugs before they spread through the body. *ACS Cent. Sci.* **2019**, *5* (3), 419-427.

(10) Prasad, P.; Gupta, A.; Sasmal, P. K. Aggregation-induced emission active metal complexes: A promising strategy to tackle bacterial infections. *Chem. Commun.* **2021**, *57* (2), 174-186.

(11) Engler, A. C.; Wiradharma, N.; Ong, Z. Y.; Coady, D. J.; Hedrick, J. L.; Yang, Y.-Y. Emerging trends in macromolecular antimicrobials to fight multi-drug-resistant infections. *Nano Today* **2012**, *7* (3), 201-222.

(12) Fischbach, M. A.; Walsh, C. T. Antibiotics for emerging pathogens. *Science* **2009**, *325* (5944), 1089-1093.

(13) Dickens, E.; Ahmed, S. Principles of cancer treatment by chemotherapy. *Surgery (Oxford)* **2018**, *36* (3), 134-138.

(14) Collins, K.; Jacks, T.; Pavletich, N. P. The cell cycle and cancer. *Proc. Natl. Acad. Sci. U. S. A.* **1997**, *94* (7), 2776-2778.

(15) Chhikara, B. S.; Parang, K. Global Cancer Statistics 2022: the trends projection analysis. *Chem. Biol. Lett.* **2023**, *10* (1), 451-451.

(16) Hu, Q.; Sun, W.; Wang, C.; Gu, Z. Recent advances of cocktail chemotherapy by combination drug delivery systems. *Adv. Drug Delivery Rev.* **2016**, *98*, 19-34.

(17) Lundqvist, E. Å.; Fujiwara, K.; Seoud, M. Principles of chemotherapy. *Int. J. Gynecol. Obstet.* **2015**, *131*, S146-S149.

(18) Malhotra, V.; Perry, M. C. Classical chemotherapy: mechanisms, toxicities and the therapeutc window. *Cancer Biol. Ther.* **2003**, *2* (sup1), 1-3.

(19) Shepherd, G. M. Hypersensitivity reactions to chemotherapeutic drugs. *Clinical reviews in allergy & immunology* **2003**, *24*, 253-262.

(20) Tiwari, M. Antimetabolites: established cancer therapy. *J. Cancer Res. Ther.* **2012**, *8* (4).

(21) Peters, G. J. Novel developments in the use of antimetabolites. *Nucleosides, Nucleotides and Nucleic Acids* **2014**, *33* (4-6), 358-374.

(22) Box, V. G. The intercalation of DNA double helices with doxorubicin and nagalomycin. *J. Mol. Graph Mod.* **2007**, *26* (1), 14-19.

(23) Hilmer, S. N.; Cogger, V. C.; Muller, M.; Le Couteur, D. G. The hepatic pharmacokinetics of doxorubicin and liposomal doxorubicin. *Drug Metab. Dispos.* **2004**, *32* (8), 794-799.

(24) Ashley, N.; Poulton, J. Mitochondrial DNA is a direct target of anti-cancer anthracycline drugs. *Biophys. Res. Commun.* **2009**, *378* (3), 450-455.

(25) Binaschi, M.; Zunino, F.; Capranico, G. Mechanism of action of DNA topoisomerase inhibitors. *Stem Cells* **1995**, *13* (4), 369-379.

(26) Verrills, N.; Kavallaris, M. Improving the targeting of tubulin-binding agents: lessons from drug resistance studies. *Curr. Pharm. Des.* **2005**, *11* (13), 1719-1733.

(27) Dumontet, C. Mechanisms of action and resistance to tubulin-binding agents. *Expert Opin. Invest. Drugs* **2000**, *9* (4), 779-788.

(28) Carvalho, C.; Santos, R. X.; Cardoso, S.; Correia, S.; Oliveira, P. J.; Santos, M. S.; Moreira, P. I. Doxorubicin: the good, the bad and the ugly effect. *Curr. Med. Chem.* **2009**, *16* (25), 3267-3285.

(29) Pugazhendhi, A.; Edison, T. N. J. I.; Velmurugan, B. K.; Jacob, J. A.; Karuppusamy, I. Toxicity of Doxorubicin (Dox) to different experimental organ systems. *Life Sci.* **2018**, *200*, 26-30.

(30) Injac, R.; Strukelj, B. Recent advances in protection against doxorubicin-induced toxicity. *Technol. Cancer Res. Treat.* **2008**, *7* (6), 497-516.

(31) Wáng, Y.-X. J.; De Baere, T.; Idée, J.-M.; Ballet, S. Transcatheter embolization therapy in liver cancer: an update of clinical evidences. *Chin. J. Cancer Res.* **2015**, *27* (2), 96-121.

(32) Patel, A. S.; Saeed, M.; Yee, E. J.; Yang, J.; Lam, G. J.; Losey, A. D.; Lillaney, P. V.; Thorne, B.; Chin, A. K.; Malik, S. Development and validation of endovascular chemotherapy filter device for removing high-dose doxorubicin: preclinical study. *J. Med. Dev.* **2014**, *8* (4), 041008-041001 - 041008-041008.

(33) Sun, V. C.-Y.; Sarna, L. Symptom management in hepatocellular carcinoma. *Clin. J. Onco.l Nurs.* **2008**, *12* (5), 759-766.

(34) Altekruse, S. F.; McGlynn, K. A.; Reichman, M. E. Hepatocellular carcinoma incidence, mortality, and survival trends in the United States from 1975 to 2005. *J. Clin. Oncol.* **2009**, *27* (9), 1485-1491.

(35) Rammohan, A.; Sathyanesan, J.; Ramaswami, S.; Lakshmanan, A.; Senthil-Kumar, P.; Srinivasan, U. P.; Ramasamy, R.; Ravichandran, P. Embolization of liver tumors: Past, present and future. *World J. Radiol.* **2012**, *4* (9), 405.

(36) Savic, L. J.; Chen, E.; Nezami, N.; Murali, N.; Hamm, C. A.; Wang, C.; Lin, M.; Schlachter, T.; Hong, K.; Georgiades, C. Conventional vs. Drug-Eluting Beads Transarterial Chemoembolization for Unresectable Hepatocellular Carcinoma—A Propensity Score Weighted Comparison of Efficacy and Safety. *Cancers* **2022**, *14* (23), 5847.

(37) Sieghart, W.; Hucke, F.; Peck-Radosavljevic, M. Transarterial chemoembolization: modalities, indication, and patient selection. *J. Hepatol.* **2015**, *62* (5), 1187-1195.

(38) Anwanwan, D.; Singh, S. K.; Singh, S.; Saikam, V.; Singh, R. Challenges in liver cancer and possible treatment approaches. *Biochim Biophys Acta Rev Cancer* **2020**, *1873* (1), 188314.

(39) J Wang, Y.-X. Transcatheter embolization therapy in liver cancer. *Recent Pat. Med. Img.* **2012**, *2* (2), 150-162.

(40) Yee, D. W.; Hetts, S. W.; Greer, J. R. 3D-Printed Drug Capture Materials Based on Genomic DNA Coatings. *ACS Appl. Mater. Interfaces* **2021**, *13* (35), 41424-41434.

(41) Roche, A.; Girish, B. V.; de Baère, T.; Baudin, E.; Boige, V.; Elias, D.; Lasser, P.; Schlumberger, M.; Ducreux, M. Trans-catheter arterial chemoembolization as first-line treatment for hepatic metastases from endocrine tumors. *Eur. Radiol.* **2003**, *13*, 136-140.

(42) Temperini, C.; Messori, L.; Orioli, P.; Bugno, C. D.; Animati, F.; Ughetto, G. The crystal structure of the complex between a disaccharide anthracycline and the DNA hexamer d (CGATCG) reveals two different binding sites involving two DNA duplexes. *Nucleic Acids Res.* **2003**, *31* (5), 1464-1469.

(43) Gnapareddy, B.; Reddy Dugasani, S.; Ha, T.; Paulson, B.; Hwang, T.; Kim, T.; Hoon Kim, J.; Oh, K.; Park, S. H. Chemical and physical characteristics of doxorubicin hydrochloride drug-doped salmon DNA thin films. *Scientific reports* **2015**, *5* (1), 1-9.

(44) Aboian, M. S.; Yu, J. F.; Gautam, A.; Sze, C.-H.; Yang, J. K.; Chan, J.; Lillaney, P. V.; Jordan, C. D.; Oh, H.-J.; Wilson, D. M. In vitro clearance of doxorubicin with a DNA-based filtration device designed for intravascular use with intra-arterial chemotherapy. *Biomed. Microdevices* **2016**, *18*, 1-9.

(45) Krishnamoorthy, S.; Grubbs, R. H. Aldehyde-Functionalized Magnetic Particles to Capture Off-Target Chemotherapeutic Agents. *ACS Omega* **2020**, *5* (45), 29121-29126.

(46) Hutchings, M. I.; Truman, A. W.; Wilkinson, B. Antibiotics: past, present and future. *Curr. Opin. Microbiol.* **2019**, *51*, 72-80.

(47) Ikuta, K. S.; Swetschinski, L. R.; Aguilar, G. R.; Sharara, F.; Mestrovic, T.; Gray, A. P.; Weaver, N. D.; Wool, E. E.; Han, C.; Hayoon, A. G. Global mortality associated with 33 bacterial pathogens in 2019: a systematic analysis for the Global Burden of Disease Study 2019. *Lancet* **2022**, *400* (10369), 2221-2248.

(48) van Elsland, D.; Neefjes, J. Bacterial infections and cancer. *EMBO reports* **2018**, *19* (11), e46632.

(49) Mukherjee, S.; Ghosh, R. N.; Maxfield, F. R. Endocytosis. *Physiol. Rev.* **1997**, *77* (3), 759-803.

(50) Canton, I.; Battaglia, G. Endocytosis at the nanoscale. *Chem. Soc. Rev.* **2012**, *41* (7), 2718-2739.

(51) Gulbins, E.; Lang, F. Pathogens, Host-Cell Invasion and Disease: Invading pathogens can co-opt even the cells of the immune system. New anti-infective drugs may arise from an understanding of this chemical warfare. *Am. Sci.* **2001**, *89* (5), 406-413.

(52) Srinivasan, R.; Santhakumari, S.; Poonguzhali, P.; Geetha, M.; Dyavaiah, M.; Xiangmin, L. Bacterial biofilm inhibition: A focused review on recent therapeutic strategies for combating the biofilm mediated infections. *Front. Microbiol.* **2021**, *12*, 676458.

(53) Doron, S.; Gorbach, S. L. Bacterial infections: overview. *International Encyclopedia of Public Health* **2008**, 273.

(54) Gerling-Driessen, U. I.; Hoffmann, M.; Schmidt, S.; Snyder, N. L.; Hartmann, L. Glycopolymers against pathogen infection. *Chem. Soc. Rev.* **2023**, *52*, 2617-2642.

(55) Cook, M. A.; Wright, G. D. The past, present, and future of antibiotics. *Sci. Transl. Med.* **2022**, *14* (657), eabo7793.

(56) Mei, R.; Heng, X.; Liu, X.; Chen, G. Glycopolymers for antibacterial and antiviral applications. *Molecules* **2023**, *28* (3), 985.

(57) Hughes, D.; Karlén, A. Discovery and preclinical development of new antibiotics. *Upsala J. Med. Sci.* **2014**, *119* (2), 162-169.

(58) Van Bambeke, F.; Van Laethem, Y.; Courvalin, P.; Tulkens, P. M. Glycopeptide antibiotics: from conventional molecules to new derivatives. *Drugs* **2004**, *64*, 913-936.

(59) Papp-Wallace, K. M.; Endimiani, A.; Taracila, M. A.; Bonomo, R. A. Carbapenems: past, present, and future. *Antimicrob. Agents Chemother.* **2011**, *55* (11), 4943-4960.

(60) Vannuffel, P.; Cocito, C. Mechanism of action of streptogramins and macrolides. *Drugs* **1996**, *51*, 20-30.

(61) Krause, K. M.; Serio, A. W.; Kane, T. R.; Connolly, L. E. Aminoglycosides: an overview. *Cold Spring Harbor Perspect. Med.* **2016**, *6* (6).

(62) Drlica, K.; Malik, M. Fluoroquinolones: action and resistance. *Curr. Trends Med. Chem.* **2003**, *3* (3), 249-282.

(63) Wagenlehner, F.; Lorenz, H.; Ewald, O.; Gerke, P. Why d-Mannose may be as efficient as antibiotics in the treatment of acute uncomplicated lower urinary tract infections—preliminary considerations and conclusions from a non-interventional study. *Antibiotics* **2022**, *11* (3), 314.

(64) Liu, M.; Li, J.; Li, B. Mannose-modificated polyethylenimine: a specific and effective antibacterial agent against Escherichia coli. *Langmuir* **2018**, *34* (4), 1574-1580.

(65) Aslam, B.; Wang, W.; Arshad, M. I.; Khurshid, M.; Muzammil, S.; Rasool, M. H.; Nisar, M. A.; Alvi, R. F.; Aslam, M. A.; Qamar, M. U. Antibiotic resistance: a rundown of a global crisis. *Infect. Drug Resist.* **2018**, 1645-1658.

(66) Larsson, D. J.; Flach, C.-F. Antibiotic resistance in the environment. *Nat. Rev. Microbiol.* **2022**, *20* (5), 257-269.

(67) Zaman, S. B.; Hussain, M. A.; Nye, R.; Mehta, V.; Mamun, K. T.; Hossain, N. A review on antibiotic resistance: alarm bells are ringing. *Cureus* **2017**, *9* (6).

(68) Kadri, S. S. Key takeaways from the US CDC's 2019 antibiotic resistance threats report for frontline providers. *Crit. Care Med.* **2020**, *48* (7), 939-945.

(69) Si, Z.; Zheng, W.; Prananty, D.; Li, J.; Koh, C. H.; Kang, E.-T.; Pethe, K.; Chan-Park, M. B. Polymers as advanced antibacterial and antibiofilm agents for direct and combination therapies. *Chem. Sci.* **2022**, *13* (2), 345-364.

(70) Kamaruzzaman, N. F. T., L.P.; Hamdan, R.H.; Choong, S.S.; Wong, W.K.; Gibson, A.J.; Chivu, A.; Pina, M.F. Antimicrobial Polymers: The Potential Replacement of Existing Antibiotics? *Int. J. Mol. Sci.* **2019**, *20*, 2747-2777.

(71) Jones, M. W.; Otten, L.; Richards, S.-J.; Lowery, R.; Phillips, D. J.; Haddleton, D. M.; Gibson, M. I. Glycopolymers with secondary binding motifs mimic glycan branching and display bacterial lectin selectivity in addition to affinity. *Chem. Sci.* **2014**, *5* (4), 1611-1616.

(72) Saxena, S.; Kandasubramanian, B. Glycopolymers in molecular recognition, biomimicking and glycotechnology: a review. *Int. J. Polym. Mater. Polym. Biomater.* **2022**, *71* (10), 756-776.

(73) Bhattacharya, K.; Kalita, U.; Singha, N. K. Tailor-made glycopolymers via reversible deactivation radical polymerization: design, properties and applications. *Polym. Chem.* **2022**, *13* (11), 1458-1483.

(74) Zhang, Y.; Chan, J. W.; Moretti, A.; Uhrich, K. E. Designing polymers with sugar-based advantages for bioactive delivery applications. *J. Controlled Release* **2015**, *219*, 355-368.

(75) Stenzel, M. H. Glycopolymers for drug delivery: opportunities and challenges. *Macromolecules* **2022**, *55* (12), 4867-4890.

(76) Ladmiral, V.; Melia, E.; Haddleton, D. M. Synthetic glycopolymers: an overview. *Eur. Polym. J.* **2004**, *40* (3), 431-449.

(77) Ting, S. S.; Min, E. H.; Escale, P.; Save, M.; Billon, L.; Stenzel, M. H. Lectin recognizable biomaterials synthesized via nitroxide-mediated polymerization of a methacryloyl galactose monomer. *Macromolecules* **2009**, *42* (24), 9422-9434.

(78) Bhatia, S.; Mohr, A.; Mathur, D.; Parmar, V. S.; Haag, R.; Prasad, A. K. Biocatalytic route to sugar-PEG-based polymers for drug delivery applications. *Biomacromolecules* **2011**, *12* (10), 3487-3498.

(79) Ahmed, M.; Narain, R. The effect of polymer architecture, composition, and molecular weight on the properties of glycopolymer-based non-viral gene delivery systems. *Biomaterials* **2011**, *32* (22), 5279-5290.

(80) Pohl, N. L.; Kiessling, L. L. Scope of multivalent ligand function: lactose-bearing neoglycopolymers by ring-opening metathesis polymerization. *Synthesis* **1999**, *1999* (S 01), 1515-1519.

(81) Strong, L. E.; Kiessling, L. L. A general synthetic route to defined, biologically active multivalent arrays. *J. Am. Chem. Soc.* **1999**, *121* (26), 6193-6196.

(82) Pramudya, I.; Chung, H. Recent progress of glycopolymer synthesis for biomedical applications. *Biomater. Sci.* **2019**, *7* (12), 4848-4872.

(83) Miura, Y. Design and synthesis of well-defined glycopolymers for the control of biological functionalities. *Polym. J.* **2012**, *44* (7), 679-689.

(84) Miura, Y. Synthesis and biological application of glycopolymers. *J. Polym. Sci., Part A: Polym. Chem.* **2007**, *45* (22), 5031-5036.

(85) Sun, X.-L.; Grande, D.; Baskaran, S.; Hanson, S. R.; Chaikof, E. L. Glycosaminoglycan mimetic biomaterials. 4. Synthesis of sulfated lactose-based glycopolymers that exhibit anticoagulant activity. *Biomacromolecules* **2002**, *3* (5), 1065-1070.

(86) Kundie, F.; Azhari, C. H.; Muchtar, A.; Ahmad, Z. A. Effects of filler size on the mechanical properties of polymer-filled dental composites: A review of recent developments. *J. Phys. Sci.* **2018**, *29* (1), 141-165.

(87) Parry, A. L.; Clemson, N. A.; Ellis, J.; Bernhard, S. S.; Davis, B. G.; Cameron, N. R. 'Multicopy multivalent'glycopolymer-stabilized gold nanoparticles as potential synthetic cancer vaccines. *J. Am. Chem. Soc.* **2013**, *135* (25), 9362-9365.

(88) Huang, Y.-L.; Wu, C.-Y. Carbohydrate-based vaccines: challenges and opportunities. *Expert Rev. Vaccines* **2010**, *9* (11), 1257-1274.

(89) Milošević, N.; Rütter, M.; Ventura, Y.; Kezerle, Y.; Feinshtein, V.; David, A. Attenuation of neutrophil-mediated liver injury in mice by drug-free E-selectin binding polymer. *J. Controlled Release* **2020**, *319*, 475-486.

(90) Sun, P.; Wang, G.; Hou, H.; Yuan, P.; Deng, W.; Wang, C.; Lu, X.; Fan, Q.; Huang, W. A water-soluble phosphorescent conjugated polymer brush for tumor-targeted photodynamic therapy. *Polym. Chem.* **2017**, *8* (38), 5836-5844.

(91) Tengdelius, M.; Lee, C.-J.; Grenegård, M.; Griffith, M.; Påhlsson, P.; Konradsson, P. Synthesis and biological evaluation of fucoidan-mimetic glycopolymers through cyanoxyl-mediated free-radical polymerization. *Biomacromolecules* **2014**, *15* (7), 2359-2368.
(92) Chen, G. The past ten years of carbohydrate polymers in ACS Macro Letters. ACS Publications: 2021; Vol. 10, pp 1145-1150.
(93) Becer, C. R.; Gibson, M. I.; Geng, J.; Ilyas, R.; Wallis, R.; Mitchell, D. A.; Haddleton, D. M. High-affinity glycopolymer binding to human DC-SIGN and disruption of DC-SIGN interactions with HIV envelope glycoprotein. *J. Am. Chem. Soc.* **2010**, *132* (43), 15130-15132.
(94) Deng, C.; Li, F.; Hackett, J. M.; Chaudhry, S. H.; Toll, F. N.; Toye, B.; Hodge, W.; Griffith, M. Collagen and glycopolymer based hydrogel for potential corneal application. *Acta Biomater.* **2010**, *6* (1), 187-194.
(95) Igde, S.; Röblitz, S.; Müller, A.; Kolbe, K.; Boden, S.; Fessele, C.; Lindhorst, T. K.; Weber, M.; Hartmann, L. Linear precision glycomacromolecules with varying interligand spacing and linker functionalities binding to Concanavalin A and the bacterial lectin FimH. *Macromol. Biosci.* **2017**, *17* (12), 1700198.
(96) Tibbitt, M. W.; Dahlman, J. E.; Langer, R. Emerging frontiers in drug delivery. *J. Am. Chem. Soc.* **2016**, *138* (3), 704-717.
(97) Englert, C.; Brendel, J. C.; Majdanski, T. C.; Yildirim, T.; Schubert, S.; Gottschaldt, M.; Windhab, N.; Schubert, U. S. Pharmapolymers in the 21st century: Synthetic polymers in drug delivery applications. *Prog. Polym. Sci.* **2018**, *87*, 107-164.
(98) Miao, T.; Wang, J.; Zeng, Y.; Liu, G.; Chen, X. Polysaccharide-based controlled release systems for therapeutics delivery and tissue engineering: from bench to bedside. *Adv. Sci.* **2018**, *5* (4), 1700513.

(99) Hariyadi, D. M.; Islam, N. Current status of alginate in drug delivery. *Adv. Pharmacol. Pharm. Sci.* **2020**, *2020*.

(100) Cheung, R. C. F.; Ng, T. B.; Wong, J. H.; Chan, W. Y. Chitosan: an update on potential biomedical and pharmaceutical applications. *Mar. Drugs* **2015**, *13* (8), 5156-5186.

(101) Wu, D.; Zhu, L.; Li, Y.; Zhang, X.; Xu, S.; Yang, G.; Delair, T. Chitosan-based colloidal polyelectrolyte complexes for drug delivery: a review. *Carbohydr. Polym.* **2020**, *238*, 116126.

(102) Tiwari, P.; Panthari, P.; Katare, D. P.; Kharkwal, H. Natural polymers in drug delivery. *World J. Pharm. Pharm. Sci* **2014**, *3* (9), 1395-1409.

(103) Huang, G.; Huang, H. Application of hyaluronic acid as carriers in drug delivery. *Drug delivery* **2018**, *25* (1), 766-772.

(104) Necas, J.; Bartosikova, L.; Brauner, P.; Kolar, J. Hyaluronic acid (hyaluronan): a review. *Vet. Med.* **2008**, *53* (8), 397-411.

(105) Ciolacu, D. E.; Nicu, R.; Ciolacu, F. Cellulose-based hydrogels as sustained drug-delivery systems. *Materials* **2020**, *13* (22), 5270.

(106) Sannino, A.; Demitri, C.; Madaghiele, M. Biodegradable cellulose-based hydrogels: design and applications. *Materials* **2009**, *2* (2), 353-373.

(107) Mohammadi, S.; Jabbari, F.; Babaeipour, V. Bacterial cellulose-based composites as vehicles for dermal and transdermal drug delivery: a review. *Int. J. Biol. Macromol.* **2023**, *242*, 124955.

(108) Funasaka, T.; Raz, A.; Nangia-Makker, P. Galectin-3 in angiogenesis and metastasis. *Glycobiology* **2014**, *24* (10), 886-891.

(109) Pearson, S.; Vitucci, D.; Khine, Y. Y.; Dag, A.; Lu, H.; Save, M.; Billon, L.; Stenzel, M. H. Light-responsive azobenzene-based glycopolymer micelles for targeted drug delivery to melanoma cells. *Eur. Polym. J.* **2015**, *69*, 616-627.

(110) Dag, A.; Lu, H.; Stenzel, M. Controlling the morphology of glyco-nanoparticles in water using block copolymer mixtures: the effect on cellular uptake. *Polym. Chem.* **2015**, *6* (45), 7812-7820.

(111) Levit, M.; Zashikhina, N.; Vdovchenko, A.; Dobrodumov, A.; Zakharova, N.; Kashina, A.; Rühl, E.; Lavrentieva, A.; Scheper, T.; Tennikova, T. Bio-inspired amphiphilic block-copolymers based on synthetic glycopolymer and poly (amino acid) as potential drug delivery systems. *Polymers* **2020**, *12* (1), 183.

(112) Mettu, R.; Chen, C.-Y.; Wu, C.-Y. Synthetic carbohydrate-based vaccines: challenges and opportunities. *J. Biomed. Sci.* **2020**, *27*, 1-22.

(113) Costantino, P.; Rappuoli, R.; Berti, F. The design of semi-synthetic and synthetic glycoconjugate vaccines. *Expert Opin. Drug Discovery* **2011**, *6* (10), 1045-1066.

(114) Jones, C. Vaccines based on the cell surface carbohydrates of pathogenic bacteria. *An. Acad. Bras. Cienc.* **2005**, *77*, 293-324.

(115) Picco, G.; Julien, S.; Brockhausen, I.; Beatson, R.; Antonopoulos, A.; Haslam, S.; Mandel, U.; Dell, A.; Pinder, S.; Taylor-Papadimitriou, J. Over-expression of ST3Gal-I promotes mammary tumorigenesis. *Glycobiology* **2010**, *20* (10), 1241-1250.

(116) Buskas, T.; Ingale, S.; Boons, G. J. Towards a fully synthetic carbohydrate-based anticancer vaccine: synthesis and immunological evaluation of a lipidated glycopeptide containing the tumor-associated Tn antigen. *Angew. Chem.* **2005**, *117* (37), 6139-6142.

(117) Dziadek, S.; Hobel, A.; Schmitt, E.; Kunz, H. A fully synthetic vaccine consisting of a tumor-associated glycopeptide antigen and a T-cell epitope for the induction of a highly specific humoral immune response. *Angew. Chem.* **2005**, *44* (46), 7630-7635.

(118) Vichier-Guerre, S.; Lo-Man, R.; Bay, S.; Deriaud, E.; Nakada, H.; Leclerc, C.; Cantacuzene, D. Short synthetic glycopeptides successfully induce antibody responses to carcinoma-associated Tn antigen. *J. Pept. Res.* **2000**, *55* (2), 173-180.

(119) Hoffmann-Röder, A.; Kaiser, A.; Wagner, S.; Gaidzik, N.; Kowalczyk, D.; Westerlind, U.; Gerlitzki, B.; Schmitt, E.; Kunz, H. Synthetic antitumor vaccines from tetanus toxoid conjugates of MUC1 glycopeptides with the Thomsen–Friedenreich antigen and a fluorine-substituted analogue. *Angew. Chem.* **2010**, *49* (45), 8498-8503.

(120) Riley, T.; Lyras, D.; Douce, G. Status of vaccine research and development for Clostridium difficile. *Vaccine* **2019**, *37* (50), 7300-7306.

(121) Lessa, F. C.; Mu, Y.; Bamberg, W. M.; Beldavs, Z. G.; Dumyati, G. K.; Dunn, J. R.; Farley, M. M.; Holzbauer, S. M.; Meek, J. I.; Phipps, E. C. Burden of Clostridium difficile infection in the United States. *N. Engl. J. Med.* **2015**, *372* (9), 825-834.

(122) Adamo, R.; Romano, M. R.; Berti, F.; Leuzzi, R.; Tontini, M.; Danieli, E.; Cappelletti, E.; Cakici, O. S.; Swennen, E.; Pinto, V. Phosphorylation of the synthetic hexasaccharide repeating unit is essential for the induction of antibodies to Clostridium difficile PSII cell wall polysaccharide. *ACS chemical biology* **2012**, *7* (8), 1420-1428.

(123) Wei, M.; Li, X.; Serpe, M. J. Stimuli-responsive microgel-based surface plasmon resonance transducer for glucose detection using a competitive assay with concanavalin A. *ACS Appl. Polym. Mater.* **2019**, *1* (3), 519-525.

(124) Poole, J.; Day, C. J.; von Itzstein, M.; Paton, J. C.; Jennings, M. P. Glycointeractions in bacterial pathogenesis. *Nat. Rev. Microbiol.* **2018**, *16* (7), 440-452.

(125) Deisingh, A.; Thompson, M. Strategies for the detection of Escherichia coli O157: H7 in foods. *J. Appl. Microbiol.* **2004**, *96* (3), 419-429.

(126) Sauer, M. M.; Jakob, R. P.; Luber, T.; Canonica, F.; Navarra, G.; Ernst, B.; Unverzagt, C.; Maier, T.; Glockshuber, R. Binding of the bacterial adhesin FimH to its natural, multivalent high-mannose type glycan targets. *J. Am. Chem. Soc.* **2018**, *141* (2), 936-944.

(127) Sokurenko, E. V.; Chesnokova, V.; Dykhuizen, D. E.; Ofek, I.; Wu, X.-R.; Krogfelt, K. A.; Struve, C.; Schembri, M. A.; Hasty, D. L. Pathogenic adaptation of Escherichia coli by natural variation of the FimH adhesin. *Proc. Natl. Acad. Sci. U. S. A.* **1998**, *95* (15), 8922-8926.

(128) Sharon, N. Carbohydrates as future anti-adhesion drugs for infectious diseases. *Biochim Biophys Acta Rev* **2006**, *1760* (4), 527-537.

(129) Mydock-McGrane, L. K.; Hannan, T. J.; Janetka, J. W. Rational design strategies for FimH antagonists: new drugs on the horizon for urinary tract infection and Crohn’s disease. *Expert Opin. Drug Discovery* **2017**, *12* (7), 711-731.

(130) Gouin, S. G. Repurposing Escherichia coli antiadhesives in Crohn's disease. *Future Med. Chem.* **2016**, *8* (16), 1903-1906.

(131) Kuhaudomlarp, S.; Gillon, E.; Varrot, A.; Imberty, A. LecA (PA-IL): A galactose-binding lectin from Pseudomonas aeruginosa. *Lectin Purification and Analysis: Methods and Protocols* **2020**, 257-266.

(132) Wang, J.; Zhou, J.; Yuzhuo, D.; Hu, X.-G.; Chen, Y. Glycopolymers based on carbohydrate or vinyl backbones and their biomedical applications. *Polym. Chem.* **2023**.

(133) Qin, Q.; Lang, S.; Huang, X. Synthetic linear glycopolymers and their biological applications. *J. Carbohydr. Chem.* **2021**, *40* (1-3), 1-44.

(134) Tavares, M.; Pechar, M.; Chytil, P.; Etrych, T. Polymer-Based Drug-Free Therapeutics for Anticancer, Anti-Inflammatory, and Antibacterial Treatment. *Macromol. Biosci.* **2021**, *21*, 2100135. DOI: 10.1002/mabi.202100135.

(135) Fasting, C.; Schalley, C. A.; Weber, M.; Seitz, O.; Hecht, S.; Koksch, B.; Dernedde, J.; Graf, C.; Knapp, E. W.; Haag, R. Multivalency as a chemical organization and action principle. *Angew. Chem. Int. Ed.* **2012**, *51* (42), 10472-10498.

(136) Lundquist, J. J.; Toone, E. J. The cluster glycoside effect. *Chemical reviews* **2002**, *102* (2), 555-578.

(137) Hanheiser, N.; Parshad, B.; Povolotsky, T. L.; Khatri, V.; Achazi, K.; Bhatia, S. Synthesis and Comparison of Linear Polymannosides for Direct Binding with Escherichia Coli. *Macromolecular Chemistry and Physics*, 2300339.

(138) Yan, X.; Sivignon, A.; Yamakawa, N.; Crepet, A.; Travelet, C.; Borsali, R.; Dumych, T.; Li, Z.; Bilyy, R.; Deniaud, D. Glycopolymers as antiadhesives of E. coli strains inducing inflammatory bowel diseases. *Biomacromolecules* **2015**, *16* (6), 1827-1836.

(139) Fan, Z.; Liu, B.; Wang, J.; Zhang, S.; Lin, Q.; Gong, P.; Ma, L.; Yang, S. A novel wound dressing based on Ag/graphene polymer hydrogel: effectively kill bacteria and accelerate wound healing. *Adv. Funct. Mater.* **2014**, *24* (25), 3933-3943.

(140) Ma, S.; Zhan, S.; Jia, Y.; Zhou, Q. Superior antibacterial activity of Fe3O4-TiO2 nanosheets under solar light. *ACS Appl. Mater. Interfaces* **2015**, *7* (39), 21875-21883.

(141) Yeroslavsky, G.; Girshevitz, O.; Foster-Frey, J.; Donovan, D. M.; Rahimipour, S. Antibacterial and antibiofilm surfaces through polydopamine-assisted immobilization of lysostaphin as an antibacterial enzyme. *Langmuir* **2015**, *31* (3), 1064-1073.

(142) Gibney, K. A.; Sovadinova, I.; Lopez, A. I.; Urban, M.; Ridgway, Z.; Caputo, G. A.; Kuroda, K. Poly (ethylene imine) s as antimicrobial agents with selective activity. *Macromol. Biosci.* **2012**, *12* (9), 1279-1289.

(143) Hall, B. A.; Wadsworth, O. J.; Breiner, L. M.; Chappell, J. C.; Brenner, A. S.; McCord, J. P.; Lowell, A. N.; Schulz, M. D. Inherent antibacterial properties of mannose-containing polynorbornene glycomaterials. *Chem. Commun.* **2025**, *61* (23), 4539-4542.

Chapter 2. Modification of Cellulose in Cotton Fabric for Chemotherapy Drug Capture

Ophelia J. Wadsworth[a], Landon Dehart[a], Simran Kala[a], and Michael D. Schulz[a,b]

[a] *Department of Chemistry, Virginia Polytechnic Institute and State University, Blacksburg, VA 24061*

[b] *Macromolecules Innovation Institute, Virginia Polytechnic Institute and State University, Blacksburg, VA 24061*

2.1. Abstract

Transarterial chemoembolization (TACE), a procedure in which chemotherapy drugs are directly administered to tumors via catheter, is the standard therapeutic treatment for hepatocellular carcinoma (HCC) patients who are not candidates for liver resection or transplantation. Doxorubicin (Dox) is one of the most used chemotherapy drugs to treat HCC and while TACE offers site specific delivery, approximately 50% of the administered drug exits the tumor and enters systemic circulation, causing adverse side effects such as cardiomyopathy and congestive heart failure. Inspired by previous research using DNA-based materials to mitigate off-target toxicity during TACE procedures, we modified cotton substrates by appending DNA to the surface via silane linkers. We observed an unexpected trend among the Dox capture efficacy of the modified and unmodified cotton substrates. While we expected the substrates modified with the isocyanate and epoxide-functionalized silanes with DNA to demonstrate greater Dox capture efficacy compared to those modified with DNA only and silane only, we instead observed that the DNA-only modified substrate demonstrated competitive Dox capture performance to those with silane only and silane with DNA. We then measured the DNA concentration before and after DNA adsorption reactions to calculate the amount of DNA adsorbed to the substrates. Absorption measurements revealed an increase in DNA concentration, owing to DNA denaturation. Future

work to modify the cotton surfaces with DNA may include decreasing the adsorption temperature below the denaturation temperature of the DNA and extending the reaction time, if necessary.

2.2. Introduction

Hepatocellular carcinoma (HCC) is the third leading cause of cancer mortality in the United States. Often undetected until late stages, HCC has a mortality rate of 95% within five years of diagnosis.[1-3] While transplantation or resection are primary treatment options, many patients do not qualify and are prescribed chemotherapy to improve their chances of survival.[4, 5] Transarterial chemoembolization (TACE), a procedure in which chemotherapy drugs are directly administered to the tumors via catheter, is the standard therapeutic treatment for these patients.[6-9] Despite this site-specific delivery, approximately 50% of the administered drug exits the liver and circulates throughout the body, harming healthy cells as well. Consequently, liver cancer patients experience severe side effects, which limit the chemotherapy dose that can be administered.[9-11] Doxorubicin (Dox) (**Fig. 2.1A**), an anthracycline anti-tumor agent, is one of the most commonly used chemotherapy drugs to treat HCC.[12-14] Dox intercalates between DNA strands to form stable Dox-DNA complexes,[15] disrupting DNA replication and RNA synthesis.[14, 16-18] While increasing the amount of Dox administered proportionally increases tumor cell death, the toxic effects to non-target tissue include cardiomyopathy and congestive heart failure.[19-21] Irreversible damage has been observed in patients receiving cumulative doses greater than 360 mg. Consequently, the cumulative Dox dose administered to HCC patients does not exceed this threshold, regardless of therapeutic efficacy.[22-24]

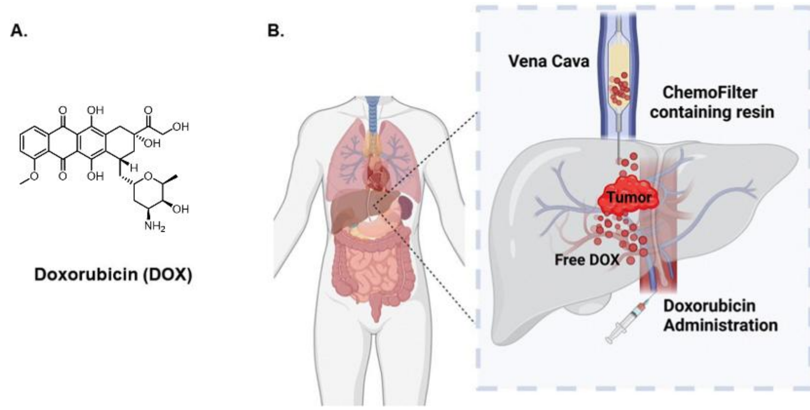

Figure 2.1. (A) Molecular structure of doxorubicin (Dox); (B) schematic of chemofilter deployed in the vena cava to capture Dox before it enters the bloodstream[25]

To mitigate or eliminate off-target toxicity during TACE procedures, Patel *et al.* proposed using a filtration device, deployed via catheter downstream from the liver, to capture excess Dox leaving the liver vasculature. This chemofilter (**Fig. 2.1B**) approach can be combined with the TACE procedure, which has already proven to be a successful treatment method to localize chemotherapy drugs in the liver.[2, 26-28] The first chemofilter used sulfonated ion-exchange resins to electrostatically bind to Dox. Within 10 minutes, Dox concentration was reduced by 52% in porcine serum, and these materials were successfully deployed in the inferior vena cava via catheter in a porcine model.[2] A second-generation filter device used immobilized DNA to capture Dox from porcine serum and porcine blood. Within 1 minute, the Dox concentration decreased by 91% and 82% in serum and blood, respectively.[11] Genomic DNA was also coated onto the surfaces of magnetic nanoparticles[29] and cured onto 3D-printed cubic lattices[26] to generate materials that captured considerably more Dox than the uncoated substrates. Subsequent work investigated using block copolymer membranes,[27] functionalized porous absorbers,[30] aldehyde-functionalized iron-oxide magnetic particles,[31] and polymer-nucleobase composites.[25] While all of these materials successfully captured Dox from various media and demonstrated potential for *in vivo* drug-capture applications, the use of DNA has proven to be the most effective approach to sequestrating Dox during TACE. **(Table 2.1)**. The superior Dox capture performance of DNA-based materials was attributed to the drug's mechanism of action; however, there are high costs associated with generating these materials. The DNA-coated nanoparticles required tedious fabrication processes to attain narrow size distributions, while the 3D-printed cubic lattices were constructed using digital light processing (DLP). DLP, compared to traditional manufacturing procedures such as extrusion or injection molding, is a more challenging process that requires specialized equipment to attain high resolution at fast speeds.[32, 33]

Table 2.1. Synopsis of Dox capture results for synthetic Chemofilter materials in complex media

Comparison of DOX Capture among different polymeric materials in varying media (Data provided for the best performing materials for each material type)					**Ref.**
Capture Medium / Capture Material	PBS	Serum	Blood	*In Vivo* (Live porcine model)	
Ion-exchange membrane	76% - 10 mins 92% - 30 mins	52% - 10 mins 80% - 30 mins	N/A	85% - 3 mins 74% - 10 mins 83% - 30 mins	2
DNA in polyester mesh	95% - 1 min 98% - 5 mins	91% - 1 min	82% - 1 min 93% - 5 mins	N/A	11
DNA-coated nanoparticles	N/A	65% - 1 min 93% - 25 mins	92% - 10 mins	82% - 3 mins	28
Sulfonated block copolymer	50% - 12 mins 90% - 31 mins	N/A	N/A	N/A	26

Inspired by the enhanced capture efficacy of genomic DNA-based materials, we explored functionalizing a more cost-effective and readily available substrate with genomic DNA to match or exceed the Dox capture results reported for the DNA-based chemofilter materials. Cellulose, the chief component of cotton fabric, is an extensively researched polysaccharide that has been utilized, with surface modifications, as the basis of many biomedical materials.[34] We hypothesized that cotton fabric, modified with DNA, will produce an inexpensive and effective drug capture material that can be further explored to generate a viable Chemofilter device for *in vivo* applications.

Cotton fabric is an appealing material because the hydroxyl groups of cellulose are tunable and can be readily modified via esterification and etherification,[35, 36] copper-catalyzed alkene-azide cycloaddition, Diels-Alder cycloaddition, thiol-ene, and oxime reactions.[37] For example, Sun *et al.* functionalized the cellulose in cotton with 3-mercaptopropyltriethoxysilane to graft thiol-reactive groups that enhanced hydrophobicity and durability.[38] Additional work has successfully modified cotton fabric with varying silanes that provided terminal groups used to facilitate further surface functionalization for enhanced properties.[39-41] Silanes such as 3-glycidoxypropyltrimethoxy silane and 3-isocyanotopropyltrimethoxy silane provide electrophilic epoxide and isocyanate functional groups, respectively, that facilitate nucleophilic substitution reactions.[42]

In this work, we modified cotton substrates with DNA by covalently attaching three different silanes, two with terminal electrophiles to facilitate nucleophilic substitution with the phosphate functional group on DNA and one with a terminal alkyl chain for control experiments. DNA was also adsorbed to cotton substrates without silane linkers to determine if the linkers were critical to Dox capture efficacy. Cotton is a readily available and cost-effective material that has the necessary durability to remain intact during capture experiments and the flexibility to mount onto a device for insertion before and removal after TACE-assisted chemotherapy treatments.

2.3. Experimental

2.3.1. Instrumentation

A PHI VersaProbe III x-ray photoelectron spectrometer was used to determine the chemical identity and amounts of silane present on the cotton surfaces before and after modification. Scanning electron microscopy (SEM) was performed on a JEOL IT-500HR and samples were prepared by adhesion to an aluminum holder and coated with gold. A Flexstation II Fluorescence Microplate Reader was used to measure Dox capture kinetics within a 60-minute period.

2.3.2. Materials

Cotton fabric was purchased from Amazon Business. Doxorubicin hydrochloride (Dox) was purchased from Oakwood Products Inc. Hexyltrimethoxy silane (HTMS), (3-glycidoxypropyl)trimethoxy silane (GDPTMS), and 3-isocyanotopropyltrimethoxy silane (ICPTMS) were purchased from Gelest, Inc. Herring sperm DNA was purchased from Sigma Aldrich, Inc. Toluene, hexane and ethanol (200 proof) were purchased from Fisher Scientific. All chemicals were used without further purification.

2.3.3. Synthesis and Characterization of DNA-functionalized Cotton Substrates

To fabricate cotton substrates with DNA adsorbed directly to the surface (Cotton-DNA), 1 cm x 1 cm fabric segments were stirred in ethanol at room temperature for 1 hour to remove surface impurities. After vacuum drying at 60 °C for 1 hour, each substrate was stirred in 10 mL DNA aqueous solution (3.75 g/L), heated to 80 °C for 6 hours then rinsed in DI water for 12 hours (**Fig. 2.2**).

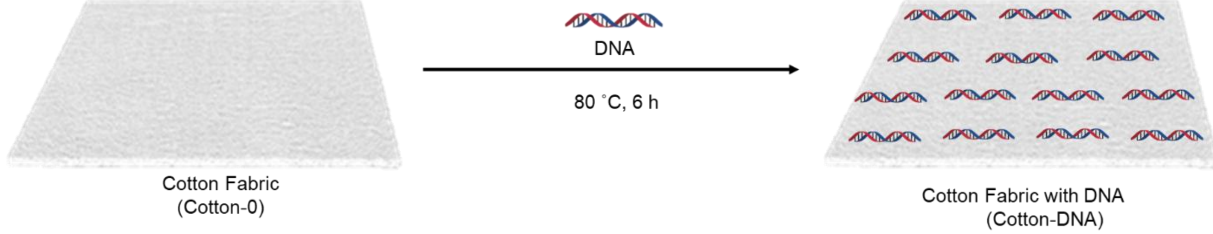

Figure 2.2. Prewashed cotton fabric functionalized with DNA

Cotton substrates modified with DNA via silane linker (Silane-DNA) were fabricated by first washing the unmodified cotton as detailed above. They were then stirred in silane solution (4% v/v) in toluene at 80 °C for 2 hours to covalently link the silane to the cotton surface (**Fig. 2.3**). After rinsing in toluene for 1 hour, they were stirred in DNA solution at 80 °C for 6 hours, rinsed in hexane for 1 hour and vacuum-dried at 40 °C for 48 hours before assessing Dox capture efficacy.

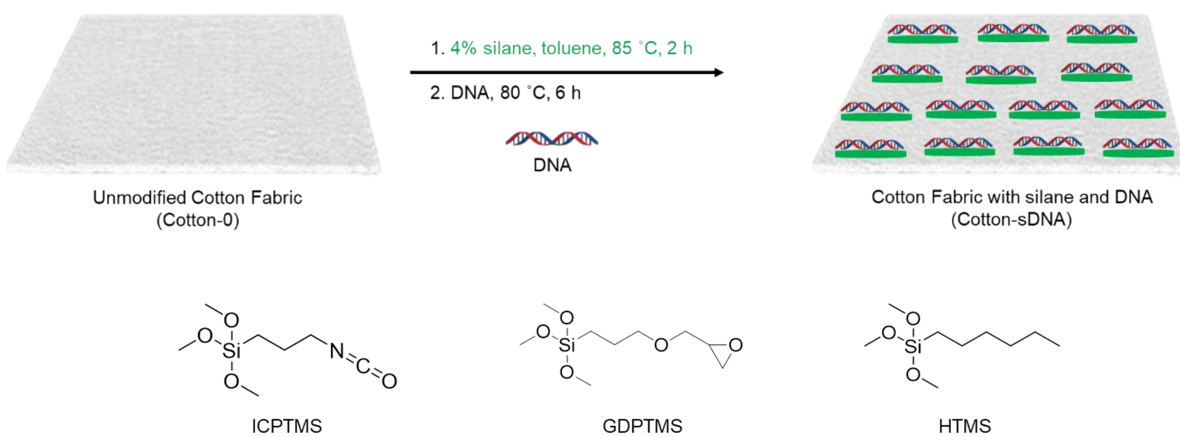

Figure 2.3. Prewashed cotton fabric functionalized with three different silanes (structures included) before further modification with DNA

Dox solutions were prepared by diluting an aqueous stock solution to 50 mg L^{-1}. The substrates were immersed in 20 mL of the diluted solution, heated to 37 °C and allowed to stir for

1 hour. 100-μL aliquots were extracted at 1-minute intervals and pipetted into 96-well plates to measure the decrease in Dox concentration *via* fluorescence spectroscopy.

2.4. Results and Discussion

Cotton, a cost-effective and readily available substrate, was modified to generate viable, DNA-based Dox capture materials. We first adsorbed DNA directly onto the surface of 1 cm x 1 cm cotton fabric segments by stirring in a DNA aqueous solution (3.75 g/L) heated to 80 °C for 6 hours. The reaction time and temperature were determined based on previous trials yielding little or no DNA adsorption at lower temperatures and shorter reaction times. Distinct changes to the surface morphology were observed after modification, as determined by SEM micrographs that showed an uneven DNA layer adsorbed to the cotton fibers (**Figure 2.4**). DNA quantification was not achieved at this time because we were unable to reliably measure the change in concentration via fluorescence spectroscopy, owing to the weak signal of the nucleic acids in DNA.[43]

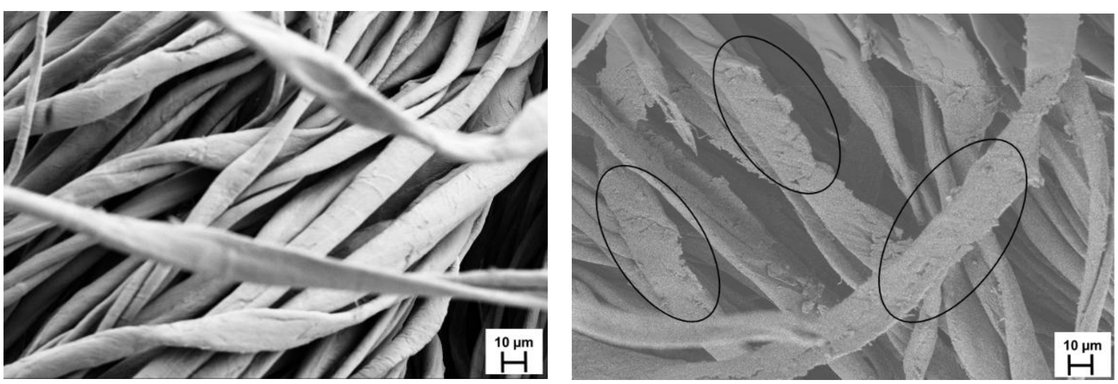

Figure 2.4. SEM micrographs of the unmodified (a) and DNA-adsorbed (b) cotton surfaces (areas where the changes were observed are circled)

We then sought to covalently bind DNA to the cotton fabric surface using various silane linkers, as they have been shown to successfully bond with hydroxyl groups on solid substrates such as glass and silicon wafers,[44, 45] and cellulose fibers.[46-49] The surface hydroxy groups reacted with silanes to form silyl ethers, while the additional functionality on each silane facilitates further modification. In this work, three different silanes were covalently linked to the surface hydroxyl groups on the cotton fabric surface; two of the silanes, ICPTMS and GDPTMS, were terminated with electrophilic moieties that would react with nucleophilic groups on the DNA while the third silane, HTMS, was terminated with a linear hexyl hydrocarbon and used as a negative control linker between the cotton surface and DNA. Subsequently, DNA was attached to the silane-modified substrates, and we evaluated the Dox capture efficacy from aqueous solutions.

We verified the silane content via X-ray photoelectron spectroscopy (XPS), which probed the surface of the cotton substrates to identify the chemical components and quantities present on the cotton surfaces before and after modification (**Table 2.2**). We expected to observe an increase in the %Si on all silane-modified substrates, an indication that silane was covalently attached to the cotton surfaces since each was thoroughly rinsed and dried after surface modification. The surface-bound silane content increased 3.5 and 3-fold for Cotton-GDPTMS and Cotton-ICPTMS, respectively, while the amount present on Cotton-HTMS remained the same as the unmodified cotton substrate (Cotton-0). HTMS was used as a control for the subsequent reaction with DNA and was expected to covalently bond to the cotton surface. The three silanes are structurally different at the terminal end; however, GDPTMS and ICPTMS have polar end groups while HTMS has a nonpolar hexyl chain. Therefore, we postulated that the overall hydrophobicity repelled the necessary contact and prevented the covalent attachment between HTMS and the hydrophilic cotton surface. An alternative possibility is that the electrophilic groups on GDPTMS and ICPTMS could also react with nucleophiles on the cellulose surface, thereby facilitating surface attachment. We also expected the %N present on the surface of Cotton-ICPTMS to increase, owing to the isocyanate functional group. XPS detected an 8-fold increase compared to Cotton-0. Furthermore, the %N detected on the surfaces of Cotton-GDPTMS and Cotton-HTMS remained the same as Cotton-0, indicating that the change in the relative surface components can be attributed to the successful modification with silane. Microscopic imaging allowed us to track physical changes to the substrates after each modification process (**Figure 2.5**). After each substrate was modified with the respective silane, the fibers of Cotton-HTMS (**b**) appeared to be unchanged while those of Cotton-GDPTMS (**c**) and Cotton-ICPTMS (**d**) displayed a rough texture when compared to the unmodified substrate (**a**). When DNA was attached, physical changes to the fibers were evident for all substrates (**e-g**).

Table 2.2. Surface components of unmodified and modified cotton substrates as determined by XPS; each value represents the average of three separate surface areas, with one standard deviation reported

Substrate	**Si (%)**	**N (%)**	**C (%)**	**O (%)**
Cotton-0 (unmodified)	1.39±0.04	0.54±0.08	58.8±1.22	39.2±1.12
Cotton-GDPTMS 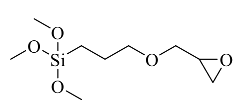	5.19±0.03	0.37±0.02	54.7±0.84	39.6±0.56
Cotton-ICPTMS 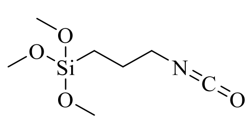	3.95±0.01	3.94	54.0±0.02	38.1±0.04
Cotton-HTMS 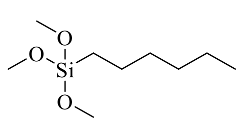	1.30±0.05	0.56±0.16	62.1±0.33	35.9±0.44

;

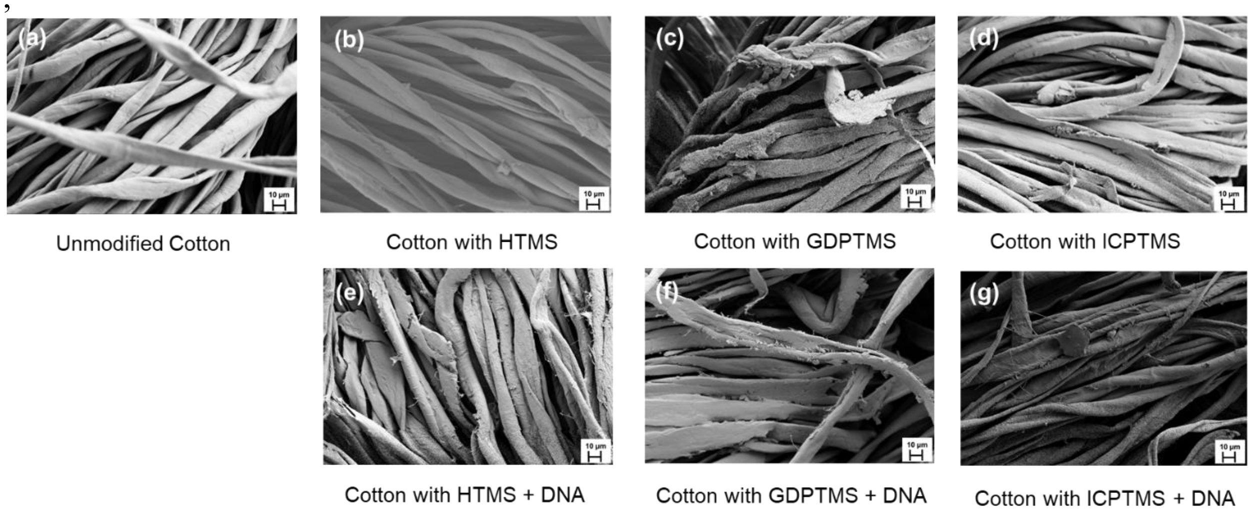

Figure 2.5. SEM imaging of unmodified cotton (a), cotton modified with silane only (b-d) and silane+DNA (e-g)

To determine the drug capture efficacy of these functionalized cotton substrates, aqueous Dox solutions were prepared by diluting a stock solution to 50 mg L^{-1}, corresponding to the standard clinical dose administered per treatment in HCC patients.[2] All substrates were individually stirred in 20 mL of Dox solution that was first heated to 37 °C. Aliquots (0.1 mL) were collected at 1-minute intervals over a 60-minute period and pipetted into 96-well plates to measure the decrease in Dox concentration *via* fluorescence spectroscopy. We first evaluated the impact of adsorbing DNA to the cotton surface on the Dox capture efficacy. To verify the role of DNA, the amount of Dox captured was compared to that captured with unmodified cotton (Cotton-0). Cotton-DNA demonstrated a 2-fold increase in capture efficacy compared to Cotton-0, indicating that DNA was essential to Dox capture (**Figure 2.6**). The small amount of Dox captured with Cotton-0 was likely due to polar/hydrophilic attractions between Dox and the surface hydroxyl groups of unmodified cotton. Cotton substrates functionalized with silanes were also evaluated for Dox capture efficacy before further surface modification with DNA. Cotton-

GDPTMS and Cotton-ICPTMS captured similar amounts of Dox, which was 1.5-fold more than Cotton-0. We deduced that GDPTMS and ICPTMS enhanced the Dox capture efficacy of the unmodified cotton substrate, most likely via polar/hydrophilic attractions between the end groups and Dox. Interestingly, the amount of Dox captured by Cotton-HTMS was equivalent to that captured by Cotton-0. Since XPS and SEM confirmed there were no physical changes to the fibers when cotton was modified with HTMS, and there were evident physical changes to the fibers when modified with GDPTMS and ICPTMS, we concluded that Cotton-HTMS was not functionalized and therefore was as effective at Dox capture as Cotton-0.

We then investigated the impact of covalently attaching DNA to the silane-functionalized substrates. We expected the addition of DNA to generate materials that would capture more Dox than the other substrates. Instead, we observed that GDPTMS-DNA and ICPTMS-DNA did not capture more Dox than their silane-only counterparts and captured less Dox than HTMS-DNA. Furthermore, the amount of Dox captured with HTMS-DNA was equivalent to that of Cotton-DNA and both demonstrated greater capture efficacy than Cotton-0 and all other modified substrates. We previously concluded that Cotton-0 and Cotton-HTMS were essentially the same material, therefore we can also conclude that Cotton-DNA and HTMS-DNA were also the same material. Overall, the addition of GDPTMS and ICPTMS silanes as linkers between the cotton surface and DNA did not promote greater Dox capture efficacy. Since XPS and SEM verified that the silanes were successfully attached to the cotton surface, and Cotton-DNA captured 2-fold more Dox than Cotton-0, we postulated that DNA was not bound to GDPTMS or ICPTMS. It is plausible that DNA did not react with the electrophilic end groups of the silanes due to its steric bulk and was therefore unable to contribute to Dox capture efficacy. One possible solution is to extend the reaction time to allow nucleophilic substitution to proceed to completion.

To examine the relationship between mass of DNA and the amount of Dox captured, we decided to quantify the amount of DNA bound to the Cotton-DNA surface. Aliquots were collected before and after the DNA adsorption reaction, the absorbance measured via fluorescence spectroscopy, and the concentration calculated using a calibration curve and Beer-Lambert's law. Measurements from three reactions were averaged and the results revealed the final DNA concentration was apparently greater than the initial concentration (17.98 mg/L and 15.87 mg/L, respectively). An increase in DNA absorbance (hyperchromicity) occurs when DNA denatures at temperatures that disrupts the hydrogen bonds between the base pairs.[50] Although denaturation temperature varies based on the organism from which it is extracted, double-stranded DNA typically denatures between 70-100 °C.[51] The temperature used for the adsorption reactions was 85 °C; consequently, we were unable to accurately quantify the amount of DNA loaded onto the cotton substrates. Further DNA adsorption reactions will be done at a temperature safely below the denaturation temperature for DNA.

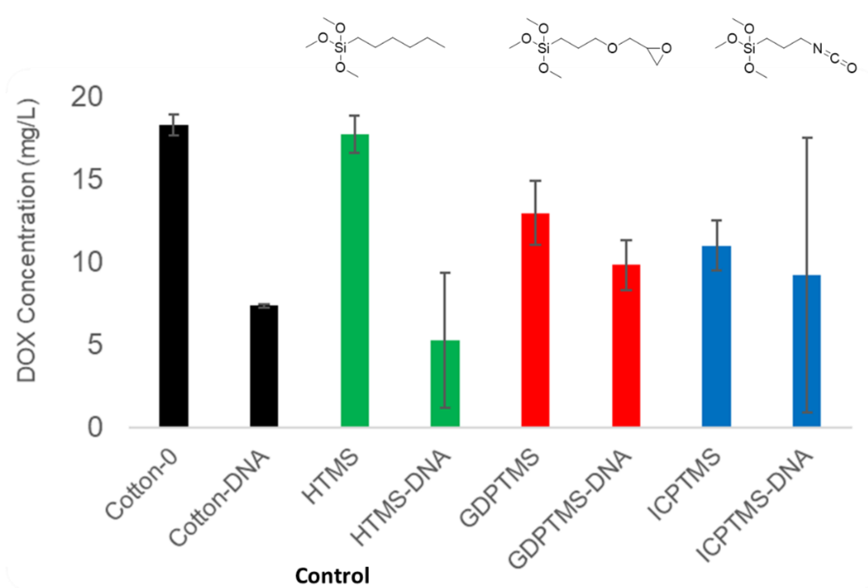

Figure 2.6. Dox capture results for unmodified and modified cotton substrates. Error bars are standard deviations of 2 measurements.

2.5. Conclusion

We modified cotton fabric to generate functionalized substrates as novel DNA-based Dox capture materials. We used XPS to verify silane adsorption and SEM to observe the physical changes to the cotton fibers after each modification process. While we expected the substrates modified with ICPTMS and GDPTMS with DNA to demonstrate greater Dox capture efficacy, we instead observed that the substrate modified with DNA only (Cotton-0) captured 2-fold more Dox than all other substrates. We reasoned that steric hindrance played a role in hindering the nucleophilic substitution reaction between DNA and the electrophilic functional groups of GDPTMS and ICPTMS. This challenge could potentially be solved by extending the reaction time. To evaluate the amount DNA responsible for enhanced capture efficacy observed with Cotton-0, we measured the DNA concentration before and after DNA adsorption reactions to calculate the amount of DNA adsorbed to the substrates. Absorption measurements revealed an apparent increase in DNA concentration, likely owing to DNA denaturation. Future work to determine the degree of DNA functionalization will include decreasing the adsorption temperature below DNA's denaturation temperature and extending the reaction time, if necessary.

2.6. References

(1) J Wang, Y.-X. Transcatheter embolization therapy in liver cancer. *Recent Pat. Med. Img.* **2012**, *2* (2), 150-162.

(2) Patel, A. S.; Saeed, M.; Yee, E. J.; Yang, J.; Lam, G. J.; Losey, A. D.; Lillaney, P. V.; Thorne, B.; Chin, A. K.; Malik, S. Development and validation of endovascular chemotherapy filter device for removing high-dose doxorubicin: preclinical study. *J. Med. Dev.* **2014**, *8* (4), 041008-041001 - 041008-041008.

(3) Sun, V. C.-Y.; Sarna, L. Symptom management in hepatocellular carcinoma. *Clin. J. Onco.l Nurs.* **2008**, *12* (5), 759-766.

(4) Altekruse, S. F.; McGlynn, K. A.; Reichman, M. E. Hepatocellular carcinoma incidence, mortality, and survival trends in the United States from 1975 to 2005. *J. Clin. Oncol.* **2009**, *27* (9), 1485-1491.

(5) Rammohan, A.; Sathyanesan, J.; Ramaswami, S.; Lakshmanan, A.; Senthil-Kumar, P.; Srinivasan, U. P.; Ramasamy, R.; Ravichandran, P. Embolization of liver tumors: Past, present and future. *World J. Radiol.* **2012**, *4* (9), 405.

(6) Savic, L. J.; Chen, E.; Nezami, N.; Murali, N.; Hamm, C. A.; Wang, C.; Lin, M.; Schlachter, T.; Hong, K.; Georgiades, C. Conventional vs. Drug-Eluting Beads Transarterial Chemoembolization for Unresectable Hepatocellular Carcinoma—A Propensity Score Weighted Comparison of Efficacy and Safety. *Cancers* **2022**, *14* (23), 5847.

(7) Sieghart, W.; Hucke, F.; Peck-Radosavljevic, M. Transarterial chemoembolization: modalities, indication, and patient selection. *J. Hepatol.* **2015**, *62* (5), 1187-1195.

(8) Anwanwan, D.; Singh, S. K.; Singh, S.; Saikam, V.; Singh, R. Challenges in liver cancer and possible treatment approaches. *Biochim Biophys Acta Rev Cancer* **2020**, *1873* (1), 188314.

(9) Wáng, Y.-X. J.; De Baere, T.; Idée, J.-M.; Ballet, S. Transcatheter embolization therapy in liver cancer: an update of clinical evidences. *Chin. J. Cancer Res.* **2015**, *27* (2), 96-121.

(10) Tacar, O.; Sriamornsak, P.; Dass, C. R. Doxorubicin: an update on anticancer molecular action, toxicity and novel drug delivery systems. *J. Pharm. Pharmacol.* **2013**, *65* (2), 157-170.

(11) Aboian, M. S.; Yu, J. F.; Gautam, A.; Sze, C.-H.; Yang, J. K.; Chan, J.; Lillaney, P. V.; Jordan, C. D.; Oh, H.-J.; Wilson, D. M. In vitro clearance of doxorubicin with a DNA-based filtration device designed for intravascular use with intra-arterial chemotherapy. *Biomed. Microdevices* **2016**, *18*, 1-9.

(12) Marelli, L.; Stigliano, R.; Triantos, C.; Senzolo, M.; Cholongitas, E.; Davies, N.; Tibballs, J.; Meyer, T.; Patch, D. W.; Burroughs, A. K. Transarterial therapy for hepatocellular carcinoma: which technique is more effective? A systematic review of cohort and randomized studies. *Cardiovasc. Interv. Radiol.* **2007**, *30*, 6-25.

(13) Buijs, M.; Vossen, J. A.; Frangakis, C.; Hong, K.; Georgiades, C. S.; Chen, Y.; Liapi, E.; Geschwind, J.-F. H. Nonresectable hepatocellular carcinoma: long-term toxicity in patients treated with transarterial chemoembolization—single-center experience. *Radiology* **2008**, *249* (1), 346-354.

(14) Jain, D. Cardiotoxicity of doxorubicin and other anthracycline derivatives. *J. Nucl. Cardiol.* **2000**, *7*, 53-62.

(15) Jawad, B.; Poudel, L.; Podgornik, R.; Steinmetz, N. F.; Ching, W.-Y. Molecular mechanism and binding free energy of doxorubicin intercalation in DNA. *Phys. Chem. Chem. Phys.* **2019**, *21* (7), 3877-3893.

(16) Liu, G.; Jin, Q.; Liu, X.; Lv, L.; Chen, C.; Ji, J. Biocompatible vesicles based on PEO-b-PMPC/α-cyclodextrin inclusion complexes for drug delivery. *Soft Matter* **2011**, *7* (2), 662-669.

(17) Temperini, C.; Messori, L.; Orioli, P.; Bugno, C. D.; Animati, F.; Ughetto, G. The crystal structure of the complex between a disaccharide anthracycline and the DNA hexamer d (CGATCG) reveals two different binding sites involving two DNA duplexes. *Nucleic Acids Res.* **2003**, *31* (5), 1464-1469.

(18) Gnapareddy, B.; Reddy Dugasani, S.; Ha, T.; Paulson, B.; Hwang, T.; Kim, T.; Hoon Kim, J.; Oh, K.; Park, S. H. Chemical and physical characteristics of doxorubicin hydrochloride drug-doped salmon DNA thin films. *Sci. Rep.* **2015**, *5* (1), 1-9.

(19) August, D.; Verma, N.; Vaerten, M.; Shah, R.; Andrews, J.; Brenner, D. Pharmacokinetic evaluation of percutaneous hepatic venous isolation for administration of regional chemotherapy. *J. Surg. Oncol.* **1995**, *4* (4), 205-216.

(20) Cheung-Ong, K.; Giaever, G.; Nislow, C. DNA-damaging agents in cancer chemotherapy: serendipity and chemical biology. *Chem. Biol.* **2013**, *20* (5), 648-659.

(21) Minotti, G.; Menna, P.; Salvatorelli, E.; Cairo, G.; Gianni, L. Anthracyclines: molecular advances and pharmacologic developments in antitumor activity and cardiotoxicity. *Pharmacol. Rev.* **2004**, *56* (2), 185-229.

(22) Carvalho, C.; Santos, R. X.; Cardoso, S.; Correia, S.; Oliveira, P. J.; Santos, M. S.; Moreira, P. I. Doxorubicin: the good, the bad and the ugly effect. *Curr. Med. Chem.* **2009**, *16* (25), 3267-3285.

(23) Pugazhendhi, A.; Edison, T. N. J. I.; Velmurugan, B. K.; Jacob, J. A.; Karuppusamy, I. Toxicity of Doxorubicin (Dox) to different experimental organ systems. *Life Sci.* **2018**, *200*, 26-30.

(24) Injac, R.; Strukelj, B. Recent advances in protection against doxorubicin-induced toxicity. *Technol. Cancer Res. Treat.* **2008**, *7* (6), 497-516.

(25) Su, G. A.; Wadsworth, O. J.; Muller, H. S.; Archer, W. R.; Hetts, S. W.; Schulz, M. D. Polymer–nucleobase composites for chemotherapy drug capture. *J. Mater. Chem. B* **2023**, *11* (35), 8449-8455.

(26) Yee, D. W.; Hetts, S. W.; Greer, J. R. 3D-Printed Drug Capture Materials Based on Genomic DNA Coatings. *ACS Appl. Mater. Interfaces* **2021**, *13* (35), 41424-41434.

(27) Chen, X. C.; Oh, H. J.; Yu, J. F.; Yang, J. K.; Petzetakis, N.; Patel, A. S.; Hetts, S. W.; Balsara, N. P. Block copolymer membranes for efficient capture of a chemotherapy drug. *ACS Macro Lett.* **2016**, *5* (8), 936-941.

(28) Roche, A.; Girish, B. V.; de Baère, T.; Baudin, E.; Boige, V.; Elias, D.; Lasser, P.; Schlumberger, M.; Ducreux, M. Trans-catheter arterial chemoembolization as first-line treatment for hepatic metastases from endocrine tumors. *Eur. Radiol.* **2003**, *13*, 136-140.

(29) Blumenfeld, C. M.; Schulz, M. D.; Aboian, M. S.; Wilson, M. W.; Moore, T.; Hetts, S. W.; Grubbs, R. H. Drug capture materials based on genomic DNA-functionalized magnetic nanoparticles. *Nat. Commun.* **2018**, *9* (1), 1-7.

(30) Oh, H. J.; Aboian, M. S.; Yi, M. Y.; Maslyn, J. A.; Loo, W. S.; Jiang, X.; Parkinson, D. Y.; Wilson, M. W.; Moore, T.; Yee, C. R. 3D printed absorber for capturing chemotherapy drugs before they spread through the body. *ACS Cent. Sci.* **2019**, *5* (3), 419-427.

(31) Krishnamoorthy, S.; Grubbs, R. H. Aldehyde-Functionalized Magnetic Particles to Capture Off-Target Chemotherapeutic Agents. *ACS Omega* **2020**, *5* (45), 29121-29126.

(32) Zhao, Z.; Tian, X.; Song, X. Engineering materials with light: recent progress in digital light processing based 3D printing. *J. Mater. Chem. C* **2020**, *8* (40), 13896-13917.

(33) Zhu, G.; Hou, Y.; Xu, J.; Zhao, N. Reprintable polymers for digital light processing 3D printing. *Adv. Funct. Mater.* **2021**, *31* (9), 2007173.

(34) Edgar, K. J. Cellulose esters in drug delivery. *Cellulose* **2007**, *14*, 49-64.

(35) Fox, S. C.; Li, B.; Xu, D.; Edgar, K. J. Regioselective esterification and etherification of cellulose: a review. *Biomacromolecules* **2011**, *12* (6), 1956-1972.

(36) Edgar, K.; Arnold, K.; Blount, W.; Lawniczak, J.; Lowman, D. Synthesis and properties of cellulose acetoacetates. *Macromolecules* **1995**, *28* (12), 4122-4128.

(37) Meng, X.; Edgar, K. J. "Click" reactions in polysaccharide modification. *Prog. Polym. Sci.* **2016**, *53*, 52-85.

(38) Yeqiu, L.; Jinlian, H.; Yong, Z.; Zhuohong, Y. Surface modification of cotton fabric by grafting of polyurethane. *Carbohydr. Polym.* **2005**, *61* (3), 276-280.

(39) Mondal, M.; Islam, M.; Ahmed, F. Modification of cotton fibre with functionalized silane coupling agents vinyltriethoxysilane and aminopropyltriethoxysilane. *J. Text. Sci. Eng* **2018**, *8*, 1-8.

(40) Alassod, A.; Shahriari-Khalaji, M.; Wang, Y.; Balilonda, A.; Al Hinnawi, M. F.; Yang, S. Functionalization of aminoalkylsilane-grafted cotton for antibacterial, thermal, and wettability properties. *RSC Adv.* **2022**, *12* (32), 20906-20918.

(41) Abidi, N.; Hequet, E.; Tarimala, S. Functionalization of cotton fabric with vinyltrimethoxysilane. *Text. Res. J.* **2007**, *77* (9), 668-674.

(42) Goyal, S. Silanes: Chemistry and applications. *J. Indian Prosthodont. Soc.* **2006**, *6* (1), 14-18.

(43) Gustavsson, T.; Markovitsi, D. Fundamentals of the intrinsic DNA fluorescence. *Acc. Chem. Res.* **2021**, *54* (5), 1226-1235.

(44) Sterzynska, K.; Budna, J.; Frydrych-Tomczak, E.; Hreczycho, G.; Malinska, A.; Maciejewski, H.; Zabel, M. Silane-modified surfaces in specific antibody-mediated cell recognition. *Folia Histochemica et Cytobiologica* **2014**, *52* (3), 250-255.

(45) Godula, K.; Rabuka, D.; Nam, K. T.; Bertozzi, C. R. Synthesis and Microcontact Printing of Dual End-Functionalized Mucin-like Glycopolymers for Microarray Applications. *Angew. Chem.* **2009**, *121* (27), 5073-5076.

(46) Abdelmouleh, M.; Boufi, S.; ben Salah, A.; Belgacem, M. N.; Gandini, A. Interaction of silane coupling agents with cellulose. *Langmuir* **2002**, *18* (8), 3203-3208.

(47) Abdelmouleh, M.; Boufi, S.; Belgacem, M. N.; Dufresne, A.; Gandini, A. Modification of cellulose fibers with functionalized silanes: effect of the fiber treatment on the mechanical performances of cellulose–thermoset composites. *J. Appl. Polym. Sci.* **2005**, *98* (3), 974-984.

(48) Sun, D.; Wang, W.; Yu, D. Highly hydrophobic cotton fabrics prepared with fluorine-free functionalized silsesquioxanes. *Cellulose* **2017**, *24*, 4519-4531.

(49) Lin, T.-C.; Chang, J.-S.; Lee, D.-J. Hydrophobic cotton fabric with 3-mercaptopropyltriethoxysilane/polyhedral oligomeric silsesquioxane/1-octadecanethiol modification for oil/water separation. *Int. J. Biol. Macromol.* **2023**, *253*, 126748.

(50) D'Abramo, M.; Castellazzi, C. L.; Orozco, M.; Amadei, A. On the nature of DNA hyperchromic effect. *J. Phys. Chem. B* **2013**, *117* (29), 8697-8704.

(51) Thomas, R. The denaturation of DNA. *Gene* **1993**, *135* (1-2), 77-79.

Chapter 3. Methacrylic acid-based Resins for Chemotherapy Drug Capture Applications

Ophelia J. Wadsworth,[a] Gillian A. Su,[a] H. Suzanne Muller,[a] Steven W. Hetts,[b] and Michael D. Schulz.[a,c]
[a] *Department of Chemistry, Virginia Polytechnic Institute and State University, Blacksburg, VA 24061, USA*

[b] *Departments of Radiology, Biomedical Imaging, and Neurological Surgery, University of California, San Francisco, CA 94143-0628, USA*

[c] *Macromolecules Innovation Institute, Virginia Polytechnic Institute and State University, Blacksburg, VA 24061, USA*

3.1. Abstract

Doxorubicin (Dox), a common antitumor drug, causes irreversible cardiomyopathy and congestive heart failure. An emerging approach to addressing this challenge is to deploy chemotherapy-binding materials in the veins draining a tumor or tumor-bearing organ, thereby intercepting runoff chemotherapy before it causes off-target toxicity. In this work, we synthesized poly(methacrylic acid) resins as drug-capture materials to electrostatically bind to Dox, which is positively charged at pH 7.4. We verified the importance of resin charge by evaluating Dox capture efficiency at low pH and with uncharged control materials based on poly(methyl methacrylate). We observed that the amount of Dox captured by the charged resins increased 18-fold over neutral counterparts, indicating that electrostatic binding was critical. We further investigated the effect of increasing flexibility on drug capture efficacy by varying the crosslink density and crosslinker length. When resins were crosslinked with ethylene glycol dimethacrylate (1EG), increasing crosslink density increased Dox capture. Dox capture also decreased when longer crosslinkers were used. These results suggest that some network rigidity is required for optimal Dox binding, but that the hydrophobicity of the matrix and density of the resin must also be considered. These

findings underscore the importance of balancing electrostatic attraction, network rigidity, hydrophobic effects when designing drug-capture materials.

3.2. Introduction

Hepatocellular carcinoma (HCC) is the third leading cause of cancer mortality in the United States. Often undetected until late stages, HCC has a mortality rate of 95% within five years of diagnosis.[1-3] While transplantation or resection are primary treatment options, many patients do not qualify and are instead prescribed chemotherapy.[4, 5] Transarterial chemoembolization (TACE), a procedure in which chemotherapy drugs are directly administered to the tumors via catheter, is the standard therapeutic treatment for these patients.[6-9] Despite this site-specific delivery, approximately 50% of the administered drug exits the liver and circulates throughout the body, harming healthy tissues as well. Consequently, liver cancer patients experience severe side effects, which limit the chemotherapy dose that can be administered.[9-11]

Doxorubicin (Dox) (**Fig. 3.1A**), an anthracycline anti-tumor agent that disrupts DNA replication and repair, remains one of the most common chemotherapy drugs used to treat HCC.[12, 13] While increasing the amount of Dox administered proportionally increases tumor cell death, it also has toxic effects on non-target tissue including cardiomyopathy and congestive heart failure.[14-16] Irreversible damage has been observed in patients receiving cumulative doses greater than 360 mg. Consequently, the cumulative Dox dose administered to HCC patients does not exceed this threshold, regardless of therapeutic efficacy.[17-19]

To mitigate or eliminate off-target toxicity during TACE procedures, Patel *et al.* proposed using a filtration device, deployed via catheter downstream from the liver, to capture excess Dox leaving the liver vasculature. This chemofilter approach (**Fig. 3.1B**) can be integrated with the TACE procedure, which has already proven to be a successful treatment method to localize chemotherapy drugs in the liver.[2, 20-22] The first Chemofilter used sulfonated ion-exchange resins to electrostatically bind to Dox. Within 10 minutes, Dox concentration was reduced by 52% in porcine serum, and these materials were successfully deployed in the inferior vena cava via catheter in a porcine model.[2] Subsequently, additional work investigated using block copolymer membranes, [21] immobilized genomic DNA,[20, 23] functionalized porous absorbers,[24] DNA-functionalized iron oxide particles,[25] and polymer-nucleobase composites.[26] All successfully captured Dox from various media and demonstrated potential for *in vivo* drug-capture applications.

Inspired by this work, we explored using molecularly imprinted polymers (MIPs) to capture Dox from complex solutions. MIPs are crosslinked polymers synthesized in the presence of a template molecule, which is encapsulated within the polymer network. The template is then removed, leaving cavities that are matched to the molecular size and shape of the template and producing specific binding sites to selectively capture the target molecule.[27-30] Previously prepared MIPs have successfully removed organic contaminants such as pharmaceutical drugs,[31, 32] polycyclic aromatic hydrocarbons,[28, 29, 33] and pesticides[27, 34, 35] from groundwater samples. These target molecules have certain structural similarities with common chemotherapy agents, including Dox, suggesting that MIPs may also be suitable for drug-capture applications.[36]

To prepare Dox-capturing MIPs, methacrylic acid (MA) was copolymerized in the presence of Dox with ethylene glycol dimethacrylate (1EG) as a crosslinking agent (**Table 3.S1**); however, complete template (Dox) removal using several suitable solvents and varying temperatures (**Table 3.S2**) was unsuccessful (**Fig. 3.S1**). These observations indicated that Dox was strongly bound to the resin. We hypothesized that Dox was either electrostatically bound to the negatively charged carboxylate, owing to its protonated amine, or encapsulated in the polymer network. Consequently, we shifted our focus to evaluating these capture mechanisms using non-templated resins.

In this work, we synthesized poly(methacrylic acid) (PMA) resins to assess how polymer charge affects Dox capture efficacy. We also evaluated the impact of crosslinking density and flexibility on capture performance. We hypothesized that 1) the carboxylate groups on the PMA resin would engage in electrostatic interactions with the protonated amine groups of Dox, leading to drug capture, and 2) the change in crosslink density would impact the degree to which the resin swells and the rate at which Dox diffuses into the network.

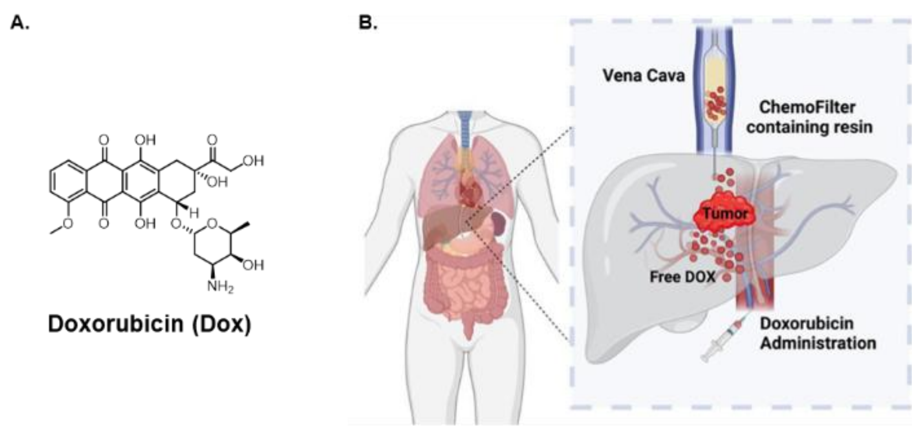

Figure 3.1. (A) Molecular structure of doxorubicin (Dox); (B) schematic of Chemofilter deployed in the vena cava to capture Dox before it enters the bloodstream[26]

3.3. Experimental

3.3.1. Instrumentation

An Agilent Technologies Cary 60 UV-Vis spectrometer with a stainless-steel probe (10 mm pathlength) was used to measure solution absorbance changes associated with Dox binding to the resins. Scans were collected every 30 s for 20 mins from 600-200 nm with an average scan time of 0.0125 s, 1 nm interval and a scan rate of 4800 nm $s^{-1.}$ A Varian 670-IR Fourier Transform Infrared Spectrometer was used to measure the relevant absorbance bands.

3.3.2. Materials

Doxorubicin hydrochloride (Dox), methacrylic acid (MA) and dimethyl sulfoxide (DMSO) were purchased from Oakwood Chemical Co. Methyl methacrylate (MMA), ethylene glycol dimethacrylate (1EG), diethylene glycol dimethacrylate (2EG), triethylene glycol dimethacrylate (3EG) and 2,2-azobisisobutyronitrile (AIBN) were purchased from Sigma Aldrich. Phosphate-buffered saline (with calcium and magnesium) was purchased from Fisher Scientific. MA, MMA, 1EG, and 3EG were filtered through a basic aluminum oxide plug to remove the inhibitors. AIBN was recrystallized from methanol before use. All other chemicals were used as received.

3.3.3. Methods

Synthetic methods were adapted from published procedures for resins synthesized to capture micropollutants in contaminated ground water.[27] Monomer (1 eq.), dimethacrylate crosslinker (0.25 – 2.0 molar eq.), and AIBN (0.01 molar eq.) were placed in a 50 mL round bottom flask with DMSO and purged for 15 minutes while stirring. The flask was then heated to 65 °C for 2 h (**Scheme 3.1**). Each crosslinker was also polymerized in the absence of the monomers to generate homopolymer networks. The crosslinked products were crushed and vigorously stirred in excess acetone for 2 h to remove DMSO, which would disrupt the capture efficiency of the materials synthesized,[37-39] before vacuum drying overnight at 60 °C. The dried resins were crushed again, rewashed with acetone and redried before FTIR characterization (**Figs. 3.S3 to 3.S14**) and Dox capture experiments were conducted. **Table 1** lists the monomers, crosslinkers, and resin products synthesized.

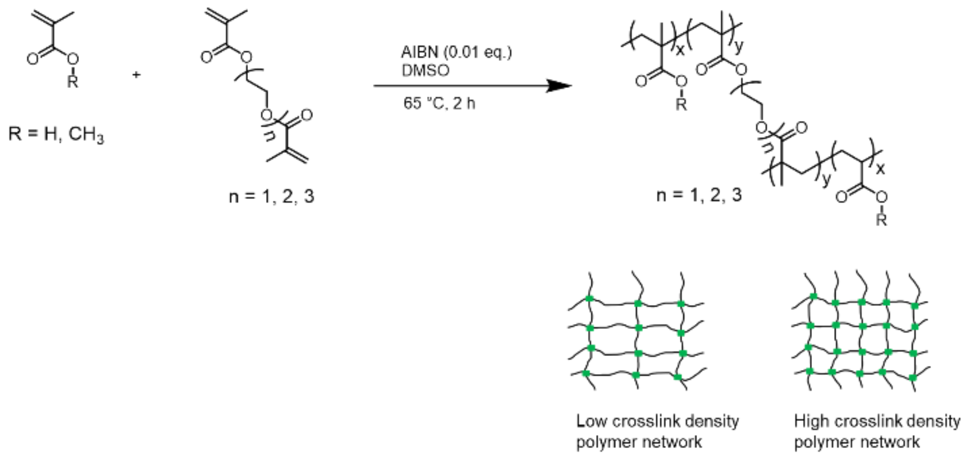

Scheme 3.1. Free-radical copolymerization of monomer with mono, di and tri-ethylene glycol dimethacrylate crosslinkers

Neutral Dox solutions were prepared by first dissolving 12.5 mg Dox in 12.5 g DI water then filling a 250-mL volumetric flask with PBS (pH ≈ 7.4) to attain a 0.05 mg mL^{-1} concentration. Acidic Dox solutions were prepared by dissolving 12.5 mg Dox, 25 mg $CaCl_2$, 25 mg $MgCl_2$, 1.32 mL acetic acid and 0.640 g sodium acetate in 250 mL DI water (pH ≈ 3.6). Dox capture was evaluated by first generating a calibration curve using a UV-Vis spectrometer equipped with a 1 cm pathlength probe. Measurements were conducted in PBS and acidic solutions to determine the molar extinction coefficient (ε) according to the Beer-Lambert law (**Fig. 3.S2**). Subsequent changes in absorbance over time were then used to quantify Dox uptake. In accordance with procedures established in our previous work,[26] 75 g of Dox solution was placed in a beaker, then a filter cup was suspended to facilitate separation between the UV-Vis probe and the resin. The Dox solution was stirred and heated to 37 °C before the initial concentration was measured. Immediately after, 100 mg of resin was added to the Dox solution between the beaker and the filter cup and absorbance was measured once every 30 s over a 20-minute period.

Table 3.1. Methacrylic acid and methyl methacrylate-based resins synthesized for Dox capture characterization.

Monomer	Crosslinker	Crosslinker:monomer molar ratio	Resin
MMA (methyl methacrylate) R = CH_3	1EG (n=1)	0.5	PMMA-1EG-050
	2EG (n=2)	0.5	PMMA-2EG-050
	3EG (n=3)	0.5	PMMA-3EG-050
MA (methacrylic acid) R = H	1EG (n=1)	0.25	PMA-1EG-025
		0.50	PMA-1EG-050
		1.00	PMA-1EG-100
		2.00	PMA-1EG-200
	2EG (n=2)	0.25	PMA-2EG-025
		0.50	PMA-2EG-050
		1.00	PMA-2EG-100
		2.00	PMA-2EG-200
	3EG (n =3)	0.25	PMA-3EG-025
		0.50	PMA-3EG-050
		1.00	PMA-3EG-100
		2.00	PMA-3EG-200

3.4. Results and Discussion

PMA resins were synthesized to produce anionic resins for drug-capture applications. Methacrylic acid (MA), which is ionized at physiological pH (pKa ≈ 4.65), was used as the anionic component to facilitate electrostatic interactions with positively charged Dox. Ethylene glycol dimethacrylate (1EG) was incorporated at different ratios to generate resins with varying crosslink densities. These materials were named according to the base polymer (PMA), crosslinker (1EG) and crosslinker: monomer molar ratio (e.g., PMA-1EG-025 for a 0.25 1EG:MA molar ratio).

We first investigated the impact of electrostatic binding on the Dox capture efficacy of PMA-1EG-050. At pH 7.4 MA is ionized, and we expected the carboxylate to electrostatically bind to Dox. To verify the role of the carboxylate, the amount of Dox captured from PBS solution (pH 7.4) was compared to that captured in an acidic Dox solution buffered at pH 3.6. At this lower pH, MA will retain its neutral carboxylic acid form, eliminating the electrostatic interaction provided by the carboxylate.[40, 41] The capture efficacy of PMA-1EG-050 increased 18-fold at pH 7.4

compared to pH 3.6 (**Fig. 3.2**), indicating that electrostatic binding is critical to Dox capture. We postulated that the small amount of Dox captured in the acidic solution was due to hydrogen bonding between Dox and the carboxylic acids on the resin or interactions with residual carboxylates present at this pH (~9% ionized). To test this hypothesis, we replaced MA with methyl methacrylate (MMA), which cannot be ionized under these conditions, producing a non-ionized control. As hypothesized, the amount of Dox captured by PMMA-1EG-050 was negligible. All remaining Dox capture experiments were conducted in PBS at pH 7.4.

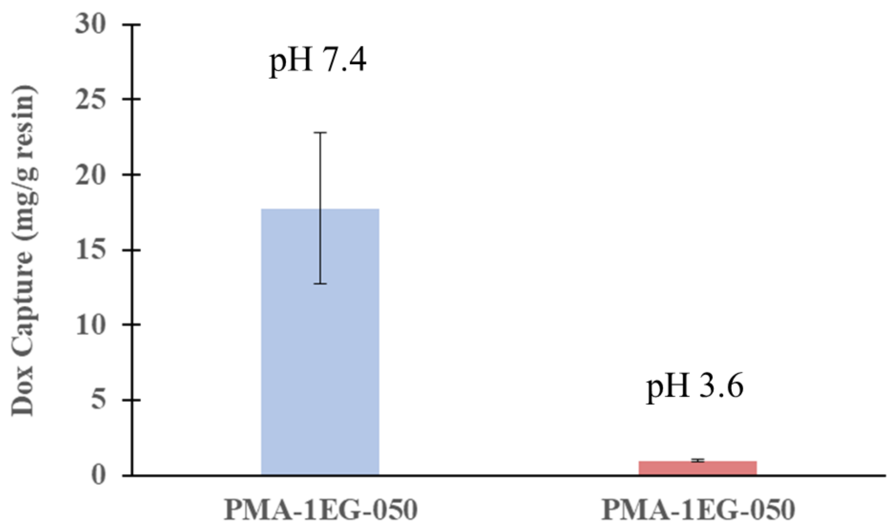

Figure 3.2. Dox capture from 0.05 mg mL^{-1} solution for PMA-1EG-050 at pH 7.4 (blue) and 3.6 (red)

Crosslinked polymers vary in their physical properties and applications based on the degree of crosslinking. Highly crosslinked polymers are stiffer, mechanically stronger, and more chemically resistant, while lightly crosslinked polymers exhibit the opposite characteristics.[42-44] Critically, the degree of crosslinking is inversely proportional to the flexibility and swelling of crosslinked polymers, which we hypothesized could impact Dox capture.[42] Consequently, we investigated how changing the crosslink density would affect the Dox capture efficacy of the PMA resins. MA was copolymerized with 1EG at 0.25, 0.50, 1.00 and 2.00 crosslinker:monomer molar ratios to generate resins with varying crosslink densities. Evaluating the Dox capture performance of these materials revealed an overall trend where increasing crosslinking density increased Dox adsorption, although the differences for the lower crosslinked materials were not statistically significant (**Fig. 3.3**). This result appears counterintuitive as increased crosslink density would generate a more rigid resin, less susceptible to swelling and Dox diffusion into the polymer network. One possible explanation is that the higher crosslink density preserves an optimal network architecture that facilitates strong Dox binding. For example, the interaction between the resin and Dox may induce a conformational rearrangement of the polymer chain that carries a higher entropic penalty in the less crosslinked materials, a penalty that is reduced when the resin is conformationally restricted by high crosslink density. An alternative possibility is that the more hydrophobic crosslinker favorably interacts with the hydrophobic portions of Dox synergistically with the electrostatic interactions between the resin carboxylates and the Dox amine ($pKa \approx 8.2$).

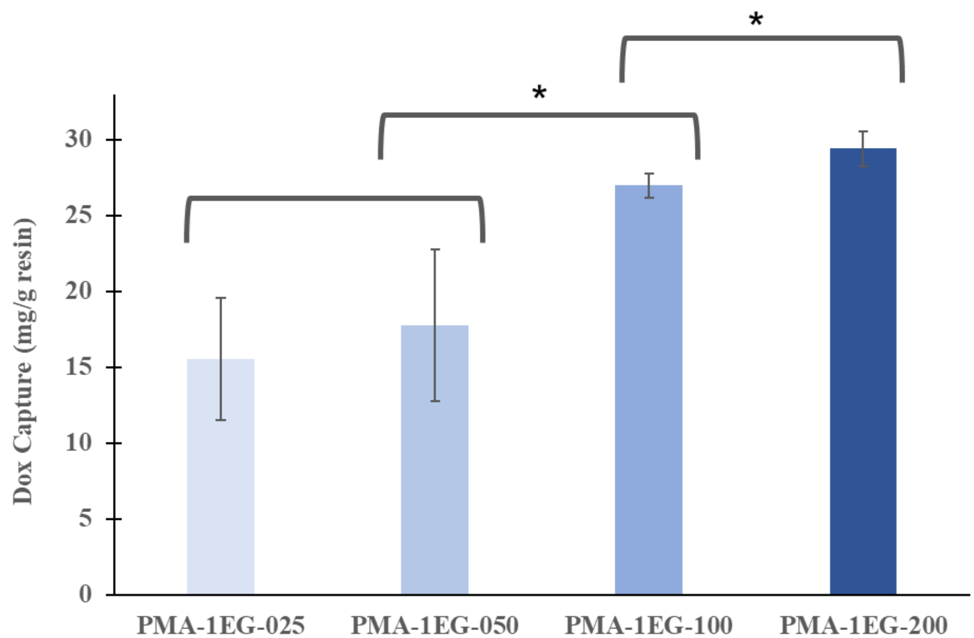

Figure 3.3. Dox capture from 0.05 mg mL^{-1} solution at pH 7.4 for PMA-1EG resins with increasing crosslinker:monomer ratios (0.25, 0.50, 1.00 and 2.00)

To distinguish between these possibilities—enhanced Dox capture driven by resin rigidity versus hydrophobic interactions—we synthesized a set of materials that varied both crosslinking density and crosslinker structure. MA was copolymerized with diethylene glycol dimethacrylate (2EG) and triethylene glycol dimethacrylate (3EG) (ethylene glycol units = 2 and 3, respectively) to produce polymer networks with increased chain mobility, thus reducing the rigidity of the resin. PMA-2EG and PMA-3EG resins with 0.25, 0.50, 1.00 and 2.00 crosslinker equivalents were used to capture Dox in PBS (pH 7.4) and the results were compared to the corresponding PMA-1EG resins. We hypothesized that if resin rigidity was driving the increase in Dox capture with increased crosslinking density, then increasing the crosslinker chain length (flexibility) would eliminate this trend, decreasing Dox capture. However, if greater hydrophobic interactions were driving the increase in Dox capture, then increasing the hydrophobic content of the resins with longer crosslinkers should increase the Dox capture.

The materials with longer crosslinkers captured less Dox at all crosslink densities, relative to the shorter 1EG crosslinked materials (**Fig. 3.4**). As crosslink density increased, this trend became more pronounced, with the highest crosslinking density producing the most effective material for the shortest crosslinker (1EG) but the least effective materials for the longer crosslinkers.

While these results support the hypothesis that network rigidity is critical for effective Dox binding, hydrophobicity is likely still playing a key role. During the absorbance measurements, we observed that the 2EG and 3EG resins were more buoyant in the Dox solution compared to the resins synthesized with 1EG. This observation may suggest that the longer crosslinkers produced more hydrophobic or less dense materials that were potentially resistant to swelling with the aqueous Dox solution. Changes in hydrophobicity or density may have negatively impacted drug capture by limiting the interaction between the Dox solution and potential binding sites on the resin.

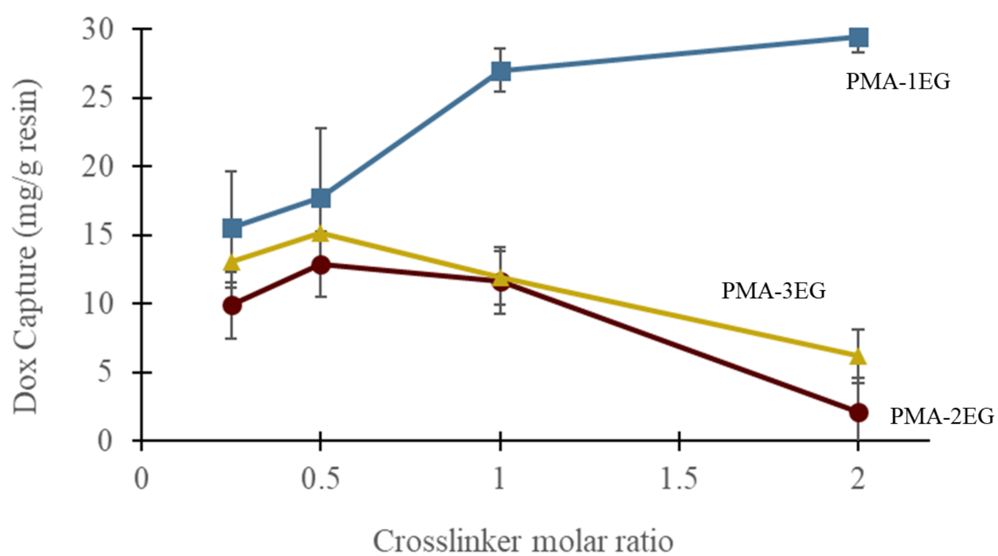

Figure 3.4. Dox capture comparison of copolymer resins synthesized with 1EG, 2EG and 3EG with increasing crosslink density (0.25, 0.50, 1.00 and 2.00 molar equivalents)

3.5. Conclusion

These findings underscore the interplay between polymer network rigidity, hydrophobicity, and density in governing the Dox capture performance of anionic resins. We observed that increasing crosslink density can enhance Dox absorption, likely by promoting a more conformationally restricted environment that facilitates electrostatic binding. Moreover, the crosslinker structure also plays a pivotal role by determining network rigidity and hydrophobicity, as excessively hydrophobic networks adversely affect overall capture. Taken together, this work highlights the importance of tuning crosslink density and crosslinker structure to optimize both electrostatic interactions and hydrophobicity to ultimately produce increasingly effective drug-capture materials.

3.6. References

1) J Wang, Y.-X. Transcatheter embolization therapy in liver cancer. *Recent Pat. Med. Img.* **2012**, *2* (2), 150-162.(1) J Wang, Y.-X. Transcatheter embolization therapy in liver cancer. *Recent Pat. Med. Img.* **2012**, *2* (2), 150-162.

(2) Patel, A. S.; Saeed, M.; Yee, E. J.; Yang, J.; Lam, G. J.; Losey, A. D.; Lillaney, P. V.; Thorne, B.; Chin, A. K.; Malik, S. Development and validation of endovascular chemotherapy filter device for removing high-dose doxorubicin: preclinical study. *J. Med. Dev.* **2014**, *8* (4), 041008-041001 - 041008-041008.

(3) Sun, V. C.-Y.; Sarna, L. Symptom management in hepatocellular carcinoma. *Clin. J. Onco.l Nurs.* **2008**, *12* (5), 759-766.

(4) Altekruse, S. F.; McGlynn, K. A.; Reichman, M. E. Hepatocellular carcinoma incidence, mortality, and survival trends in the United States from 1975 to 2005. *J. Clin. Oncol.* **2009**, *27* (9), 1485-1491.

(5) Rammohan, A.; Sathyanesan, J.; Ramaswami, S.; Lakshmanan, A.; Senthil-Kumar, P.; Srinivasan, U. P.; Ramasamy, R.; Ravichandran, P. Embolization of liver tumors: Past, present and future. *World J. Radiol.* **2012**, *4* (9), 405.

(6) Savic, L. J.; Chen, E.; Nezami, N.; Murali, N.; Hamm, C. A.; Wang, C.; Lin, M.; Schlachter, T.; Hong, K.; Georgiades, C. Conventional vs. Drug-Eluting Beads Transarterial Chemoembolization for Unresectable Hepatocellular Carcinoma—A Propensity Score Weighted Comparison of Efficacy and Safety. *Cancers* **2022**, *14* (23), 5847.

(7) Sieghart, W.; Hucke, F.; Peck-Radosavljevic, M. Transarterial chemoembolization: modalities, indication, and patient selection. *J. Hepatol.* **2015**, *62* (5), 1187-1195.

(8) Anwanwan, D.; Singh, S. K.; Singh, S.; Saikam, V.; Singh, R. Challenges in liver cancer and possible treatment approaches. *Biochim Biophys Acta Rev Cancer* **2020**, *1873* (1), 188314.

(9) Wáng, Y.-X. J.; De Baere, T.; Idée, J.-M.; Ballet, S. Transcatheter embolization therapy in liver cancer: an update of clinical evidences. *Chin. J. Cancer Res.* **2015**, *27* (2), 96-121.

(10) Tacar, O.; Sriamornsak, P.; Dass, C. R. Doxorubicin: an update on anticancer molecular action, toxicity and novel drug delivery systems. *J. Pharm. Pharmacol.* **2013**, *65* (2), 157-170.

(11) Aboian, M. S.; Yu, J. F.; Gautam, A.; Sze, C.-H.; Yang, J. K.; Chan, J.; Lillaney, P. V.; Jordan, C. D.; Oh, H.-J.; Wilson, D. M. In vitro clearance of doxorubicin with a DNA-based filtration device designed for intravascular use with intra-arterial chemotherapy. *Biomed. Microdevices* **2016**, *18*, 1-9.

(12) Liu, G.; Jin, Q.; Liu, X.; Lv, L.; Chen, C.; Ji, J. Biocompatible vesicles based on PEO-b-PMPC/α-cyclodextrin inclusion complexes for drug delivery. *Soft Matter* **2011**, *7* (2), 662-669.

(13) Jain, D. Cardiotoxicity of doxorubicin and other anthracycline derivatives. *J. Nucl. Cardiol.* **2000**, *7*, 53-62.

(14) August, D.; Verma, N.; Vaerten, M.; Shah, R.; Andrews, J.; Brenner, D. Pharmacokinetic evaluation of percutaneous hepatic venous isolation for administration of regional chemotherapy. *J. Surg. Oncol.* **1995**, *4* (4), 205-216.

(15) Cheung-Ong, K.; Giaever, G.; Nislow, C. DNA-damaging agents in cancer chemotherapy: serendipity and chemical biology. *Chem. Biol.* **2013**, *20* (5), 648-659.

(16) Minotti, G.; Menna, P.; Salvatorelli, E.; Cairo, G.; Gianni, L. Anthracyclines: molecular advances and pharmacologic developments in antitumor activity and cardiotoxicity. *Pharmacol. Rev.* **2004**, *56* (2), 185-229.

(17) Carvalho, C.; Santos, R. X.; Cardoso, S.; Correia, S.; Oliveira, P. J.; Santos, M. S.; Moreira, P. I. Doxorubicin: the good, the bad and the ugly effect. *Curr. Med. Chem.* **2009**, *16* (25), 3267-3285.

(18) Pugazhendhi, A.; Edison, T. N. J. I.; Velmurugan, B. K.; Jacob, J. A.; Karuppusamy, I. Toxicity of Doxorubicin (Dox) to different experimental organ systems. *Life Sci.* **2018**, *200*, 26-30.

(19) Injac, R.; Strukelj, B. Recent advances in protection against doxorubicin-induced toxicity. *Technol. Cancer Res. Treat.* **2008**, *7* (6), 497-516.

(20) Yee, D. W.; Hetts, S. W.; Greer, J. R. 3D-Printed Drug Capture Materials Based on Genomic DNA Coatings. *ACS Appl. Mater. Interfaces* **2021**, *13* (35), 41424-41434.

(21) Chen, X. C.; Oh, H. J.; Yu, J. F.; Yang, J. K.; Petzetakis, N.; Patel, A. S.; Hetts, S. W.; Balsara, N. P. Block copolymer membranes for efficient capture of a chemotherapy drug. *ACS Macro Lett.* **2016**, *5* (8), 936-941.

(22) Roche, A.; Girish, B. V.; de Baère, T.; Baudin, E.; Boige, V.; Elias, D.; Lasser, P.; Schlumberger, M.; Ducreux, M. Trans-catheter arterial chemoembolization as first-line treatment for hepatic metastases from endocrine tumors. *Eur. Radiol.* **2003**, *13*, 136-140.

(23) Blumenfeld, C. M.; Schulz, M. D.; Aboian, M. S.; Wilson, M. W.; Moore, T.; Hetts, S. W.; Grubbs, R. H. Drug capture materials based on genomic DNA-functionalized magnetic nanoparticles. *Nat. Commun.* **2018**, *9* (1), 1-7.

(24) Oh, H. J.; Aboian, M. S.; Yi, M. Y.; Maslyn, J. A.; Loo, W. S.; Jiang, X.; Parkinson, D. Y.; Wilson, M. W.; Moore, T.; Yee, C. R. 3D printed absorber for capturing chemotherapy drugs before they spread through the body. *ACS Cent. Sci.* **2019**, *5* (3), 419-427.

(25) Krishnamoorthy, S.; Grubbs, R. H. Aldehyde-Functionalized Magnetic Particles to Capture Off-Target Chemotherapeutic Agents. *ACS Omega* **2020**, *5* (45), 29121-29126.

(26) Su, G. A.; Wadsworth, O. J.; Muller, H. S.; Archer, W. R.; Hetts, S. W.; Schulz, M. D. Polymer–nucleobase composites for chemotherapy drug capture. *J. Mater. Chem. B* **2023**, *11* (35), 8449-8455.

(27) So, J.; Pang, C.; Dong, H.; Jang, P.; Juhyok, U.; Ri, K.; Yun, C. Adsorption of 1-naphthyl methyl carbamate in water by utilizing a surface molecularly imprinted polymer. *Chem. Phys. Lett.* **2018**, *699*, 199-207.

(28) Krupadam, R. J.; Khan, M. S.; Wate, S. R. Removal of probable human carcinogenic polycyclic aromatic hydrocarbons from contaminated water using molecularly imprinted polymer. *Water Res.* **2010**, *44* (3), 681-688.

(29) Ghasemi, S.; Nematollahzadeh, A. Molecularly imprinted polymer membrane for the removal of naphthalene from petrochemical wastewater streams. *Adv. Polym. Technol.* **2018**, *37* (6), 2288-2293.

(30) Huang, D.-L.; Wang, R.-Z.; Liu, Y.-G.; Zeng, G.-M.; Lai, C.; Xu, P.; Lu, B.-A.; Xu, J.-J.; Wang, C.; Huang, C. Application of molecularly imprinted polymers in wastewater treatment: a review. *Environ. Sci. Pollut. Res.* **2015**, *22*, 963-977.

(31) Meléndez-Marmolejo, J.; Díaz de León-Martínez, L.; Galván-Romero, V.; Villarreal-Lucio, S.; Ocampo-Pérez, R.; Medellín-Castillo, N. A.; Padilla-Ortega, E.; Rodríguez-Torres, I.; Flores-Ramírez, R. Design and application of molecularly imprinted polymers for adsorption and environmental assessment of anti-inflammatory drugs in wastewater samples. *Environ. Sci. Pollut. Res.* **2022**, *29* (30), 45885-45902.

(32) Aylaz, G.; Kuhn, J.; Lau, E. C.; Yeung, C. C.; Roy, V. A.; Duman, M.; Yiu, H. H. Recent developments on magnetic molecular imprinted polymers (MMIPs) for sensing, capturing, and monitoring pharmaceutical and agricultural pollutants. *J. Chem. Technol. Biotechnol.* **2021**, *96* (5), 1151-1160.

(33) Ncube, S.; Kunene, P.; Tavengwa, N. T.; Tutu, H.; Richards, H.; Cukrowska, E.; Chimuka, L. Synthesis and characterization of a molecularly imprinted polymer for the isolation of the 16 US-EPA priority polycyclic aromatic hydrocarbons (PAHs) in solution. *J. Environ. Manage.* **2017**, *199*, 192-200.

(34) Zhu, X.; Yang, J.; Su, Q.; Cai, J.; Gao, Y. Selective solid-phase extraction using molecularly imprinted polymer for the analysis of polar organophosphorus pesticides in water and soil samples. *J. Chromatogr. A* **2005**, *1092* (2), 161-169.

(35) Boulanouar, S.; Combès, A.; Mezzache, S.; Pichon, V. Synthesis and application of molecularly imprinted polymers for the selective extraction of organophosphorus pesticides from vegetable oils. *J. Chromatogr. A* **2017**, *1513*, 59-68.

(36) Archer, W. R.; Hall, B. A.; Thompson, T. N.; Wadsworth, O. J.; Schulz, M. D. Polymer sequestrants for biological and environmental applications. *Polymer International* **2019**, *68* (7), 1220-1237.

(37) Meouche, W.; Laatikainen, K.; Margaillan, A.; Silvonen, T.; Siren, H.; Sainio, T.; Beurroies, I.; Denoyel, R.; Branger, C. Effect of porogen solvent on the properties of nickel ion imprinted polymer materials prepared by inverse suspension polymerization. *Eur. Polym. J.* **2017**, *87*, 124-135.

(38) Bird, L.; Herdes, C. The porogen effect on the complexation step of trinitrotoluene–methacrylic acid: towards efficient imprinted polymer sensors. *Mol. Syst. Des. Eng.* **2018**, *3* (1), 89-95.

(39) Yu, S.; Ng, F. L.; Ma, K. C. C.; Mon, A. A.; Ng, F. L.; Ng, Y. Y. Effect of porogenic solvent on the porous properties of polymer monoliths. *J. Appl. Polym. Sci.* **2013**, *127* (4), 2641-2647.

(40) Dong, H.; Du, H.; Qian, X. Theoretical prediction of p K a values for methacrylic acid oligomers using combined quantum mechanical and continuum solvation methods. *J. Phys. Chem. A* **2008**, *112* (49), 12687-12694.

(41) Lide, D. R. *CRC handbook of chemistry and physics*; CRC press, 2004.

(42) Paul, G.; Begni, F.; Melicchio, A.; Golemme, G.; Bisio, C.; Marchi, D.; Cossi, M.; Marchese, L.; Gatti, G. Hyper-cross-linked polymers for the capture of aromatic volatile compounds. *ACS Appl. Polym. Mater.* **2019**, *2* (2), 647-658.

(43) Shen, J.; Lin, X.; Liu, J.; Li, X. Effects of cross-link density and distribution on static and dynamic properties of chemically cross-linked polymers. *Macromolecules* **2018**, *52* (1), 121-134.

(44) Huang, J.; Turner, S. R. Hypercrosslinked polymers: a review. *Polym. Rev.* **2018**, *58* (1), 1-41.

3.7. Supporting Information

Table 3.S1. Mole ratios of monomer, crosslinker and Dox template incorporated in the syntheses of molecular imprinted polymers (MIP)

Mole Ratios of MIP Reagents		
Monomer	**Cross-linker**	**Dox Template**
1	3	0.02
1	2	0.02
1	1	0.02
1	7	0.01
1	5	0.01
1	2.5	0.01
1	1	0.01
1	5	0.005
1	3	0.005
1	2	0.005

Table 3.S2. Dox template removal conditions employed to generate molecular imprinted resins

Procedures used to remove Dox template		
Solvent	Temperature (°C)	Duration (h)
Water	RT	48
Water	60	72
Water	Reflux	48
Acetone	RT	24
Acetone	50	24
DMSO	RT	48
DMSO	100	48
DMSO	150	48

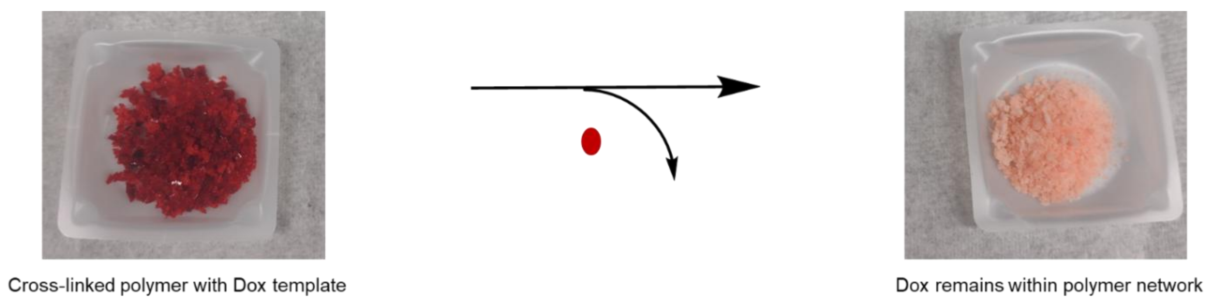

Figure 3.S1. MIP resin before and after Dox template removal attempts.

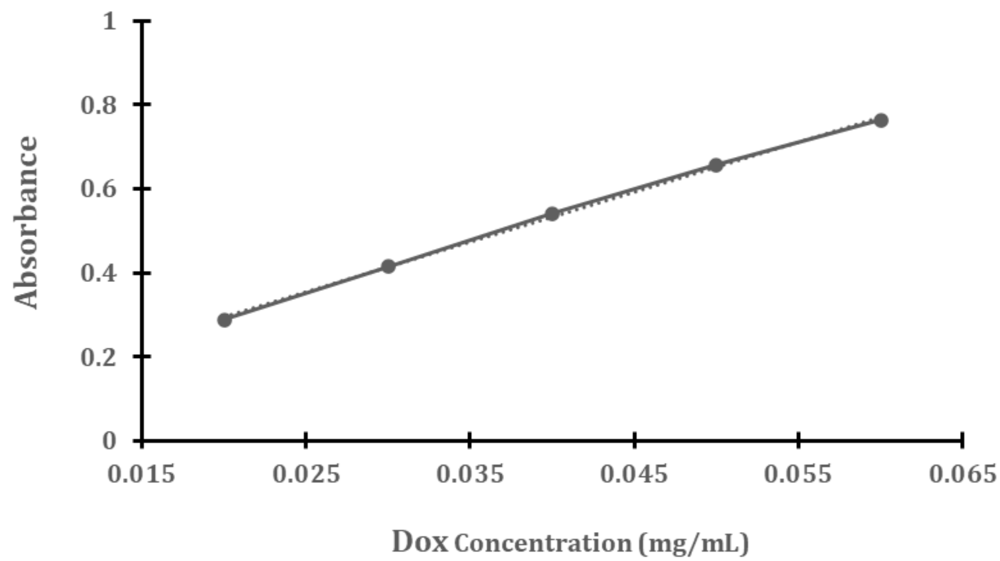

Figure 3.S2. Dox calibration plot using UV-vis spectroscopy

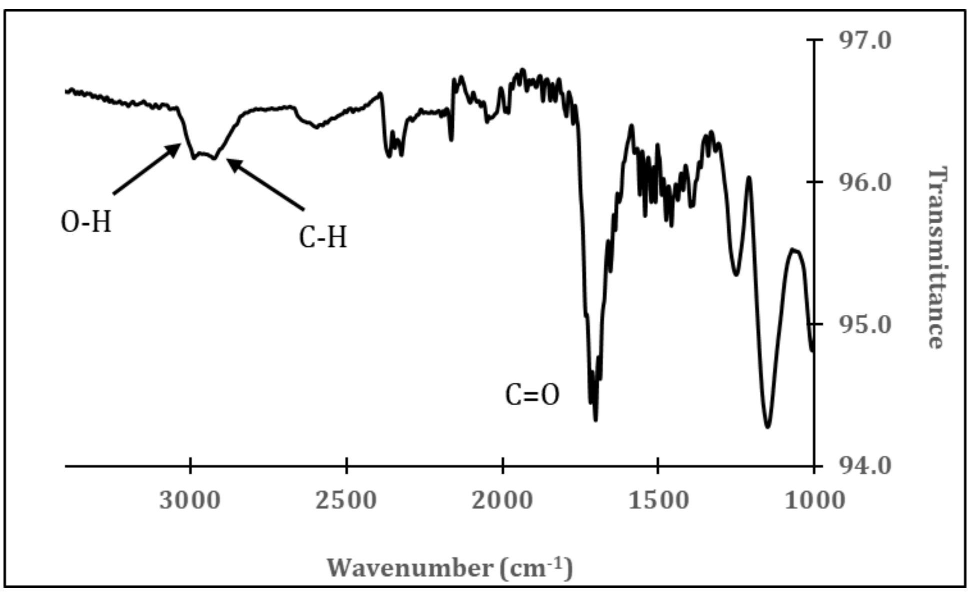

Figure 3.S3. FTIR spectrum of PMA-1EG-025 confirming incorporation of MA and 1EG with vibration bands corresponding to O-H of MA and C=O of MA and IEG

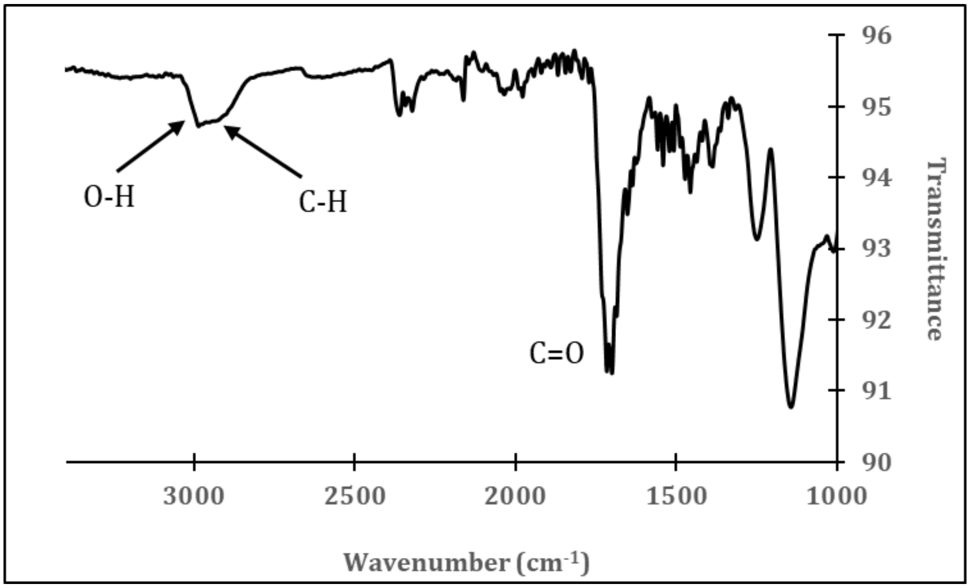

Figure 3.S4. FTIR spectrum of MA-1EG-050 confirming incorporation of MA and 1EG with vibration bands corresponding to O-H of MA and C=O of MA and IEG

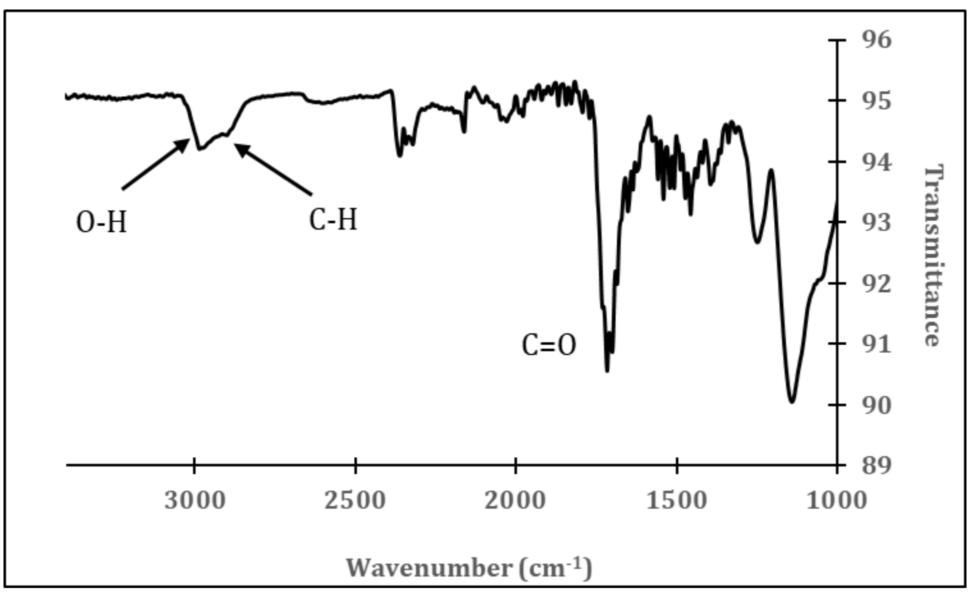

Figure 3.S5. FTIR spectrum of MA-1EG-100 confirming incorporation of MA and 1EG with vibration bands corresponding to O-H of MA and C=O of MA and IEG

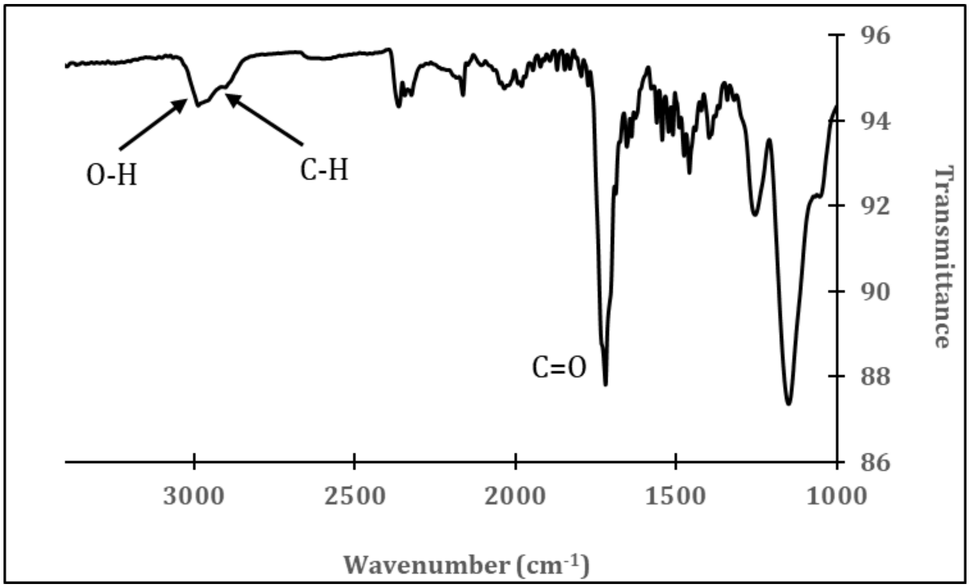

Figure 3.S6. FTIR spectrum of MA-1EG-200 confirming incorporation of MA and 1EG with vibration bands corresponding to O-H of MA and C=O of MA and IEG

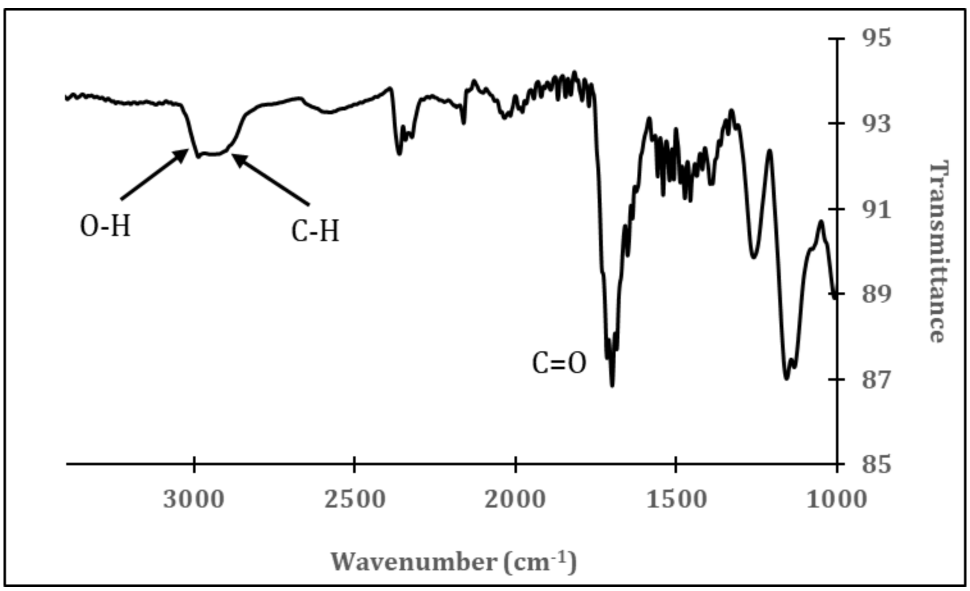

Figure 3.S7. FTIR spectrum of MA-2EG-025 confirming incorporation of MA and 1EG with vibration bands corresponding to O-H of MA and C=O of MA and 2EG

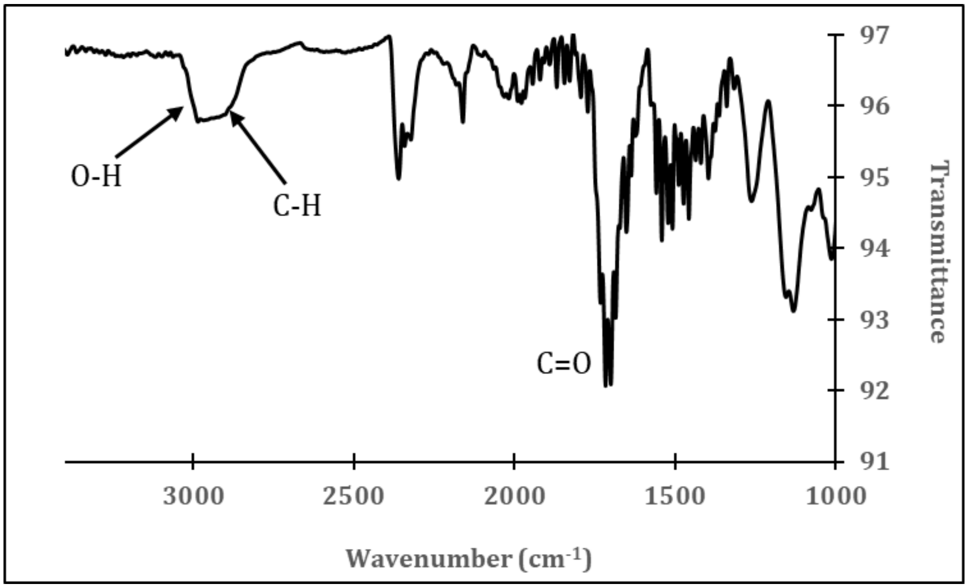

Figure 3.S8. FTIR spectrum of MA-2EG-050 confirming incorporation of MA and 1EG with vibration bands corresponding to O-H of MA and C=O of MA and 2EG

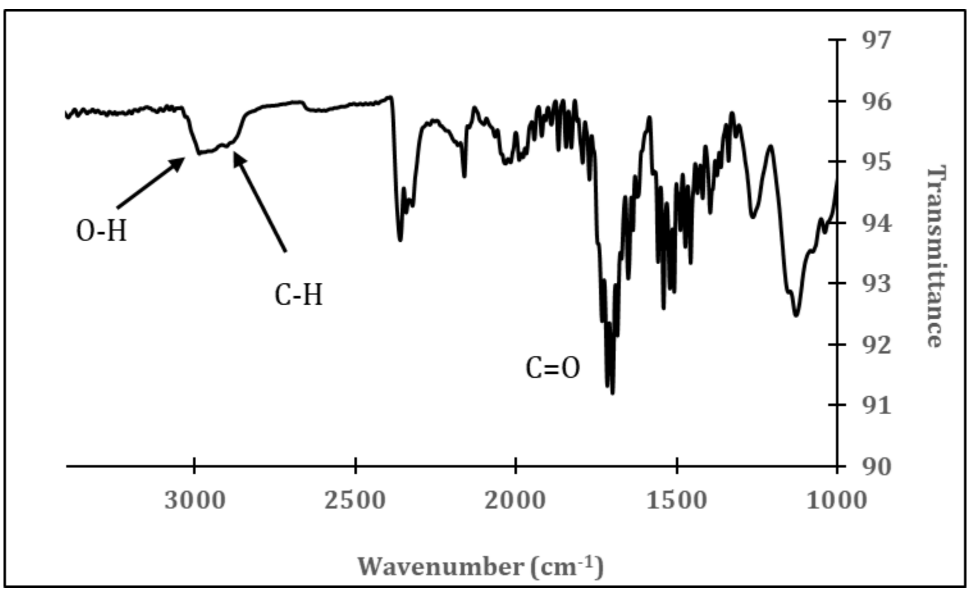

Figure 3.S9. FTIR spectrum of MA-2EG-100 confirming incorporation of MA and 1EG with vibration bands corresponding to O-H of MA and C=O of MA and 2EG

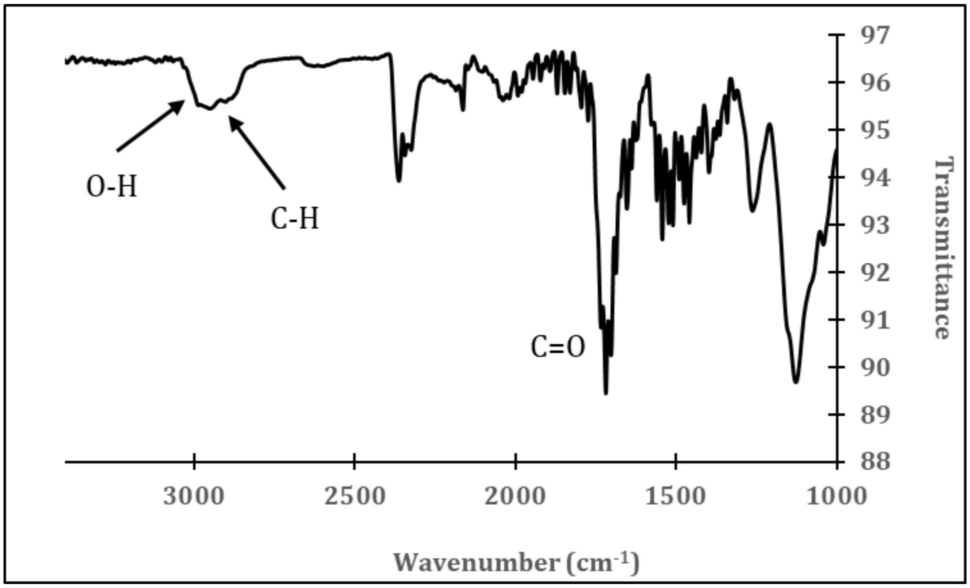

Figure 3.S10. FTIR spectrum of MA-2EG-200 confirming incorporation of MA and 2EG with vibration bands corresponding to O-H of MA and C=O of MA and 2EG

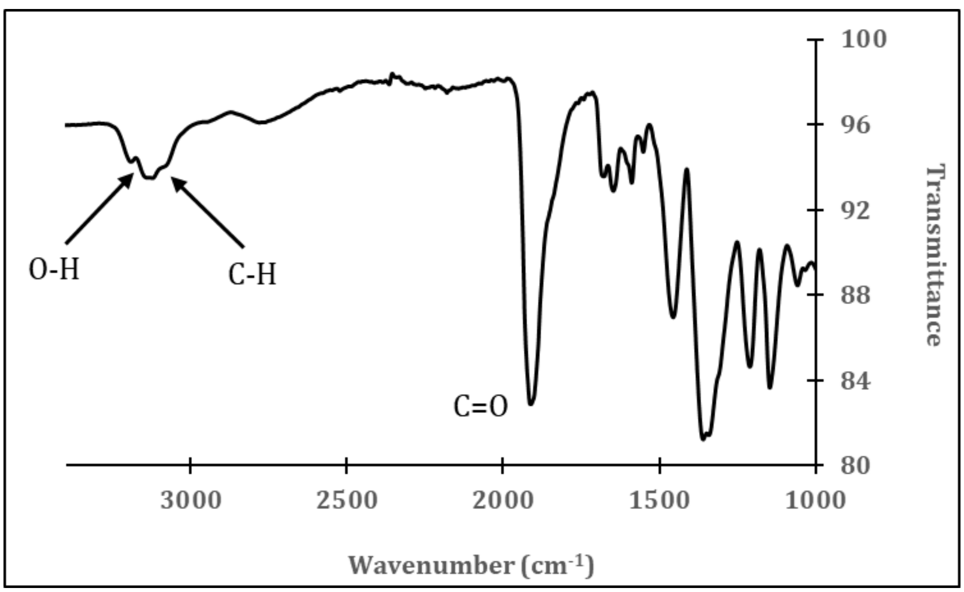

Figure 3.S11. FTIR spectrum of MA-3EG-025 confirming incorporation of MA and 1EG with vibration bands corresponding to O-H of MA and C=O of MA and 3EG

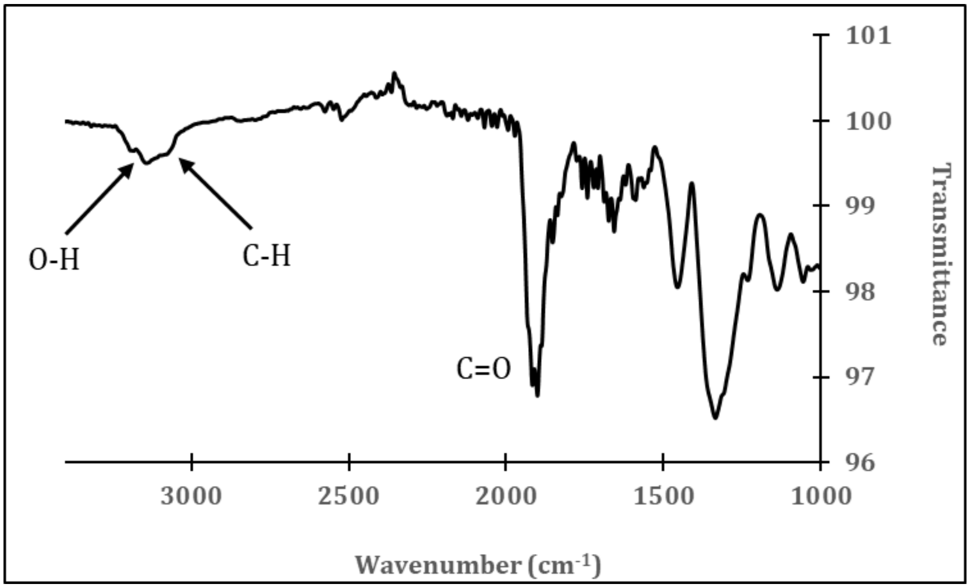

Figure 3.S12. FTIR spectrum of MA-3EG-050 confirming incorporation of MA and 3EG with vibration bands corresponding to O-H of MA and C=O of MA and 3EG

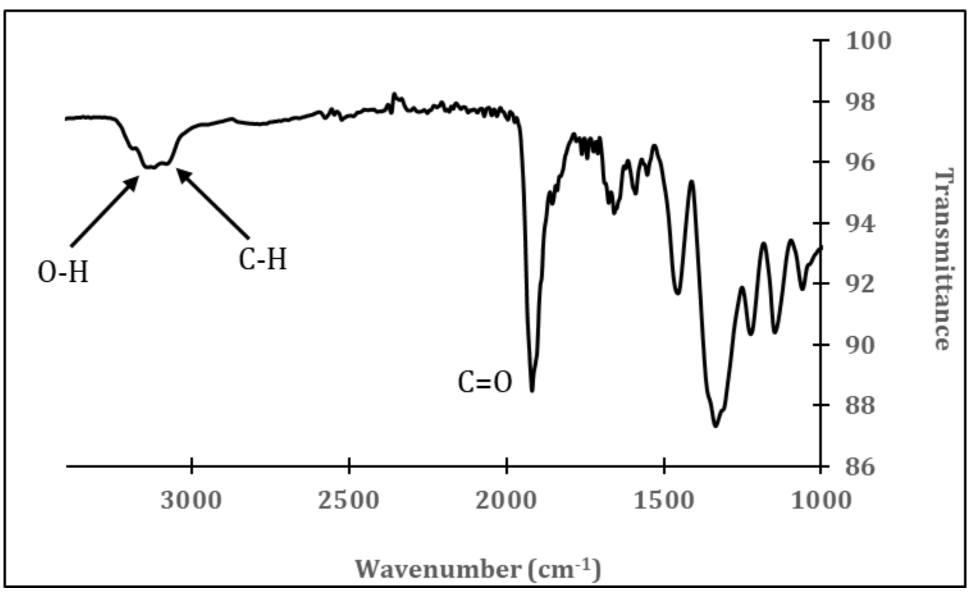

Figure 3.S13. FTIR spectrum of MA-3EG-100 confirming incorporation of MA and 3EG with vibration bands corresponding to O-H of MA and C=O of MA and 3EG

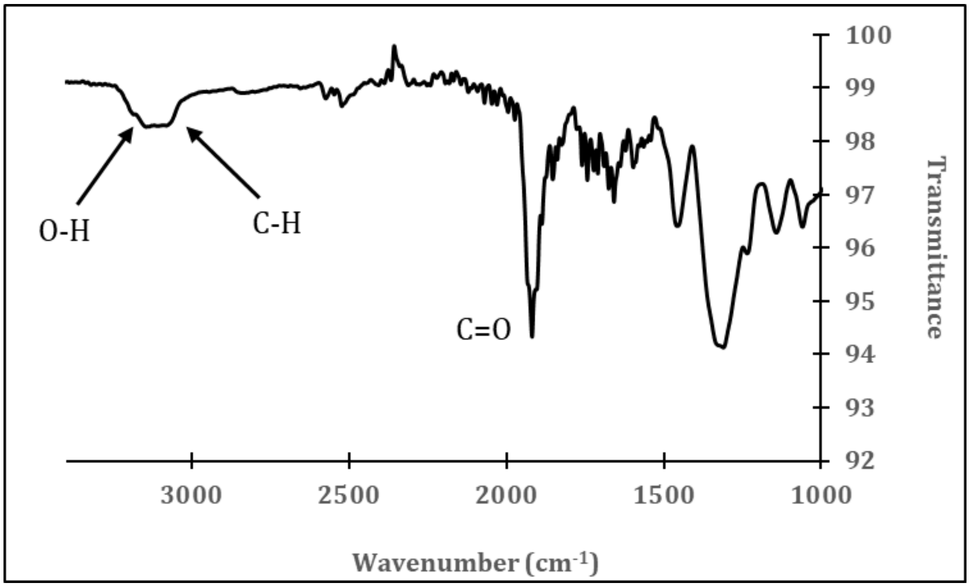

Figure 3.S14. FTIR spectrum of MA-3EG-200 confirming incorporation of MA and 3EG

Chapter 4. Synthesis and Post-polymerization Modification of Mannose-Containing Glycopolymers to Improve Antimicrobial Properties while Reducing Hemolytic Activity

Ophelia J. Wadsworth,[a] Brady A. Hall,[a] and Michael D. Schulz.[a,b,c]

[a] *Department of Chemistry, Virginia Polytechnic Institute and State University, Blacksburg, VA 24061, USA*

[b] *Macromolecules Innovation Institute, Virginia Polytechnic Institute and State University, Blacksburg, VA 24061, USA*

[c] *Center for Emerging, Zoonotic, and Arthropod-borne Pathogens, Virginia Polytechnic Institute and State University, Blacksburg, VA 24061, USA*

4.1. Abstract

Antibiotics have significantly mitigated the global impact of bacterial infections; however, many bacterial strains have adapted resistance mechanisms over time, leading to diminished antibiotic efficacy. Glycopolymers are a promising class of alternative antibacterial therapeutics to treat infections attributable to antibiotic resistant bacterial strains. The sugar-containing sidechains may mitigate bacterial infections by competing for the binding sites on the bacterial surfaces. In our previous work, we synthesized linear mannose-containing polynorbornene glycopolymers (25-250 kDa) and evaluated their antimicrobial properties in the absence of traditional antibiotic moieties such as cationic groups. Broth dilution and hemolysis assays revealed a dependence of inhibition and hemolytic activities on molecular weight, with higher molecular weight polymers demonstrating enhanced inhibition of *E. coli* and greater lysis of red blood cells. Inspired by the inherent antimicrobial properties of these glycopolymers, we sought to enhance the antimicrobial properties while simultaneously reducing the hemolytic activity by tuning the functionality and hydrophobicity of the polymer backbone. Post-polymerization modification was accomplished via thiol-ene addition to the polymer backbone with thiolated-mannose or cysteamine at 0.5 and

1.0 ligand to polymer molar ratios. Thiolated-mannose was employed as a ligand to increase mannose density, potentially enhancing lectin-receptor binding interactions while cysteamine would incorporate cationic charges, which are known to disrupt bacterial membranes. A series of sixteen mannose-containing polynorbornene glycopolymers were synthesized and will be characterized via ^{13}C NMR to confirm backbone modification, indicated by a reduction or disappearance of the C=C signals between 130-140 ppm. The degree of functionalization will be quantified using elemental analysis. Comprehensive biological assays will follow to assess the antimicrobial and hemolytic performances and determine the structure-activity relationships. By successfully polymerizing a mannose-functionalized norbornene monomer followed by post-polymerization modification with thiolated-mannose and cysteamine, we generated a set of materials with precise architecture that differs only in their pendant functionalities. We demonstrated that the backbone alkenes of these glycopolymers are amenable to thiol-ene click chemistry, allowing for the efficient post-polymerization installation of additional glycans or cationic moieties. This modular and versatile synthetic platform lays the groundwork for future studies aimed at systematically probing the structure–activity relationships of these antimicrobial glycomaterials.

4.2. Introduction

Bacterial infection-related deaths have been categorized as an urgent priority globally and are projected to increase annually, with an estimated mortality rate of 10 million per year by 2050.[1] Antibiotics have significantly mitigated the global impact of bacterial infections; however, many bacterial strains have adapted resistance mechanisms over time, leading to diminished antibiotic efficacy.[2] Overprescription of these drugs has enabled bacterial strains to develop resistance at a faster rate, rendering some infections untreatable.[3-5] Consequently, there is now an overwhelming need for new antibacterial therapeutics with equal or enhanced efficacy that can evade the drug-resistance that plagues current antibiotics.[6, 7]

Glycopolymers, synthetic macromolecules that incorporate various pendant carbohydrates as sidechains[8, 9] are widely explored as alternative therapeutics to treat infections attributable to antibiotic-resistant bacterial strains. Carbohydrates (glycans) are critical to biological functions such as cell signaling, inflammation, immune responses and molecular recognition.[10-14] For example, pathogens initiate infection by attaching to the surface of host cells.[15] This critical step involves adhesion via ligand-receptor binding between glycan specific lectins on the bacterial cell and receptors on host cells before invasion and infection begin.[16-20] The pathogenic bacterium *E. coli* uses its type 1 fimbriae lectin to bind to mannose receptors of tissue cells in the urinary tract or its type P pili lectin to bind to galactose receptors on the surface of kidney cells, promoting infection.[21, 22] Glycopolymers are promising alternative antibacterial therapeutics to treat infections attributable to antibiotic-resistant bacterial strains, because their sugar-containing sidechains can mitigate bacterial infections by competing for the binding sites on the bacterial surfaces. Additionally, development of resistance is less likely, since the lectin-receptor binding interaction is critical to bacterial adhesion and infection.

Mannose-based glycopolymers have been investigated for their antibacterial properties, however; to the best of our knowledge, mannose was only incorporated as a comonomer that facilitated specific recognition with *E. coli* while the cationic moiety disrupted the bacterial membrane.[4] Mannose-based homopolymers have demonstrated enhanced binding affinity for *E. coli*;[23-25] however, the highest molecular weight reported was 64 kDa. To determine the effect of molecular weight on bacterial growth inhibition, we previously synthesized linear mannose-containing polynorbornene glycopolymers (25-250 kDa) via ring-opening metathesis polymerization (ROMP) and evaluated their antibacterial properties in the absence of traditional antibiotic moieties such as cationic groups.[26] Broth dilution and hemolysis assays revealed a dependence of inhibition and hemolytic activities on molecular weight, with higher molecular weight polymers demonstrating enhanced inhibition of *E. coli* and greater lysis of red blood cells. We postulated that the higher molecular weight polymers produced more polyvalent binding interactions with the bacterial cell surface. This stronger interaction may have facilitated membrane permeation, allowing the glycopolymer to inhibit bacterial growth by targeting an intracellular site. Simultaneously, the hydrophobic backbone produced greater hemolytic activity due to cell membrane disruption.[27] Regardless, the higher molecular weight polymers demonstrated greater bacterial inhibition, exhibiting inherent antimicrobial properties.

Inspired by the inherent antimicrobial properties of the mannose-containing glycopolymers, we sought to improve the inhibition activity while simultaneously reducing the hemolytic activity via post-polymerization modification of the polymer backbone. The olefin functional groups present in the polymer backbone facilitated thiol-ene addition that we leveraged to generate materials with more mannose binding sites. Four molecular weights were modified with 0.5 and 1.0 molar equivalents of thiolated-mannose. Thiolated-mannose was incorporated to increase mannose density, potentially enhancing lectin-receptor binding interactions. We postulated that the modified polymers would exhibit greater potency as growth inhibitors of *E. coli*, owing to the additional binding interactions. We also incorporated cysteamine to evaluate its contribution to the potency of the modified materials, as cationic charges are known to disrupt bacterial membranes.[28, 29] These modifications allow us to explore how glycan density and cationic charge influence the efficacy of the inherently antimicrobial materials reported in our previous work.[26]

4.3. Experimental

4.3.1. Instrumentation

Size exclusion chromatography (SEC) was performed using the Wyatt Technologies chromatograph with Shimadzu light scattering and refractive index detectors. Carbon nuclear magnetic resonance (^{13}C NMR) spectra were acquired using a Neo 500 MHz spectrometer (2000 scans, 5 sec delay). Samples were dissolved in deuterated chloroform or deuterated dimethyl sulfoxide to generate 30 mg mL^{-1} solutions. The Biotage Isolera One was used to purify the synthesized precursors via flash chromatography with 50 g columns as the stationary phase.

4.3.2. Materials

1,2,3,4,6-Penta-O-acetyl-a-D-mannopyranose (AcMan) was purchased from Biosynth. Boron trifluoride dietherate, dimethyl sulfoxide (DMSO) and dimethyl formamide (DMF) were purchased from Oakwood Products. 2-Hydroxy ethyl acrylate (HEA), 6-mercaptohexan-1-ol and dicyclopentadiene were purchased from Sigma Aldrich. Cyclopentadiene was distilled from dicyclopentadiene according to literature procedure. Toluene, methanol, and dichloromethane were purchased from Fischer Scientific. Grubbs Gen 2 catalyst was acquired from Ambeed, Inc and used to prepare Grubbs Gen 3 catalyst, which was used within two hours of preparation. 2,2-Dimethoxy-2-phenylacetophenone (DMPA) was purchased from Ambeed and used without purification.

4.3.3. Synthesis of Mannose Glycomonomers

AcMan (19.5 g, 0.0500 mol), HEA (8.00 mL, 0.0750 mol), and 100 mL DCM were added to a 250 mL round bottom flask and purged while stirring. The solution was cooled to 0 °C while boron trifluoride diethyl etherate ($BF_3.OEt_2$, 36.0 mL, 0.290 mol) was added at a rate of 0.1 mL min^{-1}. The reaction was stirred at 0 °C for 1 hour then warmed to 25 °C for 48 hours. The reaction mixture was diluted with 400 mL DCM before neutralizing with 300 mL saturated $NaHCO_3$. The organic layer was separated and washed with 1 x 300 mL saturated $NaHCO_3$, 2 x 300 mL DI water, then 1 x 300 mL brine. The organic layer was dried over $MgSO_4$ and concentrated to produce 1-*O*-acryloyloxethyl-2,3,4-6-tetra-*O*-acetyl-a-D-mannopyranoside (AcMan-EA, 21.3 g, 93%) as a yellow oil that was used without further purification.

Cyclopentadiene (2.80 mL, 0.0338 mol) was added to a solution of AcMan-EA (6.00 g, 0.0135 mol) in 150 mL toluene. The mixture was refluxed and allowed to react for 72 hours. After cooling, the solvent was evaporated, and the crude yellow oil product purified via flash chromatography to produce 2-O-(2,3,4,6-tetra-O-acetyl-a-D-mannopyranosyl)hydroxylethyl 5-norbornene-2-carboxylate as a viscous oil (AcMan-ENC, 4.29 g, 62%). The product was a mixture of endo/exo norbornene (71/29) that was polymerized without separation.

4.3.4. Synthesis of Thiolated-mannose

Potassium thioacetate (52.5 g, 0.460 mol) was stirred in 300 mL dried DMF at room temperature for 30 minutes. The mixture was cooled to 0 °C while 1-bromohexan-1-ol (30 mL, 0.230 mol) was added dropwise, then allowed to stir at room temperature for 72 hours. The solution was diluted with 700 mL DI water, then extracted with 2 x 350 mL ethyl acetate. The organic layers were combined and washed with 300 mL DI water and 350 mL brine, then dried over $MgSO_4$. The solvent was removed under reduced pressure to produce *S*-(6-hydroxyhexyl) ethanethioate (6-HHET, 32.3 g, 80%) as a yellow oil that was used without further purification.

AcMan (17.7 g, 0.0454 mol) was reacted with 6-HHET (2 equivalents) in the same manner as described above for the synthesis of AcMan-EA. The crude product was purified via flash chromatography to yield 2-O-(2,3,4,6-tetra-O-acetyl-a-D-mannopyranosyl)hydroxyhexyl ethanethioate (AcMan-HHET, 9.40 g, 41%) as a yellow oil. To deprotect the thiol, AcMan-HHET

(3.40 g, 0.00671 mol) was dissolved in 30 mL DMAc, added dropwise to a solution of dithiothreitol (5.20 g, 0.0337 mol) and triethylamine (0.94 mL, 0.00684 mol) in 20 mL DMAc and allowed to stir at room temperature for 48 hours. The solution was diluted with 150 mL DI water and extracted with 3 x 100 mL DCM. The organic layer was washed with 2 x 100 mL HCl (3.00 M), 2 x 200 mL DI water, 200 mL brine and dried over $MgSO_4$. The crude product was purified via flash chromatography to produce 2-O-(2,3,4,6-tetra-O-acetyl-a-D-mannopyranosyl) hydroxy-hexyl thiol (AcMan-OxHSH, 2.10 g, 66%) as a clear oil.

4.3.5. Synthesis and Post-polymerization Modification of Mannose-containing Polynorbornene Glycopolymers

AcMan-ENC (2 g, 0.00390 mol) was dissolved in 15 mL DCM. From a stock solution of G3 catalyst in DCM, the appropriate amount of catalyst (based on the targeted molecular weights of 25.6, 51.2, 128, and 256) was added in one portion under a nitrogen atmosphere. The mixture was allowed to react for 2 hours at room temperature before termination with ethyl vinyl ether (200 equivalents). The product was precipitated in 150 mL methanol, filtered, washed with methanol, and dried under reduced pressure to produce mannose-containing norbornene parent polymers (P-AcMan).

P-AcMan (0.5 g, 0.000976 mol) was dissolved in 8 mL dioxane containing DMPA (0.2 equivalents) and thiolated mannose (0.5 or 1.0 equivalents) under a nitrogen atmosphere. The solution was irradiated with UV light for 72 hours, after which the product was precipitated in methanol, filtered, and dried. Post-polymerization modification with cysteamine was carried out similarly, except DMSO was used as the solvent and the product was precipitated in deionized water.

4.4. Results and Discussion

4.4.1. Synthesis of Mannose Glycomonomers

The synthesis of AcMan-EA was extremely efficient, producing a 93% yield. Furthermore, ten-fold larger scale reactions did not diminish the yields. The key factor to generating such high yields is the slow addition of the Lewis acid (0.1 mL min^{-1}), as faster addition rates of strong acids produce side reactions that fragments carbohydrates, consequently reducing the overall yield.[30] In this Koenigs-Knorr like reaction, the anomeric acetyl group was replaced via nucleophilic substitution by HEA. Stereoselectivity in this reaction was governed by neighboring group participation, where the 2-*O*-acyl group facilitated the formation of a 1,2-*trans* product.[31, 32] In the $^4C_1$ conformation of α-AcMan, the axial orientation of the 2-*O*-acyl group enabled participation during the departure of the anomeric leaving group, forming a transient cyclic intermediate. The intermediate occupied the top face of the ring, directing the subsequent nucleophilic attack from the bottom face. As a result, the configuration at the anomeric center was preserved, leading to selective formation of the 1,2-*trans*-glycoside.[33] The mannose-containing norbornene monomer (AcMan-ENC) was prepared by methods adopted from our previous work (**Scheme 4.1**).[26] The norbornene moiety was synthesized via Diels-Alder cycloaddition between AcMan-EA and cyclopentadiene. This synthetic route represents a departure from conventional methods, which introduce the carbohydrate to the norbornene precursor.[34-37] This reaction yields a mixture of endo/exo isomers, favoring the endo isomer as the major product.[38, 39] AcMan-EA was isolated without purification while AcMan-ENC was chromatographed and the solvent reduced to generate a yellow oil (see **Figs 4.S1 to 4.S4** for NMR characterizations).

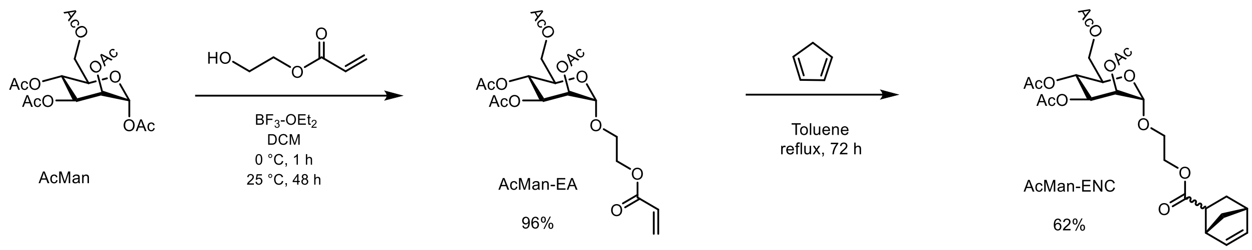

Scheme 4.1. Synthetic route to mannose-containing norbornene glycomonomer; overall yields shown below each product

4.4.2. Synthesis of Thiolated-mannose

To facilitate post-polymerization of the polymer backbone via thiol-ene addition, we first synthesized 6-hydroxyhexyl ethanethioate (6-HHET) to afford transglycosylation with peracetylated mannose (AcMan). Potassium thioacetate was stirred in DMF for 30 minutes before the slow addition of 6-bromohexan-1-ol. The protected thiol was used to prevent its addition to the anomeric position of AcMan in the subsequent step, as sulfur is more nucleophilic than oxygen. The hexyl chain length was selected to circumvent steric interference between mannose and the polymer backbone. The protected thiolated-mannose (AcMan-HHET) was extracted and purified via flash chromatography prior to deprotection with dithiothreitol (DTT) (**Scheme 4.2**). Attempts to deprotect AcMan-HHET without prior purification were unsuccessful. The selective *S*-deacetylation was inspired by native chemical ligation, a method used in peptide and protein synthesis to generate native amide bonds. The authors investigated various conditions to optimize the selective deacetylation of the glycosyl thioester derived from peracetylated glucose. They found that maintaining a mildly basic environment significantly enhanced reaction efficiency, with the highest yields obtained using dimethylacetamide as the solvent. The reaction proceeded via a transthioesterification mechanism, where the *S*-acetyl group was transferred to DTT. As this step is reversible, an excess of DTT (1.5 equivalents) was used. Under these optimized conditions, a maximum yield of 96% was achieved within one hour.[40] However, further optimization was required to achieve successful deacetylation of AcMan-HHET, which contained a hexyl thioester in place of the more reactive glycosyl thioester. To compensate for the reduced reactivity, the amount of DTT was increased to 5 equivalents, and the reaction time was extended to 48 hours. Additionally, the starting material was limited to a maximum of 6.71 mmol to achieve the optimal yield (66%). The deprotected thiolated-mannose (AcMan-OxHSH) was purified via flash chromatography to produce a yellow oil with the characteristic sulfur odor (see **Figs 4.S6 to 4.S11** for NMR characterizations).

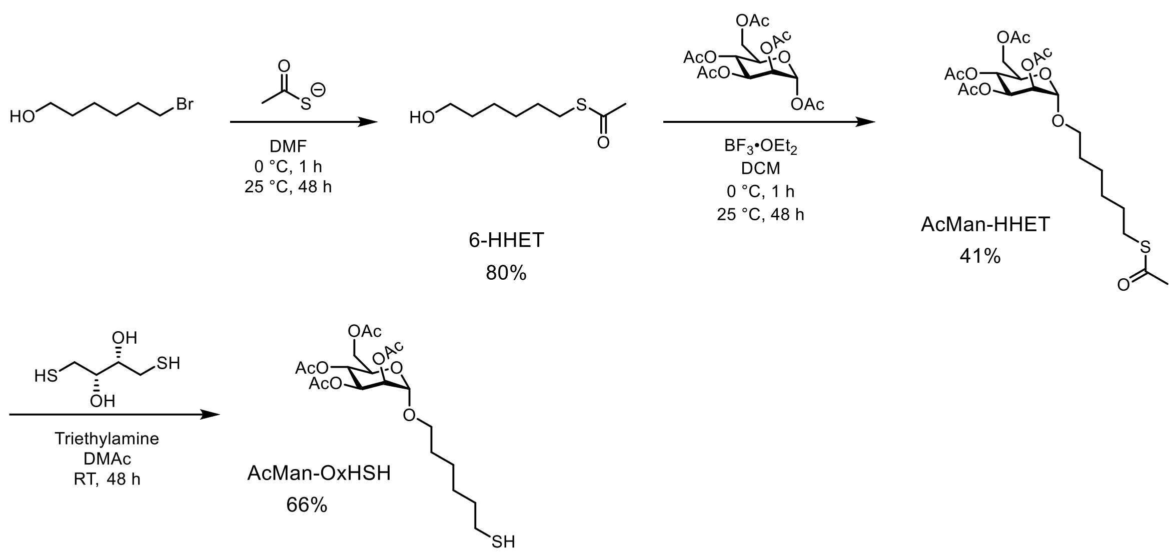

Scheme 4.2. Synthetic route AcMan-OxHSH, the deprotected mannose-thiol used to modify the polymer backbone via thiol-ene addition.

4.4.3. Synthesis and Post-polymerization Modification of Mannose-containing Polynorbornene Glycopolymers

Four molecular weights (25.6, 51.2, 128, and 256 kDa) were targeted with ROMP of the mannose-containing norbornene glycopolymer (**Scheme 4.3**). As ruthenium is known to be cytotoxic,[41, 42] the catalyst was removed by precipitating the polymer product in methanol, which dissolves G3. The catalyst and product were then separated by filtration. ^{1}H NMR was used to confirm polymer synthesis, showing complete disappearance of the norbornene alkene peaks (**Fig. 4.S5**).

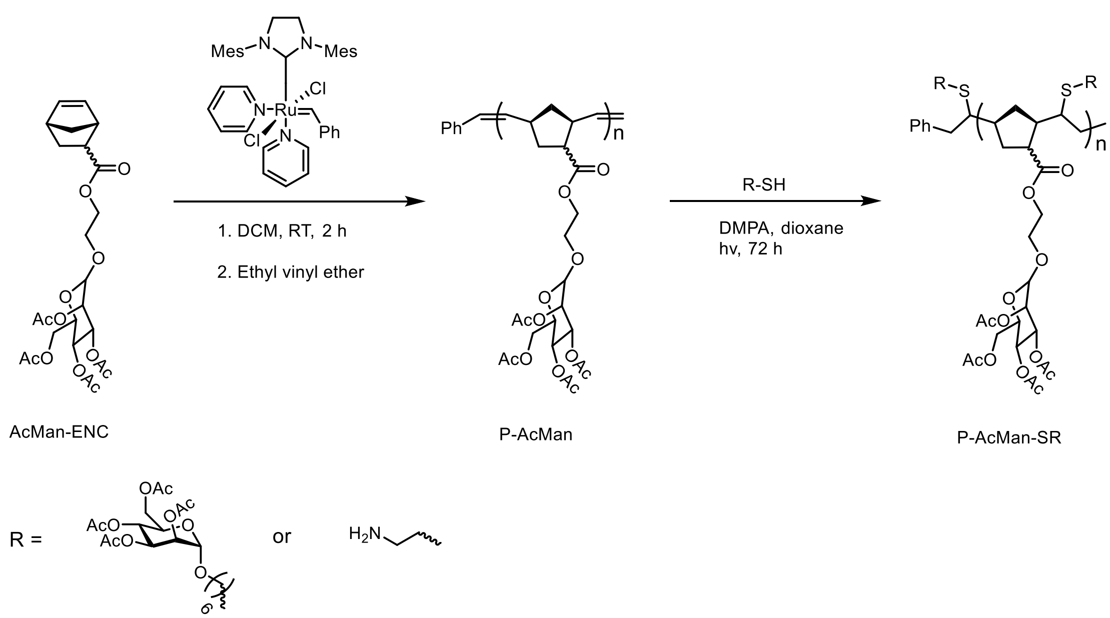

Scheme 4.3. ROMP of AcMan-ENC to generate mannose-containing polynorbornenes of four molecular weights (25.6, 51.2, 128 and 256 kDa). Post-polymerization modification of the polymer backbone was accomplished via thiol-ene addition of thiolated-mannose or cysteamine.

Post-polymerization modification was accomplished via thiol-ene addition to the alkene functional groups in the polymer backbone (**Scheme 4.3**). Prior optimization experiments revealed that the extended reaction time was necessary to observe any detectable modification to the polymer backbone, most likely attributable to steric hindrance. A series of sixteen mannose-containing polynorbornene glycopolymers was synthesized (**Table 4.1**) and will be characterized via ^{13}C NMR to confirm backbone modification, indicated by a reduction or disappearance of the C=C signals between 130-140 ppm. The degree of functionalization will be quantified using elemental analysis. Comprehensive biological assays will follow to assess the antimicrobial and hemolytic performances and determine the structure-activity relationships.

Table 4.1. Polymer molecular weights, ligand identity and ligand to polymer molar ratio used for post-polymerization modification of P-AcMan.

<table>
<tr><th>P-AcMan</th><th>Ligand</th><th>M_n (kDa)* before modification</th><th>Ligand to polymer molar ratio</th></tr>
<tr><td rowspan="16">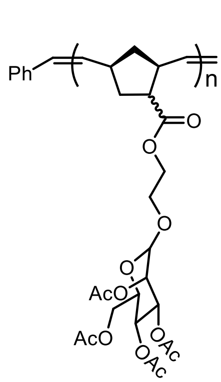
P-AcMan</td><td rowspan="8">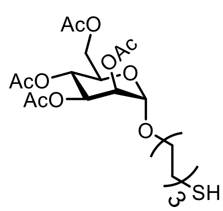
AcMan-OxHSH</td><td rowspan="2">25.6</td><td>0.5</td></tr>
<tr><td>1.0</td></tr>
<tr><td rowspan="2">51.2</td><td>0.5</td></tr>
<tr><td>1.0</td></tr>
<tr><td rowspan="2">128</td><td>0.5</td></tr>
<tr><td>1.0</td></tr>
<tr><td rowspan="2">256</td><td>0.5</td></tr>
<tr><td>1.0</td></tr>
<tr><td rowspan="8">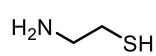
Cysteamine</td><td rowspan="2">25.6</td><td>0.5</td></tr>
<tr><td>1.0</td></tr>
<tr><td rowspan="2">51.2</td><td>0.5</td></tr>
<tr><td>1.0</td></tr>
<tr><td rowspan="2">128</td><td>0.5</td></tr>
<tr><td>1.0</td></tr>
<tr><td rowspan="2">256</td><td>0.5</td></tr>
<tr><td>1.0</td></tr>
</table>

* M_n determined by size exclusion chromatography

Previous studies of backbone modification of polynorbornenes commonly explored the oxa-norbornene derivatives, which benefit from an oxygen containing backbone that facilitates functionalization.[43-45] The reaction times were shorter than 72 hours and complete modification was characterized by disappearance of the cis and trans backbone alkene protons between 5.5 and 6.5 ppm. Furthermore, SEC analysis showed increases to the molecular weights and dispersity, owing to random addition of the ligand to the backbone moiety of polymer chains. Our approach used a hydrocarbon-based polynorbornene backbone, a significant alternate step as these materials are not widely explored for post-polymerization modification, particularly with biologically relevant molecules such as glycans and cationic compounds. We selected to characterize the modified glycopolymers using ^{13}C NMR due to overlapping proton signals of the pyranose sidechain with the backbone alkene protons.

4.5. Conclusion

Building on our successful synthesis of mannose-containing glycopolymers, this chapter presented a straightforward strategy for further functionalizing these materials with the goal of enhancing their antimicrobial properties. We demonstrated that the backbone alkenes of these glycopolymers are amenable to thiol-ene click chemistry, allowing for the efficient post-polymerization installation of additional glycans or cationic moieties. By successfully polymerizing a mannose-functionalized norbornene monomer followed by post-polymerization modification with a thiolated-mannose or cysteamine, we generated a set of materials with precise architecture that differs only in their pendant functionalities. Importantly, among the four degrees of polymerization that were targeted, the functionalized polymers were synthesized from the same initial parent polymer (polymer batch), ensuring that molecular weight, dispersity and backbone structure remained consistent. Consequently, we ensured that the comparisons of the antimicrobial and hemolytic properties will be attributable to the functional group identity, rather than underlying polymer properties. This modular and versatile synthetic platform lays the groundwork for future studies aimed at systematically probing the structure–activity relationships of these antimicrobial glycomaterials.

4.6. References

(1) Hutchings, M. I.; Truman, A. W.; Wilkinson, B. Antibiotics: past, present and future. *Curr. Opin. Microbiol.* **2019**, *51*, 72-80.

(2) Prasad, P. G., A.; Sasmal, P.K. Aggregation-induced emission active metal complexes: A promising strategy to tackle bacterial infections. *Chem. Commun.* **2021**, *57*, 174-186.

(3) Wagenlehner, F.; Lorenz, H.; Ewald, O.; Gerke, P. Why d-Mannose may be as efficient as antibiotics in the treatment of acute uncomplicated lower urinary tract infections—preliminary considerations and conclusions from a non-interventional study. *Antibiotics* **2022**, *11* (3), 314.

(4) Liu, M.; Li, J.; Li, B. Mannose-modificated polyethylenimine: a specific and effective antibacterial agent against Escherichia coli. *Langmuir* **2018**, *34* (4), 1574-1580.

(5) Aslam, B.; Wang, W.; Arshad, M. I.; Khurshid, M.; Muzammil, S.; Rasool, M. H.; Nisar, M. A.; Alvi, R. F.; Aslam, M. A.; Qamar, M. U. Antibiotic resistance: a rundown of a global crisis. *Infect. Drug Resist.* **2018**, 1645-1658.

(6) Engler, A. C.; Wiradharma, N.; Ong, Z. Y.; Coady, D. J.; Hedrick, J. L.; Yang, Y.-Y. Emerging trends in macromolecular antimicrobials to fight multi-drug-resistant infections. *Nano Today* **2012**, *7* (3), 201-222.

(7) Fischbach, M. A.; Walsh, C. T. Antibiotics for emerging pathogens. *Science* **2009**, *325* (5944), 1089-1093.

(8) Gerling-Driessen, U. I.; Hoffmann, M.; Schmidt, S.; Snyder, N. L.; Hartmann, L. Glycopolymers against pathogen infection. *Chem. Soc. Rev.* **2023**, *52*, 2617-2642.

(9) Bhattacharya, K.; Kalita, U.; Singha, N. K. Tailor-made glycopolymers via reversible deactivation radical polymerization: design, properties and applications. *Polym. Chem.* **2022**, *13* (11), 1458-1483.

(10) Rudd, P. M.; Elliott, T.; Cresswell, P.; Wilson, I. A.; Dwek, R. A. Glycosylation and the immune system. *Science* **2001**, *291* (5512), 2370-2376.

(11) Chen, S.; Fukuda, M. Cell type–specific roles of carbohydrates in tumor metastasis. *Methods Enzymol.* **2006**, *416*, 371-380.

(12) Murrey, H. E.; Hsieh-Wilson, L. C. The chemical neurobiology of carbohydrates. *Chem. Rev.* **2008**, *108* (5), 1708-1731.

(13) Walker-Nasir, E.; Kaleem, A.; Hoessli, D. C.; Khurshid, A. Galactose: a specifically recognized, terminal carbohydrate moiety in biological processes. *Curr. Org. Chem.* **2008**, *12* (11), 940-956.

(14) Council, N. R.; Earth, D. o.; Studies, L.; Sciences, B. o. L.; Sciences, B. o. C.; Importance, C. o. A. t.; Glycomics, I. o.; Glycosciences. Transforming glycoscience: a roadmap for the future. **2012**.

(15) Poole, J.; Day, C. J.; von Itzstein, M.; Paton, J. C.; Jennings, M. P. Glycointeractions in bacterial pathogenesis. *Nat. Rev. Microbiol.* **2018**, *16* (7), 440-452.

(16) Sauer, M. M.; Jakob, R. P.; Luber, T.; Canonica, F.; Navarra, G.; Ernst, B.; Unverzagt, C.; Maier, T.; Glockshuber, R. Binding of the bacterial adhesin FimH to its natural, multivalent high-mannose type glycan targets. *J. Am. Chem. Soc.* **2018**, *141* (2), 936-944.

(17) Sokurenko, E. V.; Chesnokova, V.; Dykhuizen, D. E.; Ofek, I.; Wu, X.-R.; Krogfelt, K. A.; Struve, C.; Schembri, M. A.; Hasty, D. L. Pathogenic adaptation of Escherichia coli by natural variation of the FimH adhesin. *Proc. Natl. Acad. Sci. U. S. A.* **1998**, *95* (15), 8922-8926.

(18) Sharon, N. Carbohydrates as future anti-adhesion drugs for infectious diseases. *Biochim Biophys Acta Rev* **2006**, *1760* (4), 527-537.

(19) Mydock-McGrane, L. K.; Hannan, T. J.; Janetka, J. W. Rational design strategies for FimH antagonists: new drugs on the horizon for urinary tract infection and Crohn’s disease. *Expert Opin. Drug Discovery* **2017**, *12* (7), 711-731.

(20) Gouin, S. G. Repurposing Escherichia coli antiadhesives in Crohn's disease. *Future Med. Chem.* **2016**, *8* (16), 1903-1906.

(21) Connell, I.; Agace, W.; Klemm, P.; Schembri, M.; Mărild, S.; Svanborg, C. Type 1 fimbrial expression enhances Escherichia coli virulence for the urinary tract. *Proc. Natl. Acad. Sci. U. S. A.* **1996**, *93* (18), 9827-9832.

(22) Nagahori, N.; Lee, R. T.; Nishimura, S. I.; Pagé, D.; Roy, R.; Lee, Y. C. Inhibition of adhesion of type 1 fimbriated Escherichia coli to highly mannosylated ligands. *ChemBioChem* **2002**, *3* (9), 836-844.

(23) Yan, X.; Sivignon, A.; Yamakawa, N.; Crepet, A.; Travelet, C.; Borsali, R.; Dumych, T.; Li, Z.; Bilyy, R.; Deniaud, D. Glycopolymers as antiadhesives of E. coli strains inducing inflammatory bowel diseases. *Biomacromolecules* **2015**, *16* (6), 1827-1836.

(24) Hanheiser, N.; Parshad, B.; Povolotsky, T. L.; Khatri, V.; Achazi, K.; Bhatia, S. Synthesis and Comparison of Linear Polymannosides for Direct Binding with Escherichia Coli. *Macromolecular Chemistry and Physics*, 2300339.

(25) Strong, L. E.; Kiessling, L. L. A general synthetic route to defined, biologically active multivalent arrays. *J. Am. Chem. Soc.* **1999**, *121* (26), 6193-6196.

(26) Hall, B. A.; Wadsworth, O. J.; Breiner, L. M.; Chappell, J. C.; Brenner, A. S.; McCord, J. P.; Lowell, A. N.; Schulz, M. D. Inherent antibacterial properties of mannose-containing polynorbornene glycomaterials. *Chem. Commun.* **2025**, *61* (23), 4539-4542.

(27) Ilker, M. F.; Nüsslein, K.; Tew, G. N.; Coughlin, E. B. Tuning the hemolytic and antibacterial activities of amphiphilic polynorbornene derivatives. *J. Am. Chem. Soc.* **2004**, *126* (48), 15870-15875.

(28) Xue, Y.; Xiao, H.; Zhang, Y. Antimicrobial polymeric materials with quaternary ammonium and phosphonium salts. *Int. J. Mol. Sci.* **2015**, *16* (2), 3626-3655.

(29) Kenawy, E.-R.; Kandil, S. Synthesis, antimicrobial activity and applications of polymers with ammonium and phosphonium groups. **2013**.

(30) BeMiller, J. N. Carbohydrate analysis. *Food analysis* **2017**, 333-360.

(31) Frush, H. L.; Isbell, H. S. Sugar acetates, acetylglycosyl halides and orthoacetates in relation to the Walden inversion. *J. Res. Natl. Bur. Stand.* **1941**, *27* (5), 413.

(32) Guo, J.; Ye, X.-S. Protecting groups in carbohydrate chemistry: influence on stereoselectivity of glycosylations. *Molecules* **2010**, *15* (10), 7235-7265.

(33) Elferink, H.; Mensink, R. A.; White, P. B.; Boltje, T. J. Stereoselective β-mannosylation by neighboring-group participation. *Angew. Chem.* **2016**, *128* (37), 11383-11386.

(34) Miyamoto, Y.; Fujiki, M.; Nomura, K. Synthesis of homopolymers and multiblock copolymers by the living ring-opening metathesis polymerization of norbornenes containing acetyl-protected carbohydrates with well-defined ruthenium and molybdenum initiators. *J. Polym. Sci., Part A: Polym. Chem.* **2004**, *42* (17), 4248-4265.

(35) Lee, S.-G.; Brown, J. M.; Rogers, C. J.; Matson, J. B.; Krishnamurthy, C.; Rawat, M.; Hsieh-Wilson, L. C. End-functionalized glycopolymers as mimetics of chondroitin sulfate proteoglycans. *Chem. Sci.* **2010**, *1* (3), 322-325.

(36) Choi, W.; Sun, H.; Battistella, C.; Berger, O.; Vratsanos, M. A.; Wang, M. M.; Gianneschi, N. C. Biomolecular densely grafted brush polymers: Oligonucleotides, oligosaccharides and oligopeptides. *Angew. Chem.* **2020**, *59* (45), 19762-19772.

(37) Eder, K.; Sinner, F.; Mupa, M.; Huber, C. G.; Buchmeiser, M. R. Evaluation of norbornene-β-cyclodextrin-based monomers and oligomers as chiral selectors by means of nonaqueous capillary electrophoresis. *Electrophoresis* **2001**, *22* (1), 109-116.

(38) Martin, J. G.; Hill, R. K. Stereochemistry of the Diels-Alder Reaction. *Chem. Rev.* **1961**, *61* (6), 537-562.

(39) Stefaniak, W.; Janus, E.; Milchert, E. Diels–Alder Reaction of Cyclopentadiene and Alkyl Acrylates in the Presence of Pyrrolidinium Ionic Liquids with Various Anions. *Catal. Lett.* **2011**, *141*, 742-747.

(40) Shu, P.; Zeng, J.; Tao, J.; Zhao, Y.; Yao, G.; Wan, Q. Selective S-deacetylation inspired by native chemical ligation: practical syntheses of glycosyl thiols and drug mercapto-analogues. *Green Chemistry* **2015**, *17* (4), 2545-2551.

(41) Lovison, D.; Allegri, L.; Baldan, F.; Ballico, M.; Damante, G.; Jandl, C.; Baratta, W. Cationic carboxylate and thioacetate ruthenium (II) complexes: synthesis and cytotoxic activity against anaplastic thyroid cancer cells. *Dalton Transactions* **2020**, *49* (24), 8375-8388.

(42) Peña, B.; David, A.; Pavani, C.; Baptista, M. S.; Pellois, J.-P.; Turro, C.; Dunbar, K. R. Cytotoxicity studies of cyclometallated ruthenium (II) compounds: New applications for ruthenium dyes. *Organometallics* **2014**, *33* (5), 1100-1103.

(43) Van Hensbergen, J.; Burford, R.; Lowe, A. Post-functionalization of a ROMP polymer backbone via radical thiol-ene coupling chemistry. *J. Polym. Sci., Part A: Polym. Chem.* **2013**, *51* (3), 487-492.

(44) Durmaz, H.; Butun, M.; Hizal, G.; Tunca, U. Postfunctionalization of polyoxanorbornene via sequential Michael addition and radical thiol-ene click reactions. *J. Polym. Sci., Part A: Polym. Chem.* **2012**, *50* (15), 3116-3125.

(45) Lowe, A. B.; Liu, M.; van Hensbergen, J. A.; Burford, R. P. Combining Ring-Opening Metathesis Polymerization and Thiol-Ene Coupling Chemistries: Facile Access to Novel Functional Linear and Nonlinear Macromolecules. *Macromolecular rapid communications* **2014**, *35* (4), 391-404.

4.7. Supporting Information

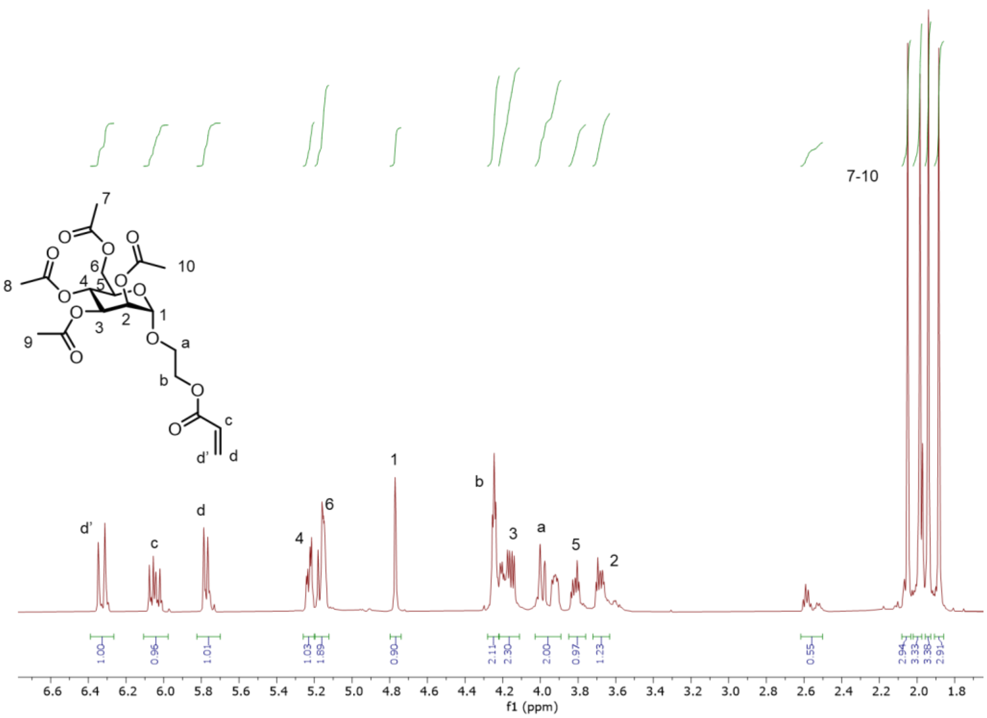

Figure 4.S1. ^{1}H NMR spectrum of AcMan-EA

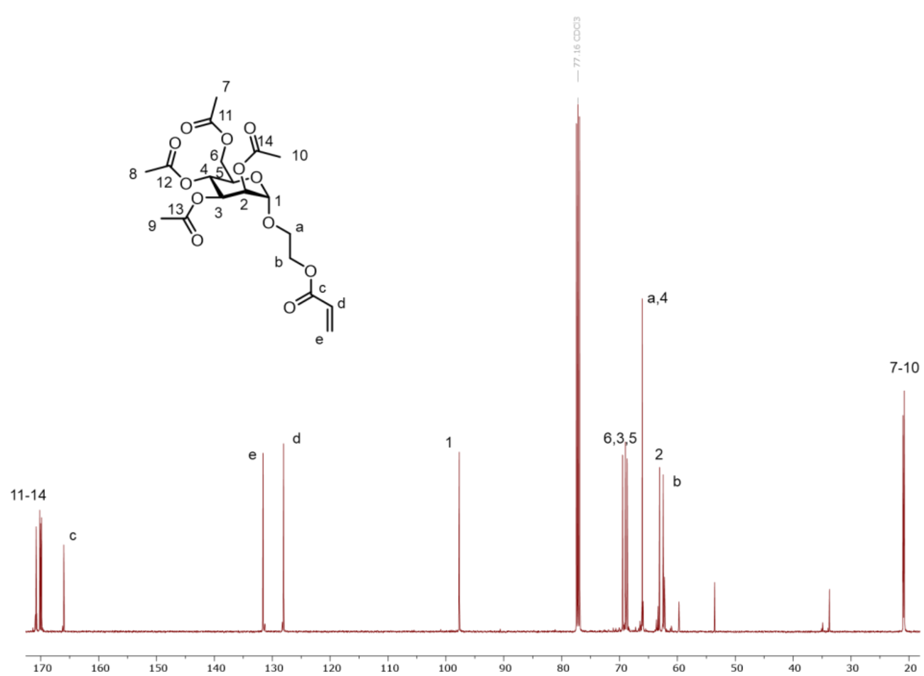

Figure 4.S2. ^{13}C NMR spectrum of AcMan-EA

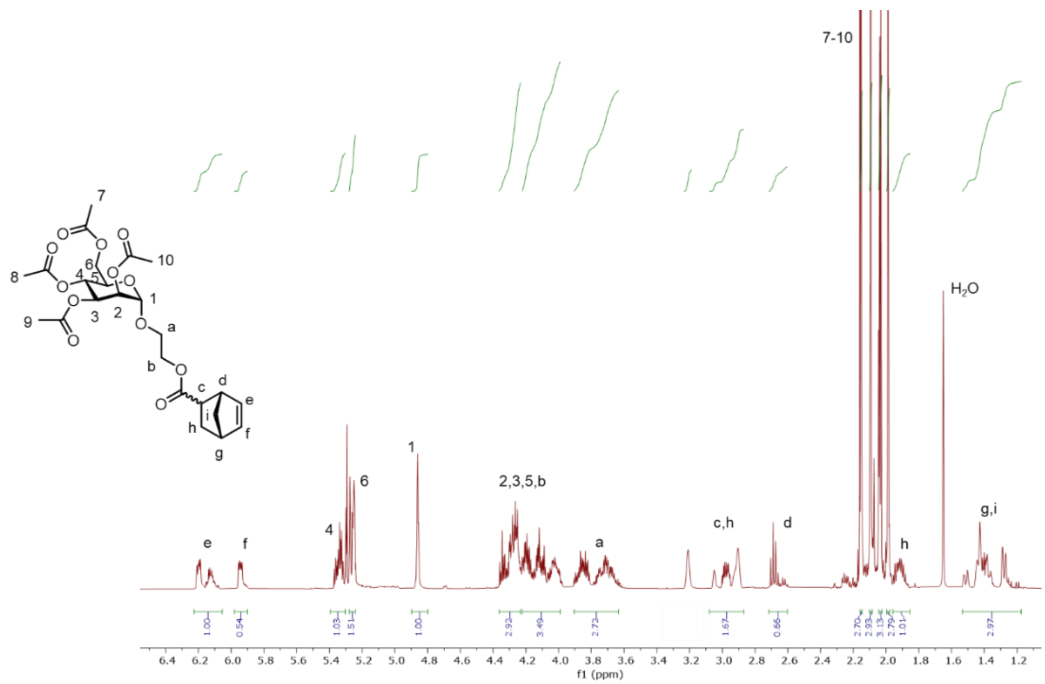

Figure 4.S3. ^{1}H NMR spectrum of AcMan-ENC

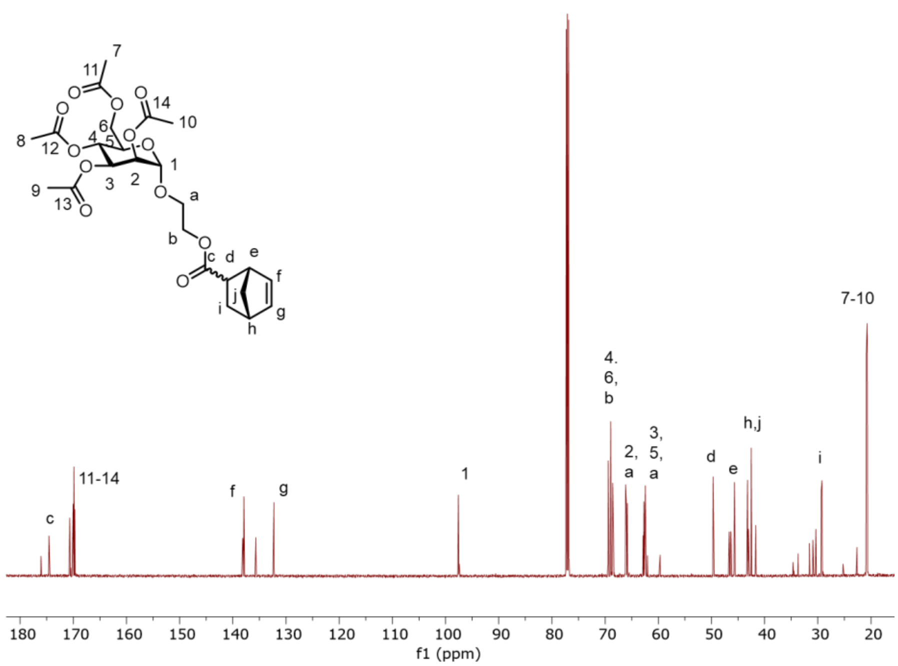

Figure 4.S4. ^{13}C NMR spectrum of AcMan-ENC

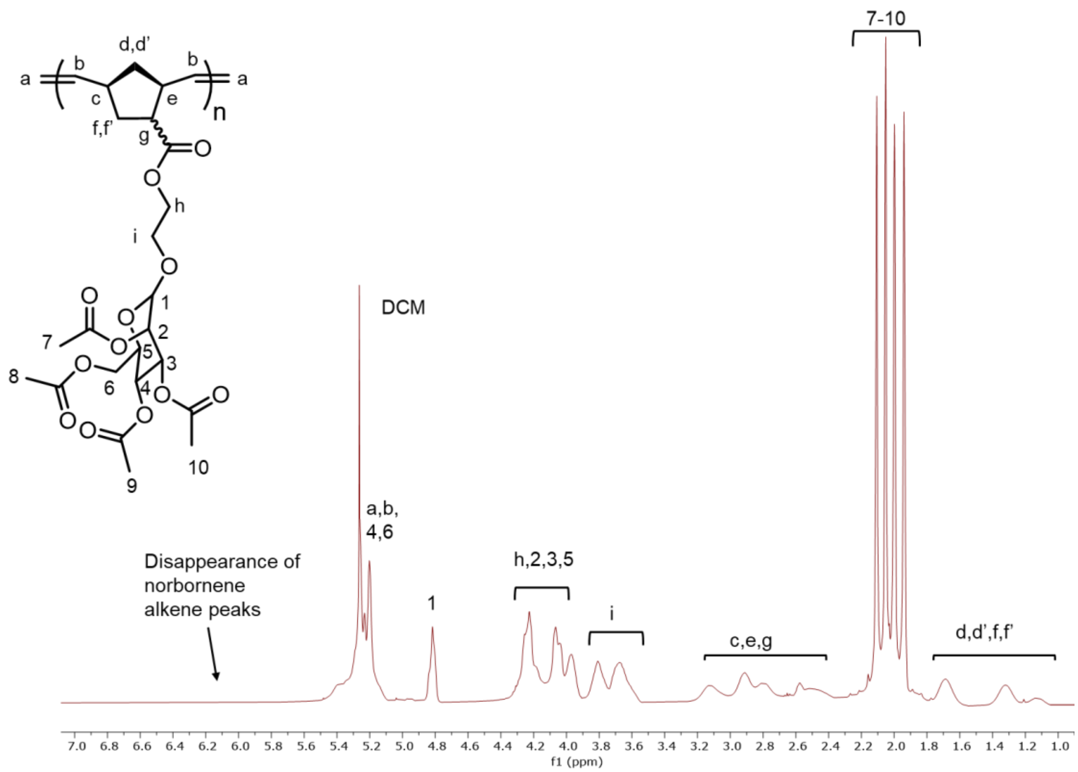

Figure 4.S5. Representative ^{1}H NMR spectrum of P-AcMan at molecular weights (25.6, 51.2, 128, and 256)

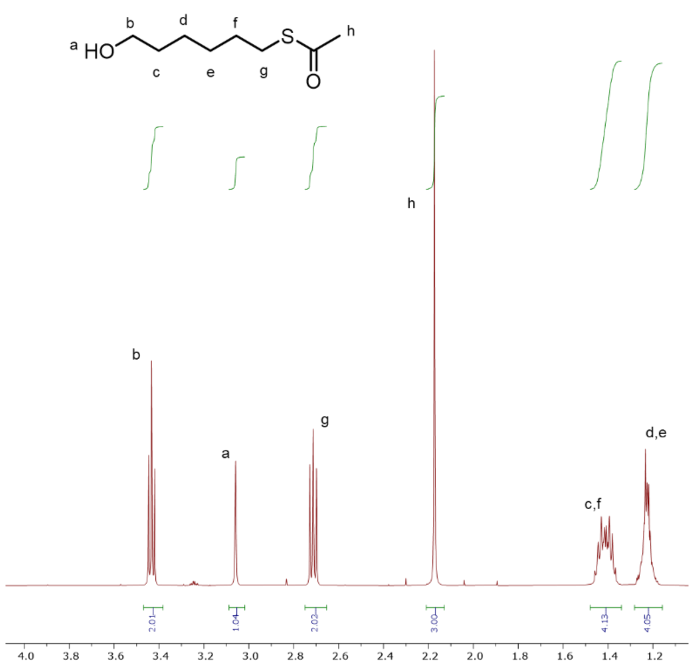

Figure 4.S6. ^{1}H NMR spectrum of 6-HHET

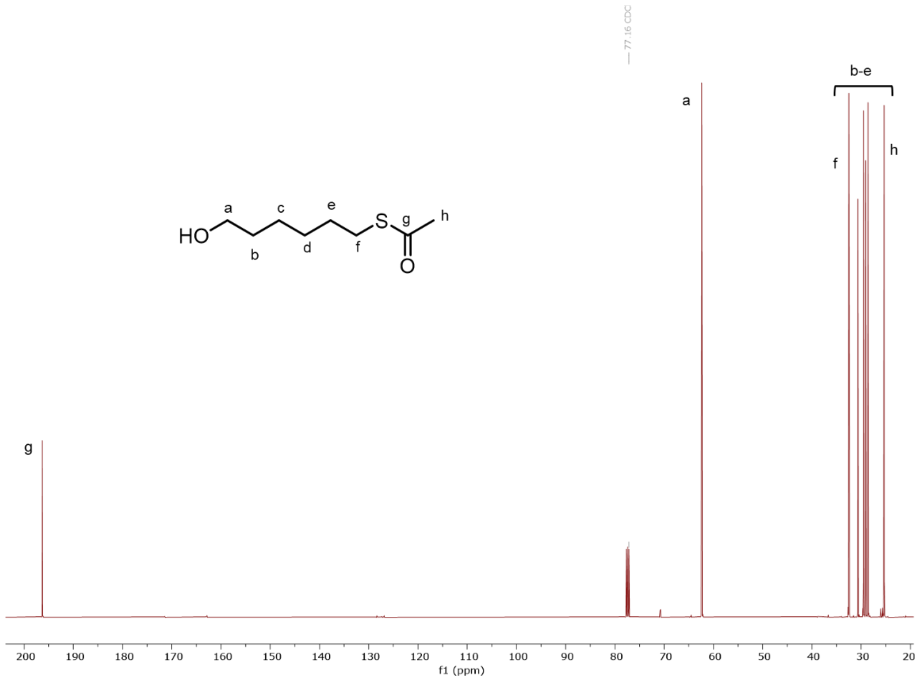

Figure 4.S7. ^{13}C NMR spectrum of 6-HHET

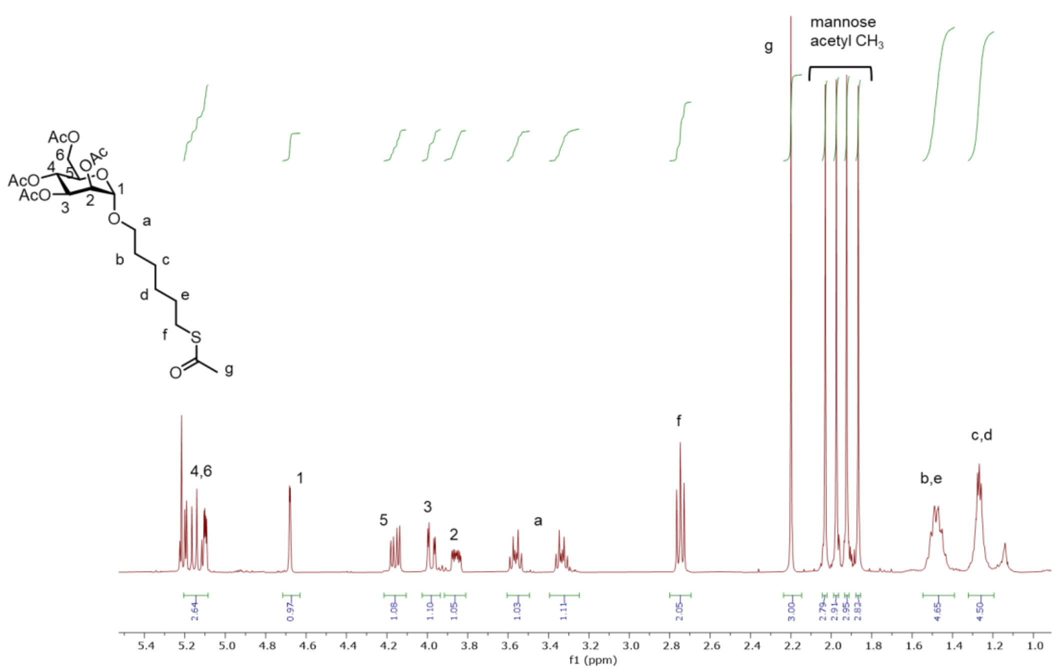

Figure 4.S8. ^{1}H NMR spectrum of AcMan-HHET

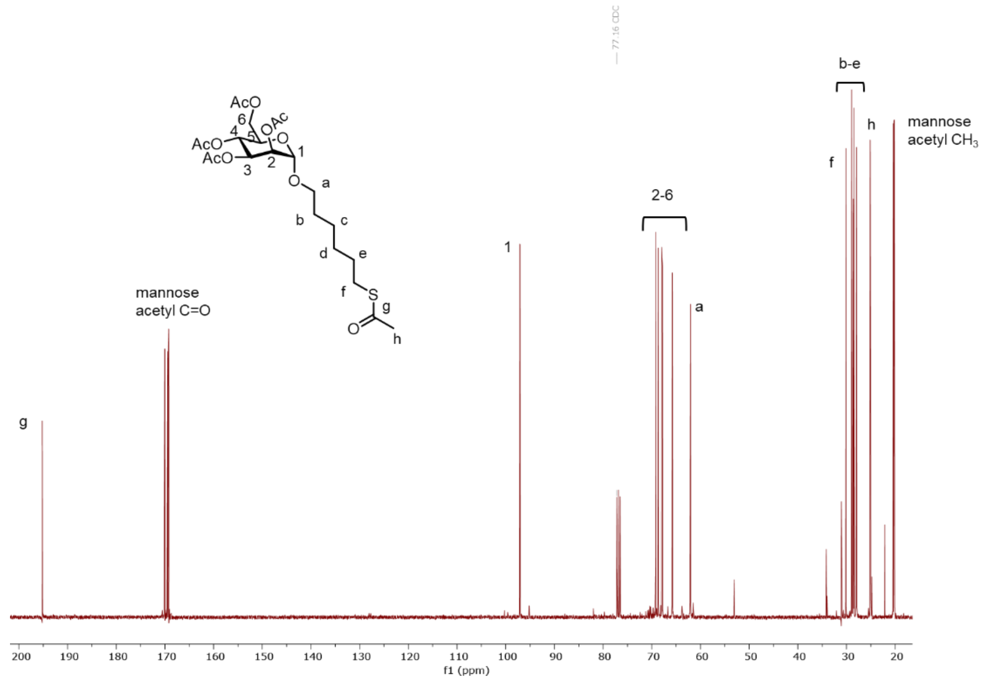

Figure 4.S9. ^{13}C NMR spectrum of AcMan-HHET

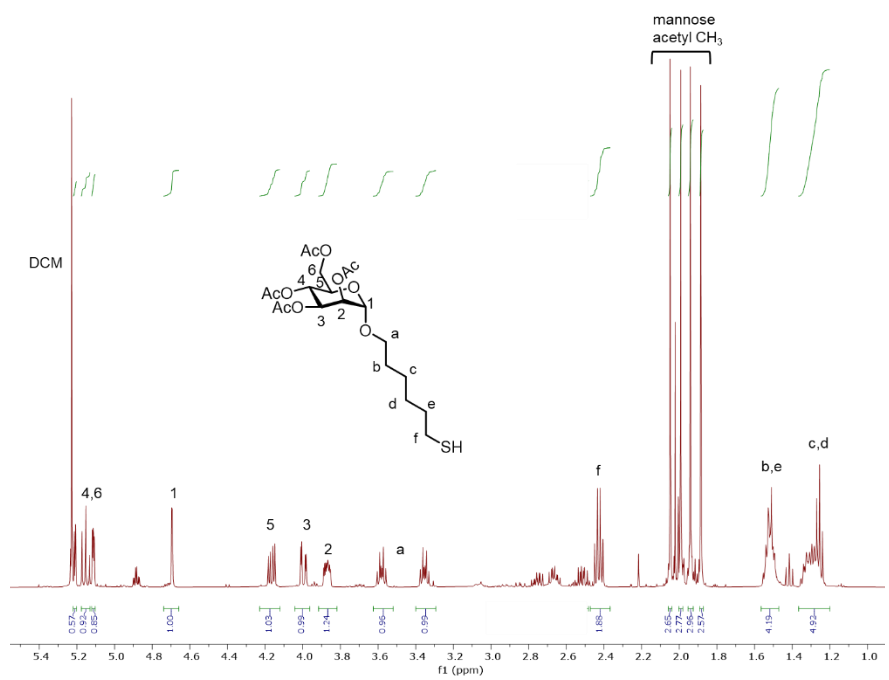

Figure 4.S10. ^{1}H NMR spectrum of AcMan-OxHSH

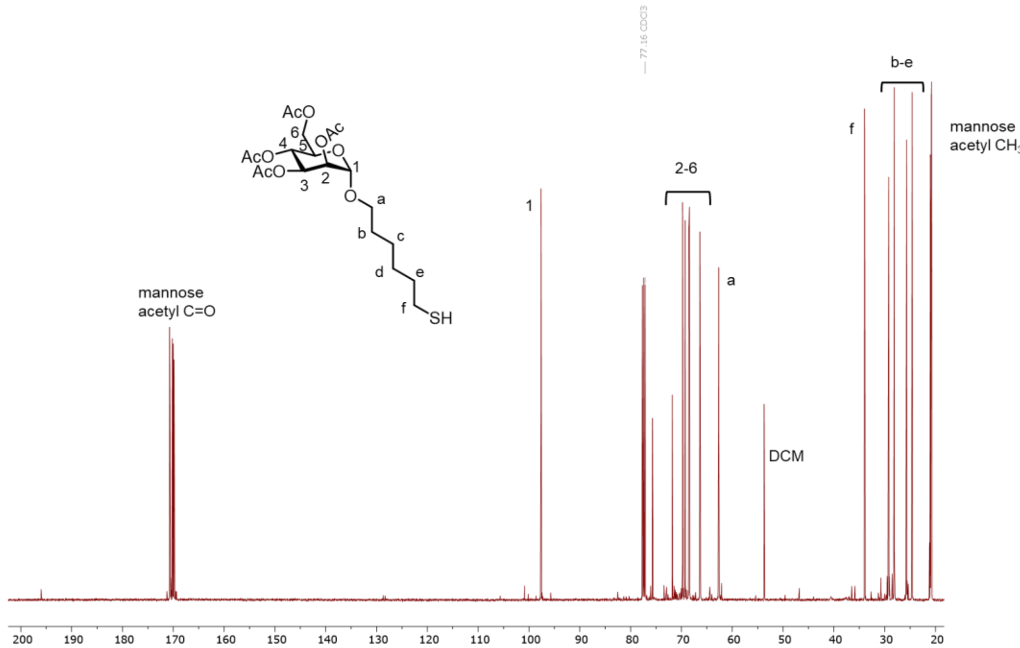

Figure 4.S11. ^{13}C NMR spectrum of AcMan-OxHSH

Chapter 5. Summary and Future Outlook

5.1. Summary and Future Outlook

The versatility of polymers as sequestrants has received much attention because they show promise to mitigate the hazards of biological and environmental contaminations.[1] Extensive research includes sequestration of organic micropollutants in the soil and wastewater,[2] radioactive materials,[3] heavy metals from wastewater sources,[4] and bacterial endotoxins in the gastrointestinal tract.[5] A more recent application is their use as drug capture materials to adsorb chemotherapy agents.[6]

Methods to limit the delivery of chemotherapy drugs to the targeted tumor are highly advantageous to mitigate toxicity to healthy tissue. Several approaches have shown promise towards sequestering the drug during chemotherapy treatment.[7-9] We investigated the use of molecularly imprinted polymers (MIPs) as effective Dox capture materials. MIPs are essentially methacrylic acid-based resins synthesized by copolymerizing MA and IEG; however, a template is incorporated to produce specific binding sites (imprints) to selectively capture the target molecule.[10-13] Since capture is driven by the imprints, complete template removal is critical to evaluating the effectiveness of these materials. For our study, Dox template removal using several suitable solvents and varying temperatures appeared to be incomplete. A worthwhile exploration is to determine the role of the residual Dox template in Dox capture from solution. Imprinted resins would be synthesized with varying crosslink densities and amount of Dox template loaded. The amount of Dox removed can be determined to calculate the residual amount adsorbed to the resin. The drug capture efficacy can then be compared to that of the corresponding non-imprinted resin. Additionally, other chemotherapy drugs can be evaluated in the same manner, especially those that have different molecular sizes and shapes.

We also investigated the use of non-templated methacrylic acid-based resins to effectively capture Dox. The performance of these materials revealed that electrostatic binding was critical to drug capture, notably between the anionic resin and positively charged Dox. Additionally, we observed an overall trend where increasing crosslinking density increased Dox adsorption. The maximum crosslinker ratio incorporated for this study was 2.00 equivalents and Dox capture results showed a two-fold increase in capture efficacy corresponding to a four-fold increase in crosslink density. Increasing the crosslink density at certain increments should reveal the crosslinker to monomer ratio at which drug capture plateaus. Additionally, incorporating a monomer such as vinyl phosphonic acid that has two anionic binding sites should enhance capture efficacy, although steric hindrance may play a role.

Turning to glycopolymers, the development of synthetic antimicrobial glycopolymers has been progressing; however, there are still challenges that impede their viability as small-molecule antibiotic replacements. Two of the prevailing concerns are reduced potency compared to traditional antibiotics and enhanced hemolytic activity.[14] Towards addressing both concerns, we modified the backbone of mannose-containing oxo-norbornene polymers to incorporate additional mannose-binding ligands while increasing overall hydrophilicity of the materials. Post-polymerization modification of the oxo-norbornene backbone was extremely challenging, as the radical intermediate is less stabilized compared to the oxa-norbornene analog. Although attempts to incorporate the oxa-norbornene backbone via Diels-Alder cycloaddition with furan and mannose-acrylate were unsuccessful, exploring reaction conditions not previously employed may change the outcome. This would facilitate higher glycan density in the polymer backbone, possibly increasing the potency of the mannose-functionalized polynorbornenes. Alternatively, introducing a higher thio-mannose ratio while modifying the oxo-norbornene backbone may also facilitate a greater degree of functionality.

The utility of polymeric sequestrants towards solving complex problems has been expanding significantly and will do so for some time. While their exploration as sequestrants to adsorb chemotherapy drugs is relatively new, they have been widely investigated as sequestrants for environmental contaminants and traditional antibiotics replacements that will evade the resistance mechanisms of pathogenic bacteria and viruses. As with any other field, an interdisciplinary approach is required to ensure that the materials developed are viable solutions and I look forward to seeing how collaborations among synthetic chemists, engineers and medical professionals will enhance patient care in the future.

5.2. References

(1) Archer, W. R.; Hall, B. A.; Thompson, T. N.; Wadsworth, O. J.; Schulz, M. D. Polymer sequestrants for biological and environmental applications. *Polym. Int.* **2019**, *68* (7), 1220-1237.

(2) Marican, A.; Durán-Lara, E. F. A review on pesticide removal through different processes. *Environ. Sci. Pollut. Res.* **2018**, *25*, 2051-2064.

(3) Husnain, S. M.; Um, W.; Chang, Y.-S. Magnetite-based adsorbents for sequestration of radionuclides: a review. *RSC Adv.* **2018**, *8* (5), 2521-2540.

(4) Diallo, M. S.; Kotte, M. R.; Cho, M. Mining critical metals and elements from seawater: opportunities and challenges. *Environ. Sci. Technol.* **2015**, *49* (16), 9390-9399.

(5) Bär, A.; Til, H.; Timonen, M. Subchronic oral toxicity study with regular and enzymatically depolymerized sodium carboxymethylcellulose in rats. *Food Chem. Toxicol.* **1995**, *33* (11), 909-917.

(6) Chen, X. C.; Oh, H. J.; Yu, J. F.; Yang, J. K.; Petzetakis, N.; Patel, A. S.; Hetts, S. W.; Balsara, N. P. Block copolymer membranes for efficient capture of a chemotherapy drug. *ACS Macro Lett.* **2016**, *5* (8), 936-941.

(7) Su, G. A.; Wadsworth, O. J.; Muller, H. S.; Archer, W. R.; Hetts, S. W.; Schulz, M. D. Polymer–nucleobase composites for chemotherapy drug capture. *J. Mater. Chem. B* **2023**, *11* (35), 8449-8455.

(8) Blumenfeld, C. M.; Schulz, M. D.; Aboian, M. S.; Wilson, M. W.; Moore, T.; Hetts, S. W.; Grubbs, R. H. Drug capture materials based on genomic DNA-functionalized magnetic nanoparticles. *Nat. Commun.* **2018**, *9* (1), 1-7.

(9) Oh, H. J.; Aboian, M. S.; Yi, M. Y.; Maslyn, J. A.; Loo, W. S.; Jiang, X.; Parkinson, D. Y.; Wilson, M. W.; Moore, T.; Yee, C. R. 3D printed absorber for capturing chemotherapy drugs before they spread through the body. *ACS Cent. Sci.* **2019**, *5* (3), 419-427.

(10) So, J.; Pang, C.; Dong, H.; Jang, P.; Juhyok, U.; Ri, K.; Yun, C. Adsorption of 1-naphthyl methyl carbamate in water by utilizing a surface molecularly imprinted polymer. *Chem. Phys. Lett.* **2018**, *699*, 199-207.

(11) Krupadam, R. J.; Khan, M. S.; Wate, S. R. Removal of probable human carcinogenic polycyclic aromatic hydrocarbons from contaminated water using molecularly imprinted polymer. *Water Res.* **2010**, *44* (3), 681-688.

(12) Ghasemi, S.; Nematollahzadeh, A. Molecularly imprinted polymer membrane for the removal of naphthalene from petrochemical wastewater streams. *Adv. Polym. Technol.* **2018**, *37* (6), 2288-2293.

(13) Murray, A.; Örmeci, B. Application of molecularly imprinted and non-imprinted polymers for removal of emerging contaminants in water and wastewater treatment: a review. *Environ. Sci. Pollut. Res.* **2012**, *19*, 3820-3830.

(14) Huang, K.-S.; Yang, C.-H.; Huang, S.-L.; Chen, C.-Y.; Lu, Y.-Y.; Lin, Y.-S. Recent advances in antimicrobial polymers: a mini-review. *Int. J. Mol. Sci.* **2016**, *17* (9), 1578.